

15th | SOLEIL USERS' MEETING

JANUARY 16th - 17th, 2020

Synchrotron SOLEIL (Saint-Aubin)

SCIENTIFIC COMMITTEE

Pierre ASSELIN (Univ. Pierre et Marie-Curie - CNRS)

Noemi CARMONA-TEJERO (Lab. de Physique des Matériaux -
Universidad Complutense - Madrid)

Anne CHARRIER (Centre Interdisciplinaire de Nanoscience de Marseille)

Nicolas DELSUC (UPMC-ENS Département de Chimie - Paris)

Emmanouil FRANTZESKAKIS (Université Paris-Sud)

Renaud GUILLEMIN (LCPMR - Paris)

Rozenn LE HIR (INRA - Centre de Versailles-Grignon)

Thomas MAROUTIAN (CNRS UMR9001 - Université Paris-Sud)

Rémi MARSAC (Université de Rennes 1 - Campus de Beaulieu - Rennes)

Benoît MASQUIDA (UMR 7156 GMGM - CNRS - Université de Strasbourg)

Karine PROVOST (Institut de Chimie et des Matériaux de Paris-Est - Thiais)

Asma TOUGERTI (Unité de Catalyse et de Chimie du Solide -
Université de Lille)

Thematic Workshop

**Techniques for integrated biology at
Synchrotron SOLEIL and its upgrade**

January 15th, 2020

Synchrotron SOLEIL (Saint-Aubin)

Information and registration:

www.synchrotron-soleil.fr/en/events/sum-2020





Welcome

The 15th SOLEIL Users' Meeting takes place on January 16th and 17th, 2020 at SOLEIL.

This invaluable forum for the synchrotron radiation users' community provides the opportunity to exchange and learn about the evolution of the machine and the beamlines. It is also the occasion to share scientific, technical and practical issues about the synchrotron radiation use.

The 2 plenary lectures deal with different aspects related to recent and future synchrotron sources evolutions.

- Condensed matter,
- Chemistry/reactivity

Scientific communications are presented during parallel sessions, selected from submitted abstracts.

The posters session and commercial exhibitions are held at SOLEIL on the afternoon of January 16th.

Then a visit of AILES, CASSIOPEE and SMIS beamlines is organized, as well as a round table about the upgrade of SOLEIL (Beamtime organisation impact).

The Roger Fourme prize award (student poster best prize) will be held before the conference dinner which takes place at SOLEIL.

Bienvenue

Le 15ème Colloque des Utilisateurs de SOLEIL se tiend les jeudi 16 et vendredi 17 janvier 2020, à SOLEIL.

Ce rendez-vous incontournable pour la communauté des utilisateurs du rayonnement synchrotron est l'occasion d'échanges et de restitutions sur l'évolution de la machine et des lignes de lumière.

Il est aussi le lieu pour échanger sur les aspects scientifiques, techniques et pratiques de l'utilisation du rayonnement synchrotron.

Les 2 conférences plénières couvrent différents thèmes de recherche de la communauté des utilisateurs de SOLEIL:

- Matière Condensée
- Chmie/réactivité

Les sessions parallèles sont composées d'exposés scientifiques originaux, sélectionnés à partir des résumés soumis.

Un temps de convivialité et de discussion est organisé à SOLEIL le jeudi 16 janvier après-midi avec la session posters et les stands d'entreprises.

A SOLEIL, sont également organisés la visite des lignes AILES, CASSIOPEE et SMIS, ainsi qu'une table ronde sur l'upgrade à SOLEIL (Impact sur l'organisation du temps de faisceau).

La remise du prix Roger Fourme (prix de meilleur poster étudiant) aura lieu avant le diner de la conférence qui a lieu au restaurant de SOLEIL.

SOLEIL Users' Meeting

January 16th - 17th, 2020

Synchrotron SOLEIL, Saint-Aubin - France

Summary

- Programme
- Plenary Session
- Parallel Sessions:
 - Ancient & New Materials
 - Dynamic, Reactivity & Chemical Analysis Diluted Matter
 - Life & Earth Sciences
- Posters Session
 - List of Student Posters
 - List of Other Posters
- Tutorials
- List of Industrial Exhibitors
- Companies Advertisements



Synchrotron SOLEIL, Saint-Aubin - France

Programme

Thursday, January 16th

SOLEIL AUDITORIUM

- 09:00 - 10:00 Registration & coffee
- 10:00 - 10:10 Welcome / Introduction
Nicolas Delsuc - *ORGUES Chairperson*
- 10:10 - 10:20 The word of SOLEIL General Director
Jean Dailant
- 10:20 - 11:05 Observation of the transition to metal hydrogen: Why and how the use of SOLEIL infrared source played a crucial role.
Paul Loubeyre - *CEA, DAM, DIF, Arpajon, France*
- 11:05 - 11:50 Hierarchical self-assembly of polyoxometalate-based hybrids driven by metal coordination and electrostatic interactions
Guillaume Izzet - *Institut Parisien de Chimie Moléculaire, Sorbonne Université, Paris, France*
- 11:50 - 12:10 Peer Review Committee Chairman - 1 Diluted matter - **Roland Thissen**
Peer Review Committee Chairman - 2 Surfaces / Interfaces - **Richard Mattana**
- 12:10 - 14:00 Lunch – **SOLEIL Restaurant**

Parallel sessions (see the detailed programme below)

- 14:00 - 16:00
- Ancient & New Materials (Cultural heritage / Structure / Electronic Properties / Surfaces & Interfaces) **SOLEIL Auditorium**
 - Dynamic, Reactivity & Chemical analysis (Diluted Matter & Chemistry) **CEA BLOCH Auditorium**
 - Life & Earth Sciences (Biology / Health & Environment / Geoscience) **SOLEIL Reception Building Auditorium**
- 16:00 - 16:30 Coffee break

Parallel sessions (see the detailed programme below)

- 16:30 - 18:00
- Ancient & New Materials (Cultural heritage / Structure / Electronic Properties / Surfaces & Interfaces) **SOLEIL Auditorium**
 - Dynamic, Reactivity & Chemical analysis (Diluted Matter & Chemistry) **CEA BLOCH Auditorium**
 - Life & Earth Sciences (Biology / Health & Environment / Geoscience) **SOLEIL Reception Building Auditorium**
- 18:00 - 20:00 Posters session / Commercial exhibition / ORGUES and AFURS Booth
Visit of Beamlines AILES, CASSIOPEE, SMIS
- 20:00 - 21:30 Buffet / Award of the best student poster



Friday, January 17th

Parallel sessions (see the detailed programme below)

- 9:00 - 11:00
- Ancient & New Materials (Cultural heritage / Structure / Electronic Properties / Surfaces & Interfaces) **SOLEIL Auditorium**
 - Dynamic, Reactivity & Chemical analysis (Diluted Matter & Chemistry) **CEA BLOCH Auditorium**
 - Life & Earth Sciences (Biology / Health & Environment / Geoscience) **SOLEIL Reception Building Auditorium**
- 11:00 - 11:30 *Coffee break - **SOLEIL Auditorium Cafeteria***
- 11:30 - 12:30 Round Table: *Upgrade: Beamtime organisation impact - **SOLEIL Auditorium***
- 12:30 - 14:00 *Lunch – **SOLEIL Restaurant***
- 14:00 - 17:00 **Chemometry in Quick XAS** tutorial (limited to the register participants)
Training room, T5 Building



Parallel Sessions Schedule

Ancient & New Materials

(Cultural heritage / Structure / Electronic Properties / Surfaces & Interfaces)

Chairpersons:

Emmanouil Frantzeskakis, Karine Provost, Noemi Carmona-Tejero,
Thomas Maroutian & Anne Charrier

Thursday, January 16th

SOLEIL AUDITORIUM

- | | |
|---------------------------|--|
| 14:00 - 14:30
(25'+5') | New 2D materials: Silicene and phosphorene
Hamid Oughaddou - Institut des Sciences Moléculaires d'Orsay, France |
| 14:30 - 15:00
(25'+5') | Electronic properties of SiO/GeO ultra-thin films from ARPES and DFT calculations
Yannick Fagot-Revurat - Institut Jean Lamour, Vandoeuvre-Les-Nancy, France |
| 15:00 - 15:20
(15'+5') | Direct observation of band gap renormalization in layered indium selenide
Zhensheng Chen - Laboratoire de Physique des Solides, Orsay, France |
| 15:20 - 15:40
(15'+5') | Influence of a metal surface on spin-crossover molecules
Amandine Bellec - Laboratoire Matériaux et Phénomènes Quantiques, Paris, France |
| 15:40 - 16:00
(15'+5') | Temperature dependent magnetization profile in Gd/Co/Pt ultrathin films
Vartika Bansal - Université Grenoble-Alpes, CNRS, INP, Institut NEEL, Grenoble, France |
| 16:00 - 16:30 | Coffee break |
| 16:30 - 17:00
(25'+5') | nanoARPES science and technique
Pavel Dudin - Synchrotron SOLEIL, Gif-sur-Yvette, France |
| 17:00 - 17:20
(15'+5') | Characterization by Synchrotron Radiation at MARS beamline, of highly irradiated 316 austenitic stainless steel
Alexandre Renault-Laborne - CEA Saclay, Gif-sur-Yvette, France |
| 17:20 - 17:40
(15'+5') | Anomalous diffraction study of germanite, a thermoelectric material
Carmelo Prestipino - Institut des Sciences Chimiques de Rennes, France |
| 17:40 - 18:00
(15'+5') | Probing photoinduced picosecond shear strain in ferroelectrics with time-resolved X-ray diffraction
Pascal Ruello - Institut des Molécules et Matériaux du Mans, France |



Parallel Sessions Schedule

Ancient & New Materials

(Cultural heritage / Structure / Electronic Properties / Surfaces & Interfaces)

Chairpersons:

Emmanouil Frantzeskakis, Karine Provost, Noemi Carmona-Tejero,
Thomas Maroutian & Anne Charrier

Friday, January 17th

SOLEIL AUDITORIUM

- 09:00 - 09:30
(25'+5') Photomagnetism in Prussian Blue analogs : Benefits from a multi-beamlines investigation
Amélie Bordage - *Institut de Chimie Moléculaire et des Matériaux d'Orsay, France*
- 09:30 - 10:00
(25'+5') PUMA, a new beamline optimised for Cultural Heritage research
Sebastian Schoeder - *Synchrotron SOLEIL, Gif-sur-Yvette, France*
- 10:00 - 10:20
(15'+5') High pressure study on the metal-organic framework MIL-101 filled with metal nanoparticles
Anna Celeste - *Synchrotron SOLEIL, Gif-sur-Yvette & Institut de Chimie et des Matériaux Paris-Est, Thiais, France*
- 10:20 - 10:40
(15'+5') Strong spin-lattice coupling in the frustrated pentagonal magnet $\text{Bi}_2\text{Fe}_4\text{O}_9$ revealed by infrared spectroscopy measurements at high pressure
Marine Verseils - *Synchrotron SOLEIL, Gif-sur-Yvette, France*
- 10:40 - 11:00
(15'+5') The use of wiggler white beam: New opportunities for high pressure science
Jean-Paul Itié - *Synchrotron SOLEIL, Gif-sur-Yvette, France*
- 11:00 - 11:30 *Coffee break*



Parallel Sessions Schedule

Dynamic, Reactivity & Chemical analysis (Diluted Matter & Chemistry)

Chairpersons:

Asma Tougerti, Nicolas Delsuc, Pierre Asselin and Renaud Guillemin

Thursday, January 16th

CEA BLOCH AUDITORIUM

- 14:00 - 14:30
(25'+5')
- The VUV photoionization of small radicals on the DESIRS beamline: Spectroscopy and cross section determination
Séverine Boyé-Péronne - Institut des Sciences Moléculaires d'Orsay, France
- 14:30 - 15:00
(25'+5')
- Photoelectron spectroscopy of liquid jets at GALAXIES and PLEIADES beamlines
Christophe Nicolas - Synchrotron SOLEIL, Gif-sur-Yvette, France
- 15:00 - 15:20
(15'+5')
- NH₃ ultrafast dissociation probed by Auger electron-ion coincidences
Ferzad Hosseini - Laboratoire de Chimie Physique-Matière et Rayonnement, Paris, France
- 15:20 - 15:40
(15'+5')
- Surface chemistry of colloidal gold nanoparticles generated by laser ablation
Anna Lévy - Institut des NanoSciences de Paris, France
- 15:40 - 16:00
(15'+5')
- Energy, environment for a sustainable development. contribution of a 4th generation Synchrotron
Valerie Briois - Synchrotron SOLEIL, Gif-sur-Yvette, France
- 16:00 - 16:30
- Coffee break
- 16:30 - 17:00
(25'+5')
- Double layer at an electrified interface, beyond the textbook: Water matters
Martina Havenith - Ruhr-Universität Bochum, Germany
- 17:00 - 17:30
(25'+5')
- Exploiting the THz Synchrotron Radiation at its highest resolution and in a broadband fashion by heterodyne techniques
Marie-Aline Martin-Drumel - Institut des Sciences Moléculaires d'Orsay, France
- 17:30 - 17:50
(15'+5')
- New line positions analysis of the ν_3 bands of ³⁵CINO₂ and ³⁷CINO₂ at 370 cm⁻¹
Anusanth Anantharajah - Laboratoire Interuniversitaire des Systèmes Atmosphériques, Créteil, France



Parallel Sessions Schedule

Dynamic, Reactivity & Chemical analysis (Diluted Matter & Chemistry)

Chairpersons:

Asma Tougeri, Nicolas Delsuc, Pierre Asselin and Renaud Guillemin

Friday, January 17th

CEA BLOCH AUDITORIUM

- | | |
|---------------------------|--|
| 09:00 - 09:30
(25'+5') | Lanthanide oxysulfide nanoplates: Growth mechanism and reactivity from ex situ and in situ spectroscopies
Sophie Carenco - <i>Laboratoire de Chimie de la Matière Condensée de Paris, France</i> |
| 09:30 - 10:00
(25'+5') | Infrared and terahertz spectroscopy under fine-controlled conditions
Pascale Roy - <i>Synchrotron SOLEIL, Gif-sur-Yvette, France</i> |
| 10:00 - 10:20
(15'+5') | Aerosol synthesis of thermally stable porous noble metals and alloys by using bi-functional templates: A mechanistic study
Marion Giraud - <i>Laboratoire ITODYS, Paris, France</i> |
| 10:20 - 10:40
(15'+5') | Monitoring catalysts at work: The advantages of combined operando EPR/XAS/ATR-IR/UV-vis spectroscopy with multivariate analysis
Jabor Rabeah - <i>Leibniz Institute, Rostock, Germany</i> |
| 10:40 - 11:00
(15'+5') | Ascorbic acid directs the anisotropic growth of silver-on-gold nanoparticles
Doru Constantin - <i>Laboratoire de Physique des Solides, Orsay, France</i> |
| 11:00 - 11:30 | <i>Coffee break</i> |



Parallel Sessions Schedule

Life & Earth Sciences (Biology / Health & Environment / Geoscience)

Chairpersons:
Benoît Masquida, Rozenn Le Hir and Remi Marsac

Thursday, January 16th

SOLEIL Reception Building AUDITORIUM

- 14:00 - 14:30
(25'+5') What about collagen in biomaterials?
Carole Aimé – *UMR Pasteur, Paris, France*
- 14:30 - 15:00
(25'+5') **Andrea Somogyi** - *Synchrotron SOLEIL, Gif-sur-Yvette, France*
- 15:00 - 15:20
(15'+5') 2D mapping bones osteosarcoma with micro-sized X-ray beam
Arnaud Bardouil - *Institut de Physique de Rennes, France*
- 15:20 - 15:40
(15'+5') A BioSAXS study of cubic liquid crystalline nanostructures involving catalase and curcumin in view of therapeutic applications
Angelina Angelova - *Institut Galien, Châtenay-Malabry, France*
- 15:40 - 16:00
(15'+5') Light-driven folding of G-quadruplex DNA structures probed by Synchrotron Radiation circular dichroism
Kevin Laouer - *Laboratoire d'Optique et Biosciences, École Polytechnique, Palaiseau, France*
- 16:00 - 16:30
Coffee break
- 16:30 - 17:00
(25'+5') Amber fossils revealed by Synchrotron imaging
Vincent Perrichot - *Géosciences Rennes, France*
- 17:00 - 17:30
(25'+5') Microfluidic chips for crystal growth and serial crystallography
Claude Sauter - *Architecture et Réactivité de l'arN, I.B.M.C., Strasbourg, France*
- 17:30 - 17:50
(15'+5') Energy, environment for a sustainable development. Contribution of a 4th generation Synchrotron
Delphine Vantelon - *Synchrotron SOLEIL, Gif-sur-Yvette, France*



Parallel Sessions Schedule

Life & Earth Sciences (Biology / Health & Environment / Geoscience)

Chairpersons:
Benoît Masquida, Rozenn Le Hir and Remi Marsac

Friday, January 17th

SOLEIL Reception Building AUDITORIUM

- 09:00 - 09:30
(25'+5')
Synchrotron time lapse imaging of lignocellulose biomass hydrolysis
Marie-Françoise Devaux ou Fabienne Guillon – *INRA, Biopolymères Interactions Assemblages, Nantes, France*
- 09:30 - 10:00
(25'+5')
PX2 - *Synchrotron SOLEIL, Gif-sur-Yvette, France*
- 10:00 - 10:20
(15'+5')
Cryo-EM structure of an archaeal translation initiation complex at 3.1 Å resolution
Pierre-Damien Coureux - *Laboratoire de Biochimie, Ecole polytechnique, Palaiseau, France*
- 10:20 - 10:40
(15'+5')
How fluorescence has enlightened antibiotic transport and resistance in Gram-negative bacteria
Muriel Masi - *Institut de Biologie Intégrative de la Cellule, Orsay, France*
- 10:40 - 11:00
(15'+5')
Anomalous magnesium: Search for the metal ions in the ribosome
Alexey Rozov - *Institut de Génétique et de Biologie Moléculaire et Cellulaire, Strasbourg, France*
- 11:00 - 11:30
Coffee break

PLENARY SESSION

PLENARY SESSION

SOLEIL AUDITORIUM

Thursday, January 16th

- PT-01** Observation of the transition to metal hydrogen: Why and how the use of SOLEIL infrared source played a crucial role.
Paul Loubeyre
- PT-02** Hierarchical self-assembly of polyoxometalate-based hybrids driven by metal coordination and electrostatic interactions
Guillaume Izzet

Observation of the Transition to Metal Hydrogen: Why and how the use of SOLEIL Infrared Source Played a Crucial Role

P. Loubeyre¹⁾, F. Occelli¹⁾ and P. Dumas²⁾

1 CEA, DAM, DIF, 91297 Arpajon. France.

2 Synchrotron SOLEIL, 91192 Gif-sur-Yvette. France.

ABSTRACT

Understanding how and when molecular solid hydrogen may transform into a metal has stimulated many theoretical works since the 30's. It is still an opened theoretical question. Also, the quest for metal hydrogen has pushed major developments of modern experimental high pressure physics and yet various claims of its observation have remained unconfirmed.

Recently, we observed and characterized the transition to metal hydrogen near 425 GPa at 80 K [1]. Previous measurements have evidenced the direct bandgap change in the visible, showing a linear decrease up to 300 GPa and so suggesting a closure of the direct bandgap, hence the insulator-metal transition, to occur about 460 GPa [2]. The most advanced theoretical calculations predict also a stability of metal hydrogen in the 400 GPa – 500 GPa pressure range[3, 4].

In this talk, we will detail our experimental strategy, following a three steps procedure namely: 1) Demonstrate the possibility to generate pressures well over 400 GPa (that is the limit of the conventional Diamond Anvil Cell (DAC)) by loading hydrogen in the recently developed Toroidal-DAC; 2) Exhibit a reliable non-intrusive signature of the insulator-metal phase transition, i.e. total IR absorption; 3) Record combined infrared, Raman and visible observation measurements to disclose the physics at stake at the insulator-metal transition. A first order transition from a molecular insulator to a protons paired metal is suggested and supported by experimental behavior.

The observation of metal hydrogen is a stepping stone towards disclosing novel quantum many-body effects. Thanks to the use of the T-DAC, the quality of the hydrogen sample, as obtained here above 400 GPa, could ease such measurements, in particular to advance on the characterization of a room temperature superconductivity. Some of the on-going experimental developments will be discussed.

REFERENCES

1. P. Loubeyre, F. Occelli and P. Dumas, arxiv.org/abs/1906.05634 (2019) and accepted for publication in Nature.
2. P. Loubeyre, F. Occelli and R. LeToullec, *Nature* 416, 613 (2002).
3. J.M. McMahon, M.A. Morales, C. Pierleoni and D.M. Ceperley, *Rev. Mod. Phys.* 84, 1607 (2012).
4. J. McMinis, R. ClayIII, D. Lee and M. Morales, *Phys. Rev. Lett.* 114, 105305 (2015).

Hierarchical Self-assembly of Polyoxometalate-based Hybrids Driven by Metal Coordination and Electrostatic Interactions

G. Izzet

Institut Parisien de Chimie Moléculaire, Sorbonne Université, UMR CNRS 8232

ABSTRACT

Polyoxometalates (POMs) are a class of discrete metal oxo clusters that bridge the gap between small oxo-metal complexes and bulk metal-oxides.^[1] Owing to their nanoscale size, their structural complexity and their sensitivity to various types of interactions, POMs are attractive molecular building units for the elaboration of complex molecular assembly with emergent properties.^[2] In this context, we are interested in synthesizing mesoscopic POM-based nanostructures via metal-directed self-assembly processes.^[3,4] The approach relies on the synthesis of POM-based building blocks bearing remote binding functions with well-suited orientations and denticities (Figure 1 left). Coordination of these hybrid building blocks to complementary metal ions afford discrete coordination oligomers. Owing to the ionic character of POMs, these primary self-assembled systems may further aggregate through intermolecular electrostatic interactions and afford larger multi-scale assemblies (Figure 1 right, top).^[5,6] This presentation will focus on the synthesis and characterization, especially by Small-angle X-ray scattering (SAXS) performed on the SWING beamline (Figure 1 right, down), of the different POM-based self-assemblies. An important emphasis will be devoted to the control of the shape of the hierarchical nano-assemblies.

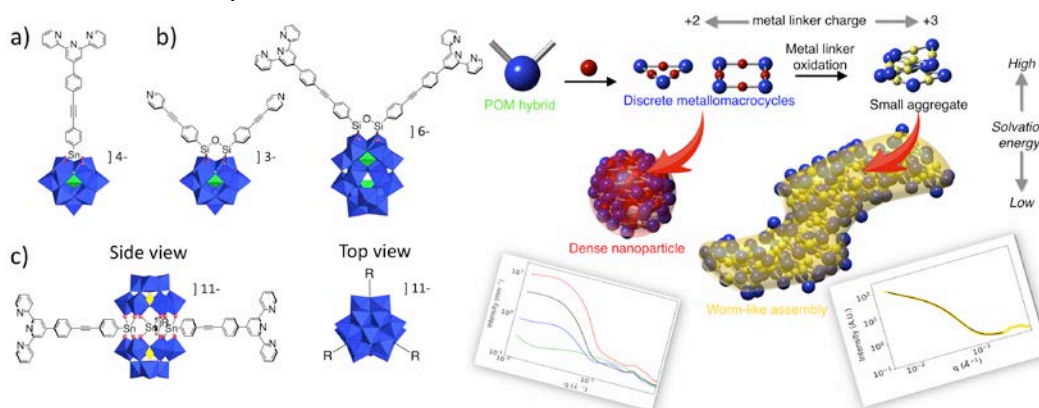


Figure 1. Left: Representation of different types of POM-based building blocks. a) monotopic; b) ditopic; c) tritopic hybrids. Right; top: Schematic representation of the formation of the nanosized aggregates by hierarchical metal driven self-assembly of a ditopic POM-based building block according to the solvent composition and the metal linker charge; down: SAXS patterns of the resulting POM-based systems.

REFERENCES

1. A. Proust, B. Matt, R. Villanneau, G. Guillemot, P. Gouzerh and G. Izzet, *Chem. Soc. Rev.* **41**, 7605-7622 (2012).
2. G. Izzet, F. Volatron and A. Proust, *Chem. Rec.* **17**, 250-266 (2017).
3. G. Izzet, A. Macdonell, C. Rinfra, M. Piot, S. Renaudineau, E. Derat, B. Abécassis, C. Afonso, and A. Proust, *Chem. Eur. J.* **21**, 19010-19015 (2015).
4. M. Piot, S. Hupin, H. Lavanant, C. Afonso, L. Bouteiller, A. Proust and G. Izzet, *Inorg. Chem.* **56**, 8490-8496, (2017).
5. G. Izzet, B. Abécassis, D. Brouri, M. Piot, B. Matt, S. A. Serapian, C. Bo and A. Proust, *J. Am. Chem. Soc.* **138**, 5093-5099 (2016).
6. M. Piot, B. Abécassis, D. Brouri, C. Troufflard, A. Proust, and G. Izzet, *Proc. Natl. Acad. Sci. U. S. A.* **36**, 8895-8900 (2018).

PARALLEL SESSIONS

PARALLEL SESSION

Ancient & New Materials

(Cultural heritage / Structure / Electronic Properties /
Surfaces & Interfaces)

SOLEIL AUDITORIUM

Thursday, January 16th

Chairpersons:

Emmanouil Frantzeskakis, Karine Provost, Noemi Carmona-Tejero,
Thomas Maroutian & Anne Charrier

- | | |
|-------|--|
| IT-01 | New 2D materials: Silicene and phosphorene
H. Oughaddou |
| IT-02 | Electronic properties of SiO/GeO ultra-thin films from ARPES and DFT calculations
Y. Fagot-Revurat |
| OC-01 | Direct observation of band gap renormalization in layered indium selenide
Z. Chen |
| OC-02 | Influence of a metal surface on spin-crossover molecules
A. Bellec |
| OC-03 | Temperature dependent magnetization profile in Gd/Co/Pt ultrathin films
V. Bansal |
| IT-03 | nanoARPES science and technique
P. Dudin |
| OC-04 | Characterization by Synchrotron Radiation at MARS beamline, of highly irradiated 316 austenitic stainless steel
A. Renault-Laborne |
| OC-05 | Anomalous diffraction study of germanite, a thermoelectric material
C. Prestipino |
| OC-06 | Probing photoinduced picosecond shear strain in ferroelectrics with time-resolved X-ray diffraction
P. Ruello |

PARALLEL SESSION

Ancient & New Materials

(Cultural heritage / Structure / Electronic Properties /
Surfaces & Interfaces)

SOLEIL AUDITORIUM

Friday, January 17th

Chairpersons:

Emmanouil Frantzeskakis, Karine Provost, Noemi Carmona-Tejero,
Thomas Maroutian & Anne Charrier

- | | |
|-------|---|
| IT-04 | Photomagnetism in Prussian Blue analogs : Benefits from a multi-beamlines investigation
A. Bordage |
| IT-05 | PUMA, a new beamline optimised for Cultural Heritage research
S. Schoeder |
| OC-07 | High pressure study on the metal-organic framework MIL-101 filled with metal nanoparticles
A. Celeste |
| OC-08 | Strong spin-lattice coupling in the frustrated pentagonal magnet $\text{Bi}_2\text{Fe}_4\text{O}_9$ revealed by infrared spectroscopy measurements at high pressure
M. Verseils |
| OC-09 | The use of wiggler white beam: New opportunities for high pressure science
J-P. Itié |

New 2D Materials: Silicene and Phosphorene

H. Oughaddou

*Institut des Sciences Moléculaires d'Orsay, ISMO-CNRS, Bât. 520, Université Paris-Sud,
F-91405 Orsay, France*

Département de Physique, Université de Cergy-Pontoise, F-95031 Cergy-Pontoise Cedex, France

ABSTRACT

The remarkable properties of graphene stem from its two-dimensional structure, with a linear dispersion of the electronic states at the corners of the Brillouin zone (BZ) forming a Dirac cone. Since then, other 2D materials have been emerged based on boron, silicon, germanium, phosphorus, tin, and metal di-chalcogenides. Indeed, even though graphene has a very high potential, its metallic character and the absence of a band gap are significant limitations for a large variety of devices.

Silicene is considered to be promising materials. Theoretical studies have shown that its structure shows similar electronic properties that graphene; such as a Dirac cone at the high symmetry point of the Brillouin zone, large charge carrier mobility and Hall effect.

Phosphorene has both an intrinsic tunable direct band gap and high carrier mobility values, which make it suitable for a large variety of optical and electronic devices. However, the synthesis of single-layer phosphorene is a major challenge because the principal process currently used to produce phosphorene is exfoliation.

In this talk, the silicene and phosphorene studies using low energy electron diffraction (LEED), high resolution angle-resolved photoemission spectroscopy (HR-ARPES), and scanning tunneling microscopy (STM) will be presented.

Electronic Properties of SiO/GeO Ultra-thin Films from ARPES and DFT Calculations

Y. Fagot-Revurat¹, T. Pierron¹, G. Kremer¹, M. Sicot¹, B. Kierren¹,
L. Moreau¹, D. Malterre¹, P. Pochet², J.C. Alvarez Quinceno³, S. Lisi⁴,
J. Coraux⁴, C. Gonzalez Pascual⁵, Y. Dappe⁶, P. Le Fèvre⁷,
F. Bertran⁷, J. Rault⁷

¹Institut Jean Lamour, UMR 7198, Université de Lorraine/CNRS, BP 70239, F-54506 Nancy, France

²CEA, INAC-SP2M, F-38054 Grenoble, France 2

³Laboratoire de Simulation Atomistique, Univ. Grenoble Alpes&CEA F-38054 Grenoble, France

⁴Univ. Grenoble Alpes, Institut NEEL, F-38000 Grenoble, France

⁵IFIMAC, Facultad de Ciencias, Universidad Autónoma de Madrid, E-28049 Madrid, Spain

⁶SPEC (CNRS URA2464), SPCSI, IRAMIS, CEA Saclay, 91191 Gif-Sur-Yvette, France

⁷SOLEIL, L'Orme des Merisiers, Saint-Aubin, BP 48, F-91192 Gif-sur Yvette, France

ABSTRACT

Ultrathin oxides films play an important role in many technological areas such as catalysis, spintronics or nanoelectronics. Silicon oxide has been shown to epitaxially grow on metals as crystalline lamellas [1-3]. On the Ru(0001) substrate, in its monolayer form, it is supposed to be chemisorbed whereas for the bilayer it is expected to form a 2D Van der Waals ultrathin oxide allowing intercalation or exfoliation [3,4]. More recently, the monolayer of germanium oxide has also been successfully grown on Ru(0001) showing a high quality structural ordering whereas as in the bilayer case it is shown to be amorphous [6]. However, in both cases, the electronic band structure was missing and this is the purpose of our recent work [7]. We present a comprehensive study of ultra-thin films of silicon and germanium oxides grown on Ru(0001) by combining LEED, STM, XPS, ARPES measurements and DFT calculations. In the monolayer case, the band structure is revealed: (i) a Dirac cone at the K point and a gap at the M point of the Silica/Germania Brillouin zone both signing the behavior of the in plane Si-O-Si (Ge-O-Ge) bonding, (ii) a signature of Si-O-Ru (Ge-O-Ru) bonding characterizing the metal/oxide coupling, (iii) a clear identification of Ru-O states coming from the precursive oxygen atoms, encapsulated in between the silica/germana layer and the Ru substrate. As a striking point, the band structure at Γ and its polarization dependence is analyzed in the light of DFT calculations. The agreement between experimental and DFT bands is acceptable for the germanium oxide monolayer but not in the case of silicon oxide evidencing the hardness to describe accurately electronic properties of such oxyde/metal interfaces. Moreover, the study of the transition from the monolayer to the bilayer evidenced an electronic decoupling of the SiO₂ layer supporting the assumption of Van Der Waals interactions.

REFERENCES

1. D. Löffler et al., Phys. Rev. Letter, 105, 146104 (2010)
2. B. Yang et al., Phys. Chem. Chem. Phys 14, 11344 (2012)
3. S. Mathur et al., Phys. Rev. B 92, 161410 (2015)
4. C. Büchner et al., ACS Nano 10(8), 7982 (2016)
5. C. Büchner and M. Heyde, Prog. Surf. Sci. 92, 341 (2017)
6. A. Lewandowski et al., Phys. Rev. B 97, 115406 (2018)
7. G. Kremer at al., ACS Nano 13, 4720–4730 (2019)

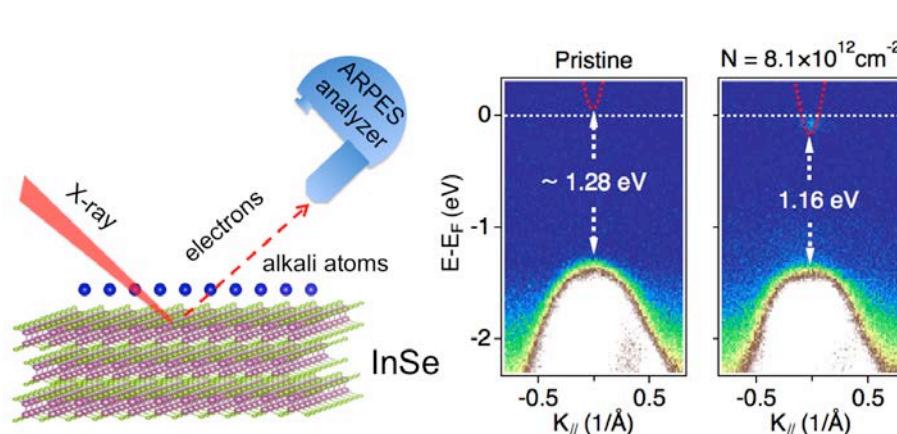
Direct Observation of Band Gap Renormalization in Layered Indium Selenide

Z. Chen

Laboratoire de Physique des Solides, CNRS, Université Paris Saclay, Orsay 91405, France

ABSTRACT

Manipulation of intrinsic electronic structures by electron or hole doping in a controlled manner in Van der Waals layered materials is the key to control their electrical and optical properties. Two dimensional (2D) indium selenide (InSe) semiconductor has attracted attention due to its direct band gap and ultrahigh mobility, as a promising material for optoelectronic devices [1-4]. In this work, we manipulate the electronic structure of InSe by in situ surface electron doping, and obtain a significant band gap renormalization of ~ 120 meV directly observed by high-resolution angle resolved photoemission spectroscopy (ARPES) [5]. This moderate doping level (carrier concentration of $8.1 \times 10^{12} \text{ cm}^{-2}$) can be achieved by electrical gating in field effect transistors (FETs), demonstrating the potential to design of broad spectral response devices.



REFERENCES

1. Z. Chen, J. Biscaras and A. Shukla, *Nanoscale*, 7, 5981-5986, (2015)
2. Z. Chen, J. Biscaras and A. Shukla, *2D materials*, 4, 2, (2017)
3. Z. Chen, Z. Zhang, J. Biscaras and A. Shukla, *Journal of Materials Chemistry C*, 6, 12407-12412, (2018).
4. Z. Chen, C. Giorgetti, J. Sjakste, R. Cabouat, V. Vénier, Z. Zhang, A. Taleb-Ibrahimi, E. Papalazarou, M. Marsi, A. Shukla, J. Peretti and L. Perfetti, *Physical Review B*, 97, 241201(R), (2018)
5. Z. Zhang, Z. Chen, M. Bouaziz, C. Giorgetti, H. Yi, J. Avila, B. Tian, A. Shukla, L. Perfetti, D. Fan, Y. Li and A. Bendounan, *ACS Nano*, DOI: 10.1021/acsnano.9b07144, (2019)

Influence of a Metal Surface on Spin-crossover Molecules

A. Bellec¹, C. Fourmental^{1,2}, C. Chacon¹, Y. Girard¹, J. Lagoute¹,
S. Rousset¹, V. Repain¹, S. Mondal³, R. Banerjee³, S. Narasimhan³,
C. Barreteau⁴, Y.J. Dappe⁴, A. Smogunov⁴, C. Enachescu⁵, M-L. Boillot⁶,
T. Mallah⁶, Y. Garreau^{1,2}, A. Coati²

1. *Laboratoire Matériaux et Phénomènes Quantiques, Université de Paris, CNRS, Paris, France*

2. *Synchrotron SOLEIL, Gif sur Yvette, France*

3. *Jawaharlal Nerhu Centre for Advanced Scientific Research, Bangalore, India*

4. *Service de Physique de l'Etat Condensé, CEA, CNRS, Saclay, France*

5. *Alexandru Ioan Cuza University, Iasi, Romania*

6. *Institut de Chimie Moléculaire et des Matériaux d'Orsay, Université Paris Saclay, CNRS, Orsay, France*

e-mail: amandine.bellec@univ-paris-diderot.fr

ABSTRACT

The use of spin-crossover molecules in electronic and spintronic devices is very appealing, considering the bistability of their spin state with various external parameters such as temperature, light, voltage, pressure, etc. Such devices display interfaces between conducting electrodes and a molecular layer that can be particularly important for the device properties. In this work, we have studied both experimentally and theoretically model interfaces between Au or Cu surfaces and a spin-crossover molecule, $(\text{Fe}^{\text{II}}((3,5\text{-}(\text{CH}_3)_2\text{Pz})_3\text{BH})_2)$, Pz for pyrazolyl, which is particularly stable upon deposition on metal surfaces. Scanning Tunneling Microscopy¹ and X-ray Absorption Spectroscopy² results show that a monolayer of this molecule on Au(111) or Cu(111) undergoes an incomplete transition with temperature, leading to a mixture (ordered or disordered) of low spin and high spin molecules at low temperature.

Recent Grazing Incidence X-ray Diffraction results allow us to demonstrate unambiguously that this mixture of spin states is due to a mechanical interaction between the molecular layer and the substrate³. Indeed, the mapping of the reciprocal space shows that a monolayer of molecule on Au(111) shows only a limited number of diffraction spots, in well-defined directions with respect to the ones of gold. Such an epitaxy is a consequence of a strong interaction with the surface that we have calculated by ab initio methods and also modelled in the framework of a mechano-elastic model. The main conclusion of those theoretical modelling is that this interaction is indeed responsible for the appearance of a mixed spin states phase at low temperature. The driving force for such a phenomenon will be explained and the generality of this finding will be discussed with regards to new results on Cu(111) and with the literature.

REFERENCES

1. K. Bairagi *et al.*, *Nature Communications*, 7, 12212 (2016).
2. K. Bairagi *et al.*, *The Journal of Physical Chemistry C*, 122, 727 (2018).
3. C. Fourmental *et al.*, *The Journal of Physical Chemistry Letters*, 10, 4103 (2019).

Temperature Dependent Magnetization Profile in Gd/Co/Pt Ultrathin Films

V. Bansal¹, J-M. Tonnerre^{1,2}, Eric Mossang¹, J. Vogel¹, S. Pizzini¹

¹Univ. Grenoble Alpes, CNRS, Grenoble INP, Institut NEEL, F-38000 Grenoble, France

²Synchrotron SOLEIL, Saint-Aubin, Boîte Postale 48, 91192 Gif-sur-Yvette Cedex, France

ABSTRACT

Domain wall (DW) dynamics in multilayer films with perpendicular magnetic anisotropy (PMA) is an important topic today, as these micromagnetic objects may be used as carriers of binary information in future ultrahigh density storage devices [1]. In thin films lacking structural inversion symmetry, i.e. thin films with different non-magnetic layers on either side, DWs can acquire Neel internal structure with a fixed chirality stabilised by the interfacial Dzyaloshinskii-Moriya interaction (DMI) [2]. This anti-symmetric exchange interaction takes place at the interface between a ferromagnetic layer and a layer exhibiting a strong spin-orbit coupling like Pt. The stability and the Néel DW dynamics, driven both by field and by spin polarised current [3,4], is influenced by the DMI, but also by the spontaneous magnetization of the layer (MS) and the effective magnetic anisotropy K_{eff} . For example, in the Pt/Co(1nm)/Gd/Pt multilayer, very large domain walls velocities (> 600 m/s) driven by a magnetic field have been observed at room temperature (RT) and attributed to a decrease of the Co magnetization due to antiferromagnetic coupling with small magnetic Gd ($T_c=293$ K) at the Gd/Co interface [3].

In this work, we investigated the magnetic properties of the system Al(7)/Gd(2)/Co(1)/Pt(4)/Ta(4)/SiO₂/Si multilayer (thickness given in nm). The motivations were to get more insights on the distribution of the out-of-plane magnetization across the Co and Gd layers. Indeed, there are no direct information about the extension of the coupling on both sides of the Co/Gd interface. Hence, it was motivating to probe how deep the interfacial magnetization of Gd extends into the Gd layer and how the magnetization of Co is modified due to the proximity effect. Moreover, it was interesting to study the evolution of the magnetization profile when the temperature is lowered crossing the compensation temperature due to the increase of the Gd magnetization [4]. For this purpose, we conducted soft X ray magnetic resonant reflectivity at the SEXTANTS beamline at synchrotron SOLEIL.

Angle dependent specular reflectivity were recorded for circular right (CR) and circular left (CL) polarized light at various incident photon energies close to the Co L_3 and Gd M_5 edges. Measurements were performed in remanence at several temperatures. The magnetization distribution is derived from the magnetic asymmetries $R=(I_{CR}-I_{CL})/(I_{CR}+I_{CL})$. At RT the whole Gd layer exhibits a graded magnetization decreasing from the Co/Gd interface up to the Gd/Al one. As we reduce T, the total magnetization increases as expected and the gradient distribution remains the main features. For the Co magnetization, a homogeneous profile at RT is found. Going to low T, the magnetization profile reveals a decrease of the magnetization at the Gd interface. This decrease could be due to the canting of some Co interfacial magnetic moments due to appearance of domains with opposite magnetization in the Gd layer.

REFERENCES

- [1] Parkin S., Hayashi M. and Thomas L., Science, 320 (2008) 190.
 [2] Thiaville A., Rohart S., Ju'e E., Cros V. and Fert A., EPL, 100 (2012) 57002.
 [3] T.H. Pham, J. Vogel, J. Sampaio, M. Va'natka, J.-C. Rojas-S'anchez, M. Bonfim, D. S. Chaves, F. Choueikani, P. Ohresser, E. Otero, A. Thiaville and S. Pizzini, Eur. Phys. Letters, 113 (2016) 67001
 [4]. R. Bläsing Tianping Ma, See-Hun Yang, Chirag Garg, Fasil Kidane Dejene, Alpha T N'Diaye, Gong Chen, Kai Liu & Stuart S.P. Parkin., Nature Communications | (2018) 9:49845

nanoARPES Science and Technique

J. Avila, S. Lorcy, P. Dudin

Synchrotron Soleil, L'Orme des Merisiers, Saint-Aubin, 91192 Gif-sur-Yvette, France

ABSTRACT

In spatially resolved ARPES (nanoARPES), standard angle resolved photoemission spectroscopy acquires spatial resolution using the light spot below 1 micron [1-3]. Using the scanning probe (microscopy) approach, we could study many systems that are challenging for traditional ARPES. We studied micro-cleaved samples in small flakes, domains of different nature in various multi-component systems, etc. In micro-device (FET, field effect transistor), the ARPES was measured as a function of gate voltage.

These and other examples of spatially resolved ARPES are described, aiming to help to disclose the potential of new technique for user community.

REFERENCES

- 1 J.Avila et al., Journal of Physics: Conference Series 425 (2013) 192023
- 2 P.Dudin et al., J. Synchrotron Rad. (2010) 17, 445–450
- 3 A.Bostwick et al, Synchrotron Radiation News 25, 5, (2012), 19-25

Characterization by Synchrotron Radiation at MARS Beamline, of Highly Irradiated 316 Austenitic Stainless Steel

D. Menut¹, A. Renault-Laborne², R. Guillou², J.L. Béchade³
J. Malaplate² and J. Vidal⁴

¹Synchrotron Soleil, F-91192 Gif-sur-Yvette, France

²CEA Saclay, Université Paris-Saclay, DEN, Service de Recherche en Métallurgie Appliquée,
F-91191 Gif-sur-Yvette, France

³CEA Saclay, Université Paris-Saclay, DEN, Service de Recherche en Métallurgie Physique,
F-91191 Gif-sur-Yvette, France

⁴EDF Lab Les Renardières, F-77818 Moret-sur-Loing, France

ABSTRACT

In the frame of extending the service life of pressurized water reactors, it is necessary to anticipate the evolution under irradiation of the microstructure of the internal structures located close to the cladding and made of austenitic stainless steel. This irradiation generates an evolution of their macroscopic properties, such as hardening, loss of strain hardening capacity, toughness reduction, eventually swelling. Mechanical and dimensional changes originate from microstructural evolution such as formation of Frank loops, dislocation lines, cavities, precipitates,...

In order to correlate the effects of these microstructural parameters to the various radiation-induced changes, studies by transmission electron microscopy were performed at CEA/DEN/DMN^{2,3,4}. Nonetheless, these studies are limited by the small number of available grain and especially by the difficulty to get access to quantitative data in the presence of a microstructure full of a great diversity of defects.

X-ray diffraction and scattering are the complementary and necessary techniques to push the limits because they help us to look beyond with more materials probed especially using synchrotron radiation, thanks to the high resolution and sensitivity of the X-ray beam and, as a result, to obtain a better statistic for low volume fraction of phases. These analyses are only available at the MARS beamline dedicated to experiments on highly radioactive matter.

Several experiments, in collaboration with EdF and MARS beamline scientist, were conducted on two types of 316 stainless steels irradiated in the PHENIX and BOR-60 experimental reactors by using three different techniques accessible

- (i) The diffraction analysis (XRD) of secondary phases in 2015 (what about the radiation induced precipitation?);
- (ii) The high resolution diffraction analysis (HR-XRD) of the austenitic matrix in 2017 (what about the solid solution evolution under irradiation?);
- (iii) The small-angle X-ray scattering (SAXS) in 2019 (what about the distribution of various nano objects under irradiation?).

In order to interpret the data about radiation-induced defects, cross analysis of samples in the as-received, thermally aged and irradiated states was performed.

The aim of this communication is to present the specific set-up used in each cases (from our knowledge, it is the very first time that such an approach using XRD, HR-XRD and SAXS for the same irradiated sample was done), the results obtained and the perspectives for these very challenging analyses performed thanks to MARS beamline.

REFERENCES

1. F.A. Garner, "Radiation Damage in Austenitic Steels," in *Comprehensive Nuclear Materials*, edited by R. J. M. Konings, Elsevier, 2012, pp. 33-95.
2. A. Renault-Laborne, J. Malaplate, C. Pokor and B. Tanguy, "Characterization of precipitates in 316 stainless steel neutron-irradiated at ~390°C by the combination of CDF-TEM, EF-TEM and HR-TEM", in *Effects of Radiation on Nuclear Materials: 26th Volume*, edited by M. Kirk et al., ASTM 1572, ASTM International, West Conshohocken, PA, 2014, pp. 74-97.
3. A. Renault-Laborne, P. Gavaille, J. Malaplate, C. Pokor and B. Tanguy, *Correlation of radiation-induced changes in microstructure/microchemistry, density and thermo-electric power of type 304L and 316 Stainless steels irradiated in the Phénix reactor*, *J. Nucl. Mater.* **460** 72-81 (2015).
4. A. Renault-Laborne, J. Garnier, J. Malaplate, P. Gavaille, F. Sefta and B. Tanguy, *Evolution of microstructure after irradiation creep in several austenitic steels irradiated up to 120 dpa at 320°C*, *J. Nucl. Mater.* **175** 209-226 (2016).

Anomalous Diffraction Study of Germanite, a Thermoelectric Material

C. Prestipino^a, L. Paradis Fortin^{a,b}, P.Lemoine^a, E.I Guilmeau^b,
B. Malaman^c, E. Elkaim^c

^a Institut des Sciences Chimiques de Rennes (UMR-CNRS 6226)

^b CRISMAT, Caen (UMR-CNRS 6508)

^c Institut Jean Lamour, Nancy (UMR-CNRS 7198)

^b Synchrotron SOLEIL, Gif sur Yvette, France

ABSTRACT

Waste heat harvesting is an essential component for the development of a sustainable energy production. Nowadays, thermoelectric generation systems are the most viable method. In particular, Cu-based sulfides with complex crystal structures have enticed much attention after the discovery of high ZT values in mineral derivative materials such as tetrahedrite $\text{Cu}_{12}\text{Sb}_4\text{S}_{13}$ ^{1,3} colusite $\text{Cu}_{26}\text{V}_2\text{Sn}_6\text{S}_{32}$ ^{4,5} and bornite Cu_5FeS_4 ^{6,7}.

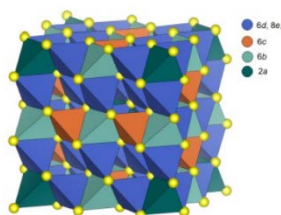


Fig.1: Crystal structure of germanite $\text{Cu}_{22}\text{Fe}_8\text{Ge}_4\text{S}_{32}$

Motivated by those pioneering studies, we are focusing on germanite $\text{Cu}_{22}\text{Fe}_8\text{Ge}_4\text{S}_{32}$, a mineral structurally similar to colusite, through the study of their crystal structure and TE properties. However, the complex cation distribution in germanite is still unknown, the general crystallographic structure ($P-43n$) (Fig 1), is a super-structure derived from cubic sphalerite ZnS ($F-43m$), in which the metallic atoms are distributed on 5 different crystallographic sites: 2a, 6c, 6d, 8e, and 12f. However, Fe, Cu and Ge show a poor contrast in XRD, but also their contrast on neutron diffraction is limited. Hence, it's difficult to discriminate between these species

from these classical diffraction techniques. X-ray resonant powder diffraction collected at the Fe, Ge, and Cu K edges collected at CRISTAL beamline with the support of laboratory X-ray single crystal diffraction and ⁵⁷Fe Mossbauer spectroscopy was able to suggest a reliable distribution of the cations.

In particular due to the elevated number of possible cation distribution (around 18000), the ensemble of resonant and non-resonant data has been analysed using a combinatorial approach consisting in the creation of an automatic script that generate the different models. and evaluate the figure of merit at each energy. An example of evaluation of a subset of configuration investigating the position of Fe using Fe K-edge data is shown in Fig 2.

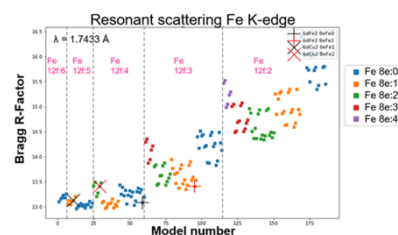


Fig. 2: R bragg factor as a function of cation distribution for diffraction collected at Fe K-edge

REFERENCES

1. Suekuni, K., Tsuruta, K., Ariga, T. and Koyano, M., Applied Physics Express 5 (2012): 051201..
2. Lu X, Morelli DT, Xia Y, Zhou F, Ozolins V, Chi H, Zhou X, Uher C. *Adv. Energy Mater.* 3 (2013) 342
3. Barbier T, Lemoine P, Gascoin S, Lebedev OI, Kaltzoglou A, Vaqueiro P, Powell AV, et al. *J. Alloys Compd.* 634 (2015) 253
4. Suekuni K, Kim FS, Takabatake T., *J. Appl. Phys.* 116 (2014) 063706
5. Bourgès C, Bouyrie Y, Supka AR, Al Rahal Al Orabi R, Lemoine P, Lebedev OI, Ohta M, et al. *J. Am. Chem. Soc.* 140 (2018) 2186
6. Guélou G, Powell AV, Vaqueiro P. *J. Mater. Chem. C* 3 (2015) 10624.
7. Pavan Kumar V, Paradis-Fortin L, Lemoine P, Caignaert V, Raveau B, Malaman B, Le Caër G, Cordier S, Guilmeau E., *Inorg. Chem.* 56 (2017) 13376

Probing Photoinduced Picosecond Shear Strain in Ferroelectrics with Time-resolved X-ray Diffraction

V. Juvé¹, R. Gu¹, S. Gable², T. Marroutian², G. Vaudel¹, S. Matzen²,
N. Chigarev³, S. Raetz³, V. E. Gusev³, M. Viret⁴, A. Jarnac⁵,
C. Laulhé⁵, B. Dkhil⁶, P. Ruello¹

¹ *Institut des Molécules et Matériaux du Mans, UMR 6283 CNRS, Le Mans Université, 72085 Le Mans, France*

² *Centre de Nanosciences et de Nanotechnologies, UMR CNRS 9000, Université Paris Saclay, 91120 Palaiseau, France*

³ *Laboratoire d'Acoustique de l'Université du Mans, UMR CNRS 6613, Le Mans Université, 72085 Le Mans, France*

⁴ *SPEC UMR CEA/CNRS, L'Orme les Merisiers, 91190 Saint-Aubin, France,*

⁵ *SOLEIL Synchrotron, L'orme des Merisiers, 91190 Saint-Aubin, France*

⁶ *Laboratoire Structures, Propriétés et Modélisation des Solides, CentraleSupélec, UMR CNRS 8580, Université Paris-Saclay, 91190 Gif-sur-Yvette, France)*

ABSTRACT

The time-resolved X-ray diffraction is currently used to study the light-induced symmetry change [1], the coherent phonon generation [2] or to measure the absolute light-induced strain in solids such as ferroic materials for example [3]. In the photoinduced strain mechanism, most of the reports deal with compressive strain field [1-3]. Usually, the photostriction measurements are only limited to the out-of-plane lattice parameter. However, in particular in ferroelectric materials where an intrinsic symmetry breaking is already present due to the ferroelectricity, the unit cell undergoes both a compressive and shear strain field when submitted to an ultrafast light pulse [4]. While already evidenced using time-resolved full optical methods [4], no direct quantitative measurements of this light-induced shear strain and its magnitude have been conducted so far. Here, we report, for the first time to our best knowledge, on the experimental determination by a time-resolved X-ray diffraction method of the photoinduced shear strain induced by the ultrafast photoexcitation of a (001)_{pc}-BiFeO₃ crystal. Time-resolved X-ray diffraction experiments performed at CRISTAL beamline (SOLEIL synchrotron) with the Low-alpha mode and grazing incidence configuration allowed to probe both in-plane and out-of-plane lattice parameters. We show that the photoinduced shear strain field leads to a different temporal behavior of Bragg peaks (h01)_{pc}/(-h01)_{pc} in BiFeO₃ while being symmetrically equivalent in the absence of laser excitation. Finally, we succeed in disentangling the absolute value of the photoinduced longitudinal and shear strains. The authors thank the French National Research Agency (ANR) for support with the project UP-DOWN (ANR-18-CE09-0026-04).

REFERENCES

1. Lindenberg et al, *Phys. Rev. Lett.* **84**, 111 (2000)
2. Larsson et al *Appl. Phys. A* **75**, 46-7478 (2002).
3. Matzen et al *Adv. Elect. Mater.* **5**, (2019).
4. Lejman et al *Nat. Comm.* **5**, 4301 (2014).

Photomagnetism in Prussian Blue Analogs: Benefits from a Multi-beamlines Investigation

A. Bordage, A. Bleuzen, G. Fornasieri

*Institut de Chimie Moléculaire et des Matériaux d'Orsay, CNRS, Université Paris-Saclay
Bât 420, rue du Doyen Georges Poitou, 91400 Orsay*

ABSTRACT

Prussian Blue Analogs (PBA; $Y_xA_4[B(CN)_6]_{(8+x)/3}$, Y = alkali cation and A,B = transition metals) are widely investigated coordination polymers because they present, for some stoichiometries, relevant photomagnetic properties for data storage devices. A reversible metal-metal charge transfer along the A—NC—B cyanide bridge can indeed be photoinduced, but it is observed at too low temperature to be used in real applications. So we work on understanding the structure-photomagnetic property relationship in photomagnetic PBAs to be able to control and adjust their working temperature. Our approach consists in a coupled laboratory-synchrotron approach, with experiments on several beamlines to fully take advantages of their experimental setups and X-ray energy ranges.

I will present 3 examples on how we choose and combine the beamlines to answer our questions on the photomagnetism of PBAs. The first two examples directly deal with the photomagnetic property in the $Rb_2Co_4[Fe(CN)_6]_{3.3}$ and $Na_2Co_4[Fe(CN)_6]_{3.3}$ PBAs, which both present a photoinduced charge transfer but with significant differences in the process. In the case of Rb_2CoFe , we performed experiments on SAMBA and DEIMOS to get a full picture of the crystallographic, electronic and magnetic structure of the PBA^{1,2}. We also investigated the effect of size reduction of the particles on the charge transfer by coupling measurements on SAMBA¹ and on BM20@ESRF. About Na_2CoFe , we combined experiments on (i) SAMBA to get information on the TM local environment, (ii) LUCIA to investigate the compound from the alkali cation side and (iii) AILES to look at the overall Co—NC—Fe cyanide bridge³. The third example is the development of a new methodology based on X-ray Magnetic Circular Dichroism (XMCD) at the K-edge of TM to quantify the small structural distortions of the cyanide bridge that seems to be the key-parameter in the photomagnetic property of PBA. First measurements for NiFe PBAs indeed showed significant variations of the Fe and Ni K-edges signals related to pressure-induced structural distortion⁴. Nevertheless, the XMCD signals at the TM K-edge are not well understood yet, and it is mandatory (i) to develop a methodology to quantify small structural distortions from these signals and (ii) to disentangle the physical effects originating TM K-edge XMCD. To develop the methodology, we are conducting a systematic XMCD investigation on non-photomagnetic model PBAs on the ODE beamline, coupled with (i) classical XAS on SAMBA and (ii) HERFD-XANES on FAME-UHD (French CRG beamline@ESRF) measurements.

REFERENCES

1. A. Bordage, R. Moulin, E. Fonda, G. Fornasieri, E. Rivière and A. Bleuzen, *J. Am. Chem. Soc.* **140**, 10332-10343 (2018).
2. S.F. Jafri, M-A. Arrio, A. Bordage, R. Moulin, A. Juhin, Ch. Cartier dit Moulin, E. Otero, Ph. Ohresser, A. Bleuzen and Ph. Sainctavit, *Inorg. Chem.* **57**, 7610-7619 (2018).
3. J. Lejeune, J-D. Cafun, G. Fornasieri, J-B. Brubach, G. Creff, P. Roy and A. Bleuzen, *Eur. J. Inorg. Chem.* **2012**, 3980-3983 (2012)
4. J-D. Cafun, J. Lejeune, J-P. Itié, F. Baudalet and A. Bleuzen, *J. Phys. Chem. C* **117**, 19645-19655 (2013)

PUMA, a New Beamline Optimised for Cultural Heritage Research

S. Schoeder

Synchrotron SOLEIL, Gif-sur-Yvette, France

High Pressure Study on the Metal-organic Framework MIL-101 Filled with Metal Nanoparticles

A. Celeste^{1;2}, A. Malouche², F. Borondics¹, B. Joseph³, A. Paolone⁴,
C. Zlotea² and F. Capitani¹

¹Synchrotron SOLEIL, L'orme des Merisiers, 91192 Saint-Aubin, Gif sur Yvette Cedex, France

²Institut de Chimie et des Materiaux Paris-Est, CNRS UMR 7182, UPEC,
2-8, rue Henri Dunant, 94320 Thiais, France

³Elettra-Sincrotrone Trieste - S.S. 14-km 163,5, 34149 Basovizza, Trieste, Italy

⁴CNR-ISC, U.O.S. Sapienza, Piazzale A. Moro 5, 00185 Roma, Italy

ABSTRACT

Metal–Organic Frameworks (MOFs) form a versatile class of porous crystalline hybrid materials where metal ions or metallic clusters are connected by organic ligands. Due to the variety of metals and organic linkers that can be used, the MOFs structure can be largely tuned. Huge pore sizes can be reached in mesoporous MOFs, where pore widths are between 2 and 50 nm. Thanks to the high surface area deriving from such an open structure, MOFs have received worldwide attention for a large range of applications, such as gas sorption, separation, H₂ storage, catalysis, drug delivery, etc [1]. It is important to stress that the sorption capacity of these systems directly depends from the surface-to-volume ratio, which can be modified through compression. The functionality of MOFs can be also modified through the insertion of guest nanoparticles (NPs) inside the porous structure [2]. The confined nanoparticles can affect the structure and the stability of the porous host through steric hindrance and chemical interactions.

Both of these effects can be altered by applying an external pressure [3].

Among all the MOFs, the mesoporous chromium(III) terephthalate MIL-101 has a rigid crystal structure with two types of quasi-spherical cages, with pore diameters close to 29 and 34 Å [4]. Recently, we have successfully embedded Pd NPs with an average diameter of 1 nm into MIL-101, for the first time with high metal loadings, up to 20 wt% (i.e. the Pd to sample mass) [5]. Here, we investigate the effect of high pressure on pristine MIL-101 and x-Pd@MIL-101 with 5 – 20 wt% by synchrotron based infrared (IR) spectroscopy and x-ray diffraction (XRD) in the 0-15 GPa pressure range. XRD measurements were carried out at the XPRESS beamline (ELETTRA) and at the Psiché beamline (SOLEIL) while the IR experiments were performed at the SMIS beamline of SOLEIL. To the best of our knowledge, this is the first time that a mesoporous MOF such as MIL-101 is studied at high pressure. We found that the behavior under pressure of the pristine MIL-101 depends on the nature of the pressure transmitting medium employed which strongly changes the pressure of amorphisation. The presence of Pd nanoparticles inside the MOF pores results in a decreased lattice compressibility but does not alter the overall structural stability in the investigated pressure range.

REFERENCES

1. G. Férey, *Chem. Soc. Rev.* **37**, 191–214 (2008).
2. C. Roesler, R. A. Fischer, *Crystengcomm* **17**, 199–217 (2015).
3. P. Ramaswamy et al., *J. Mater. Chem. A* **5**, 11047–11054 (2017).
4. A. Malouche et al., *J. Mater. Chem. A* **5**, 23043–23052 (2017)
5. G. Férey et al., *Science* **309**, 2040 (2005).

Strong Spin-lattice Coupling in the Frustrated Pentagonal Magnet $\text{Bi}_2\text{Fe}_4\text{O}_9$ Revealed by Infrared Spectroscopy Measurements at High Pressure

M. Verseils^{1,7}, K. Beauvois^{2,3}, A. Litvinchuk⁴, S. deBrion³, V. Simonet³,
E. Ressouche², V. Skumryev⁵, M. Gospodinov⁶, J-B Brubach¹
and P. Roy¹

¹ Ligne AILES-Synchrotron SOLEIL, 91190 Gif-sur-Yvette CEDEX, France

² INAC/MEM, CEA-Grenoble, 38042 Grenoble, France;

³ Institut Néel, CNRS & University, Grenoble Alpes, 38042 Grenoble, France

⁴ Texas Center for Superconductivity, University of Houston, Houston, TX 77204, États-Unis;

⁵ ICREA, Universitat Autònoma de Barcelona, 08193 Bellaterra, Barcelona, Spain;

⁶ Institute of Solid State Physics, Bulgarian Academy of Sciences, 1784 Sofia, Bulgaria;

⁷ Current address: Laboratoire Léon Brillouin, CEA-SACLAY, Gif-Sur-Yvette, France

ABSTRACT

$\text{Bi}_2\text{Fe}_4\text{O}_9$ is a common by-product in the synthesis of the multiferroic compound BiFeO_3 and has been claimed itself to display multiferroic properties [1]. The lattice formed by the two different sites of four iron Fe^{3+} magnetic atoms is quite remarkable as it materializes the first analogue of a magnetic pentagonal lattice [2]. For its peculiar lattice geometry it has attracted interest in the field of geometrical frustration. At room temperature and atmospheric pressure, the crystal structure is orthorhombic within the $Pbam$ space-group and the compounds undergoes a magnetic phase transition at 238 K from a paramagnetic state toward a non collinear magnetic state characterized by a propagation vector $\mathbf{k} = (1/2, 1/2, 1/2)$ and a large degree of frustration ($\theta_p/T_N \sim 7$) [2]. Recently it has been shown that $\text{Bi}_2\text{Fe}_4\text{O}_9$ undergoes a structural transition under pressure at 6-8 GPa toward the maximal non-isomorphic subgroup $Pbnm$, with $c' = 2c$. The driving force of the phase transition is the displacement of the O1 oxygen atom from fully constrained Wyckoff position $2b$ to a less-constrained $4c$ one [3]. Previous studies have reported the investigation of dynamical properties by mean of Raman spectroscopy both at ambient condition and at high pressure in a diamond anvil cell [3,4]. However, the vibrational modes involving O1 oxygen atoms are not Raman active but infrared active.

We will report the first polarized infrared spectroscopy measurement of $\text{Bi}_2\text{Fe}_4\text{O}_9$ performed in a DAC from 1 to 20 GPa in the far-infrared range [60-800 cm^{-1}] and at low temperature. The measurements have been performed at the AILES beamline of synchrotron SOLEIL exploiting the high-pressure/low-temperature set-up [5] coupled with the high brilliance of the radiation source in a wide spectral range on a very thin sample ($\sim 50 \mu\text{m}$) placed between diamonds with culets of 500 μm diameter. From our high quality spectra, we are able to identify the B_{3u} and B_{2u} modes within the (ab)-plane. Interestingly, while all phonon frequencies increase with pressure, the phonon mode around 200 cm^{-1} undergoes an anomalous softening with increasing pressure. In order to assign the phonon modes and reveal the microscopic mechanism of the high-pressure transition we also have performed DFT calculation at different pressures. The calculation mostly accounts for the measured phonon modes allowing the assignation of atomic motions. Our work reveals that one special lattice mode is strongly coupled with the spin degree of freedom. Understanding the mechanism at the origin of this strong coupling is interesting in the context of hybrid excitations in magnetic materials.

REFERENCES

1. A. K. Singh, *et al.*, "Substantial magnetoelectric coupling near room temperature in $\text{Bi}_2\text{Fe}_4\text{O}_9$." Applied Physics Letters **2008**, 92, 132910.
2. E. Ressouche, *et al.*, "Magnetic Frustration in an Iron-Based Cairo Pentagonal Lattice." Review Letters **2003**, 103.
3. A. Friedrich, *et al.*, "High-pressure phase transition of $\text{Bi}_2\text{Fe}_4\text{O}_9$." Journal of Physics: Condensed Matter **2012**, 24, 145401.
4. M. N. Iliev, *et al.*, "Phonon and magnon scattering of antiferromagnetic $\text{Bi}_2\text{Fe}_4\text{O}_9$." Physical Review B **2010**, 81.
5. A. Voute, *et al.*, "New high-pressure/low-temperature set-up available at the AILES beamline." Vibrational Spectroscopy **2016**, 86, 17.

The Use of Wiggler White Beam: New Opportunities for High Pressure Science

J.P. Itié, J.P. Deslandes, N. Guignot, A. King

Synchrotron SOLEIL, L'Orme des Merisiers, St Aubin BP48, 91192 Gif-sur-Yvette France

ABSTRACT

PSICHE (Pressure Structure and Imaging by Contrast at High Energy) is a SOLEIL beamline based on a under vacuum multipole wiggler. Using the white beam, both x-ray diffraction and full field tomography can be performed on the beamline, independently or simultaneously on the same sample. The beamline is mainly dedicated to experiments under extreme conditions of pressure combined or not with high temperature using large volume presses (Multi-anvils, Paris Edinburgh).

After a quick overview of the optic of the beamline, I will describe the different experimental set-up which can be implemented in the white beam hutch of the beamline, in particular the CAESAR set-up which is permanently installed on the beamline.

Then I will illustrate the possibilities of the beamline with few examples:

- Determination of the density of amorphous samples and liquids under pressure using pdf and 3D imaging
- Determination of viscosity of liquids at high pressure and high temperature (2D imaging)
- Observation of decomposition of liquids close to magmatic conditions
- Observation of the iron phase transformations by combined 3D tomography and XRD in PE cells

Finally I will show some recent developments which will improve the quality of the data and the rapidity of the acquisitions allowing some kinetic measurements.

PARALLEL SESSION

Dynamic, Reactivity & Chemical analysis (Diluted Matter & Chemistry)

CEA BLOCH AUDITORIUM

Thursday, January 16th

Chairpersons:

Asma Tougerti, Nicolas Delsuc, Pierre Asselin and Renaud Guillemin

- IT-06 The VUV photoionization of small radicals on the DESIRS beamline: Spectroscopy and cross section determination
S. Boyé-Péronne
- IT-07 Photoelectron spectroscopy of liquid jets at GALAXIES and PLEIADES beamlines
C. Nicolas
- OC-10 NH₃ ultrafast dissociation probed by Auger electron-ion coincidences
F. Hosseini
- OC-11 Surface chemistry of colloidal gold nanoparticles generated by laser ablation
A. Lévy
- OC-12 Energy, environment for a sustainable development. contribution of a 4th generation Synchrotron
V. Briois
- IT-08 Double layer at an electrified interface, beyond the textbook: Water matters
M. Havenith
- IT-09 Exploiting the THz Synchrotron Radiation at its highest resolution and in a broadband fashion by heterodyne techniques
M-A. Martin-Drumel
- OC-13 New line positions analysis of the ν_3 bands of ³⁵CINO₂ and ³⁷CINO₂ at 370 cm⁻¹
A. Anantharajah

PARALLEL SESSION

Dynamic, Reactivity & Chemical analysis (Diluted Matter & Chemistry)

CEA BLOCH AUDITORIUM

Friday, January 17th

Chairpersons:

Asma Tougeri, Nicolas Delsuc, Pierre Asselin and Renaud Guillemin

- IT-10 Lanthanide oxysulfide nanoplates: Growth mechanism and reactivity from ex situ and in situ spectroscopies
S. Carenco
- IT-11 Infrared and terahertz spectroscopy under fine-controlled conditions
P. Roy
- OC-14 Aerosol synthesis of thermally stable porous noble metals and alloys by using bi-functional templates: A mechanistic study
M. Giraud
- OC-15 Monitoring catalysts at work: The advantages of combined operando EPR/XAS/ATR-IR/UV-vis spectroscopy with multivariate analysis
J. Rabeah
- OC-16 Ascorbic acid directs the anisotropic growth of silver-on-gold nanoparticles
D. Constantin

The VUV Photoionization of Small Radicals on the DESIRS Beamline: Spectroscopy and Cross Section Determination

S. Boyé-Péronne¹, B. Gans¹, O.J. Harper¹, G.A. Garcia²,
H.R. Hrodmarsson², L. Nahon² and J.-C. Loison³

¹*Institut des Sciences Moléculaires d'Orsay, Université Paris-Saclay, CNRS*

²*Synchrotron SOLEIL, L'Orme des Merisiers, Saint Aubin*

³*Institut des Sciences Moléculaires, Université de Bordeaux, CNRS*

ABSTRACT

Gas-phase radical species, either neutral or ionized, are found in a wide variety of environments including flames, plasmas, planetary atmospheres and astrophysical media.

Although these species are largely involved in the photochemical networks of these environments, the studies of their photophysics are still scarce. Their experimental spectroscopic studies, in particular in the Vacuum Ultra-Violet (VUV), are very challenging tasks. Indeed, these unstable species require an *in situ* production with a controlled yield and very sensitive experimental setups. In this context, an original experimental approach making use of a flow-tube reactor coupled with the DELICIOUS III double electron-ion imaging spectrometer of the DESIRS beamline has been recently developed [1]. This radical source is based on the H-atom abstraction of a hydrogen-bearing molecule by reaction with fluorine atoms. The experimental conditions can be adjusted to favor the production of one or a number of radicals.

Over the past 5 years, numerous VUV photoionization studies of radicals have been performed, allowing the retrieval of new spectroscopic data on the vibronic structure of their cations [1-9]. In addition, when the experimental conditions allow a selective single-radical production, the photoionization cross section of these transient species can be determined with respect to the one of their precursors [10-13].

In this talk, I will illustrate the two outcomes of this approach by showing some selected results obtained recently on the CN [5], C₂ [8], OH [9], and NH₂ [10] radicals.

REFERENCES

- [1] G.A. Garcia et al., *J. Chem. Phys.* **142**, 164201 (2015).
- [2] G.A. Garcia et al., *J. Electron Spectrosc. Relat. Phenom.* **203**, 25 (2015).
- [3] B. Gans et al., *J. Chem. Phys.* **144**, 204307 (2016).
- [4] B. Gans et al., *J. Chem. Phys.* **146**, 011101 (2017).
- [5] G.A. Garcia et al., *J. Chem. Phys.* **147**, 013908 (2017).
- [6] B. Gans et al., *J. Phys. Chem. Lett.* **8**, 4038 (2017).
- [7] L.H. Coudert et al., *J. Chem. Phys.* **149**, 224304 (2018).
- [8] G.A. Garcia et al., *Phys. Chem. Chem. Phys.* **20**, 8707 (2018).
- [9] O.J. Harper et al., *J. Chem. Phys.* **submitted** (2019).
- [10] O.J. Harper et al., *J. Chem. Phys.* **150**, 141103 (2019).
- [11] O.J. Harper et al., *J. Chem. Phys.* **submitted** (2020).
- [12] H.R. Hrodmarsson et al., *J. Phys. Chem. A* **123**, 1521 (2019).
- [13] H.R. Hrodmarsson et al., *Phys. Chem. Chem. Phys.* **Sous presse** (2019).

Photoelectron Spectroscopy of Liquid Jets at GALAXIES and PLEIADES Beamlines

C. Nicolas and D. Céolin

*Synchrotron SOLEIL, L'Orme des Merisiers, Saint-Aubin, BP 48,
F-91192 Gif-sur-Yvette Cedex, France*

ABSTRACT

We will present the equipment we developed at SOLEIL aiming at studying various types of solutions by means of photoelectron spectroscopy. Two complementary under-vacuum microjet setups have been coupled with the electron spectrometers located at the PLEIADES and GALAXIES beamlines, allowing users to probe the electronic structure of liquids using photons having energies going from the soft (10 eV to 1000 eV) to the hard (2.3 keV to 12keV) X-ray regions, respectively. In addition of being able to selectively ionize a large number of specific core-levels and thus to focus the investigation on specific elements and their surroundings, a given solution can be probed either in its bulk or at its vacuum-liquid interface due to the possibility to generate electrons on a broad range of kinetic energies.

We will describe the two original setups by giving key technical details and what is possible or not to measure for now in our facility, as well as our last developments and improvements. The important points to be presented in a project before sending a proposal to the program review committee will also be discussed.

NH₃ Ultrafast Dissociation Probed by Auger Electron-ion Coincidences

F. Hosseini,^{1,2} O. Travnikova,¹ E. Kukk,³ C. Nicolas,² J. Bozek²
and M. Simon¹

¹Sorbonne Université, CNRS, Laboratoire de Chimie Physique-Matière et Rayonnement, Paris France

²Synchrotron SOLEIL, l'Orme des Merisiers, BP 48, F-91192 Gif-sur-Yvette Cedex, France

³Department of Physics and Astronomy, University of Turku, FI-20014 Turku, Finland

ABSTRACT

Ultrafast dissociation of core-excited NH₃ molecule is revisited by Auger electron-ion coincidences. The results give new insights to fragmentation mechanism.

Resonant excitation of a core electron to an anti-bonding molecular orbital may lead to ultrafast nuclear dynamics and even dissociation, which occurs on the same timescale and, therefore, competes with radiative or non-radiative Auger decay [1].

In this work we have revisited ultrafast dissociation (UFD) phenomenon, which occurs in core-excited NH₃ molecule, using energy-selected resonant Auger electron-ion coincidence techniques. ES-AEPICO is a unique complementary tool to high-resolution photoelectron spectroscopy as it allows disentangling fragmentation mechanisms [2]. This is because the observed resonant Auger final states can be directly correlated to the fragment ions and their behavior can be tracked as a function of the photon energy.

Narrow bandwidth photon energies across the N1s→4a₁ resonance were used to produce dissociative N1s core-excited states of NH₃. ES-AEPICO spectra were recorded at several energies across the resonance using EPICEA coincidence setup, permanently installed at PLEIADES beamline of the SOLEIL synchrotron. Detuning the photon energy allows varying the so-called effective scattering time [3] and hence influence the relative yield of the fragmentation occurring within the lifetime of the N1s core hole (~ 6 fs).

The 2D resonant Auger electron-photoion coincidence maps at different photon energies allow correlating Auger final states to different fragmentation patterns and confirming that the Auger states (381-383 eV) are related to NH₂⁺ fragments, as first observed in a previous study [3] by single-channel resonant Auger spectroscopy. Moreover, other final states of the fragments, which are hidden in resonant Auger measurements, could be identified by the coincidence measurements.

We also observe increased efficiency of UFD for positive energy detunings, which is in line with the previously calculated potential energy surface of the N1s⁻¹4a₁¹ core-excited state of NH₃ [4]. The experiments were also performed at MAXIV synchrotron in Sweden at FinEst beamline in March 2019, revealing the so-called Auger Doppler effect [5], which was previously observed only for atomic fragments.

REFERENCES

- [1] Morin P and Nenner I 1986 *PRL* **56**, 1913
- [2] Travnikova O *et al* 2013 *JPCL* **4**, 2361
- [3] Hjelte I *et al* 2003 *CPL* **370**, 781
- [4] Walsh N *et al* 2015 *PCCP* **17**, 18944
- [5] Björneholm O *et al* 2000 *PRL* **84**, 2826

Surface Chemistry of Colloidal Gold Nanoparticles Generated by Laser Ablation

A. Lévy^a, M. De Anda Villa^a, J. Gaudin^b, D. Amans^c, V. Blanchet^b,
F. Boudjada^c, J. D. Bozek^d, R. E. Grisenti^{e,f}, E. Lamour^a, G. Laurens^c,
S. Macé^a, A. R. Milosavljević^d, C. Nicolas^d, I. Papagiannouli^b,
M. Patanen^g, C. Prigent^a, E. Robert^d, S. Steydli^a, M. Trassinelli^a
and D. Vernhet^a

^a INSP, Sorbonne Université, CNRS UMR 7588, Campus P. et M. Curie, 75005 Paris, France

^b CNRS, CEA, CELIA, University of Bordeaux, UMR5107, F-33405 Talence, France

^c Université Claude Bernard Lyon 1, UMR5306 CNRS, ILM, F-69622 Villeurbanne, France

^d Synchrotron SOLEIL, Saint-Aubin, BP 48, F-91192 Gif-sur-Yvette Cedex, France

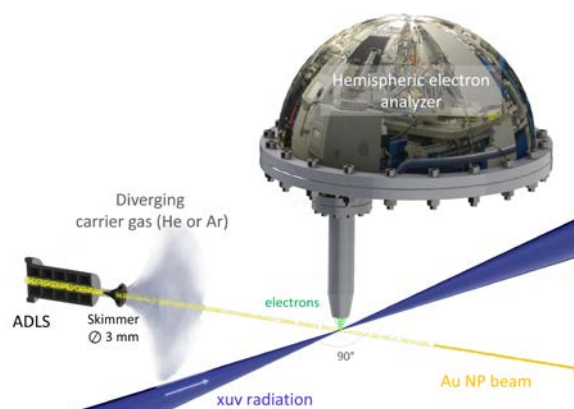
^e GSI Helmholtzzentrum für Schwerionenforschung, Planckstrasse 1, 64291 Darmstadt, Germany

^f Institut für Kernphysik, J.W. Goethe-Universität, Max-von-Laue-strasse 1, 60438 Frankfurt, Germany

^g NANOMO Research Unit, Faculty of Science, Oulu University, P.O.Box3000, FI-90014 Oulu, Finland

ABSTRACT

A promising nanoparticle (NPs) synthesis technique is based on laser irradiation of a solid target in a liquid environment. The Pulsed Laser Ablation in Liquids (PLAL) method results in the formation of ligand-free NPs which can be produced in organic or non-organic solvents. These systems are well-suited for the development of different technological applications¹ usually requiring subsequent surface functionalization. In addition, their surface chemical composition is expected to take part in the colloidal stability of the PLAL product. The resulting surface charge could be responsible of the electrostatic repulsion impeding their aggregation. However, no consensus²⁻⁶ has been drawn so far on these questions and a precise knowledge of their surface properties and composition is mandatory. An experimental investigation of the surface chemistry occurring at the PLAL NP surface will be presented based on experiments conducted at SOLEIL synchrotron facility on the PLEIADES beamline. X-ray photoelectron spectroscopy measurements performed on free-standing^{7,8} gold NPs will be reported addressing the question of (i) their surface oxidation state⁹ and (ii) the chemical composition of their first's surface atomic layers. Signatures of halide-ions and possible gold oxidized atoms on the NPs surface have been evidenced, demonstrating that this technique provides a promising new way to study bare gold surfaces and a complementary insight to their colloidal stability.



REFERENCES

1. M.-C. Daniel and D. Astruc, *Chem. Rev.* **104**, 293 (2004).
2. V. Merk, C. Rehbock, F. Becker, U. Hagemann, H. Nienhaus and S. Barcikowski, *Langmuir* **30**, 4213 (2014).
3. H. Muto, K. Yamada, K. Miyajima and F. Maune, *J. Phys. Chem. C* **111**, 17221 (2007).
4. Y. Y. Fong, J. R. Gascooke, B. R. Visser, H. H. Harris, B. C. C. Cowie, L. Thomsen, G. F. Metha and M. A. Buntine, *Langmuir* **29**, 12452 (2013).
5. J.-P. Sylvestre, S. Poulin, A. V. Kabashin, E. Sacher, M. Meunier and J. H. T. Luong, *J. Phys. Chem. B* **108**, 16864 (2004).
6. G. Palazzo, G. Valenza, M. Dell'Aglio and A. De Giacomo, *J. Colloid Interface Sci.* **489**, 47 (2017).
7. P. Liu, P. J. Ziemann, D. B. Kittelson and P. H. McMurry, *Aerosol Sci. Technol.* **22**, 293 (1995).
8. A. Lindblad, J. Söderström, C. Nicolas, E. Robert and C. Miron, *Rev. Sci. Instrum.* **84**, 113105 (2013).
9. M. De Anda Villa et al., *Langmuir* **35**, 11859 (2019).

Energy, Environment for a Sustainable Development.

Contribution of a 4th Generation Synchrotron

V. Briois¹, D. Vantelon²

¹UR1-CNRS, Synchrotron SOLEIL, L'Orme des Merisiers, BP34, 91192 Gif-sur-Yvette

²Synchrotron SOLEIL, L'Orme des Merisiers, BP34, 91192 Gif-sur-Yvette

ABSTRACT

In the frame of the scientific evolution from the current 3rd generation SOLEIL source to a 4th generation one, a series of conferences were held between January 2018 and July 2019 to discuss the opportunities of such a source in the research fields of **Energy and Environmental sciences for a Sustainable Development** [1]. Scientists among the main renowned in France had the opportunity to give their perspectives on the current technical limitations for their research domains. They thus allowed us to identify relevant techniques for which an increase in brightness and coherency as offered by a 4th generation source would be a powerful lever to overcome some of the identified bottle-necks.

Through a few representative examples of issues that could be solved with a 4th generation machine, the purpose of our presentations is to return and discuss with scientists from these communities, the necessary and expected key gains that we identified during these consultations.

REFERENCES

[1] Round Table « **Energy and Environment for a Sustainable Development** ».

Conveners: V. Briois and D. Vantelon,

Themes coordinators: F. Berenguer, C. La Fontaine, S. Belin, B. Lassalle, C. Rivard, G. Landrot.

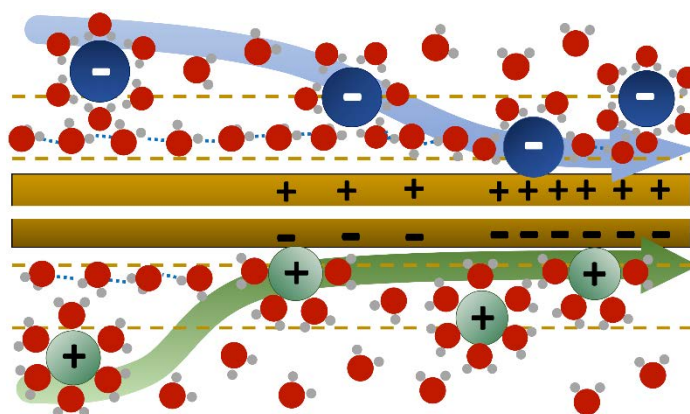
Double Layer at an Electrified Interface, beyond the Textbook: Water Matters

M. Havenith

Ruhr-Universität Bochum, Germany

ABSTRACT

The double layer at the solid/electrolyte interface is one key concept in electrochemistry, which textbooks describe through electrostatic and macroscopic observables. Here we present a combined experimental/theoretical study, which provides a molecular picture of the double layer formation in operando processes, revealing the stripping off of the NaCl electrolyte hydration shells at a Au positively/negatively charged electrode. The decisive role of water in mediating NaCl interactions at the electrode emerges. All these phenomena are directly measured by in operando THz spectroscopy, MD simulations reveal the underlying microscopic mechanisms.



Exploiting the THz Synchrotron Radiation at its Highest Resolution and in a Broadband Fashion by Heterodyne Techniques

M.-A. Martin-Drumel¹, O. Pirali^{1,2}, S. Eliet³, Z. S. Buchanan¹, J. Turut², P. Roy², F. Hindle⁴, J.-F. Lampin³, and G. Mouret⁴

¹ *Institut des Sciences Moléculaires d'Orsay (ISMO), CNRS, Univ. Paris-Sud, Université Paris-Saclay, F-91405 Orsay, France;*

² *SOLEIL synchrotron, AILES beamline, l'Orme des Merisiers, Saint-Aubin, F-91190 Gif-sur-Yvette, France;*

³ *Institut d'Electronique Microélectronique et Nanotechnologie (IEMN), Lille University, CNRS, Avenue Poincaré F-59652 Villeneuve d'Ascq Cedex, France;*

⁴ *Laboratoire de Physico-Chimie de l'Atmosphère (LPCA), Université du Littoral Côte d'Opale, Avenue Schumann F-59140 Dunkerque, France*

ABSTRACT

Despite significant efforts to improve the coverage of the so-called “terahertz (THz) gap”, technological breakthroughs are yet to impact the THz domain (arbitrarily defined as 1–10 THz). Indeed, molecular spectroscopy in this region usually entails a compromise between wide frequency coverage and high resolution. Within the frame of the HEROES¹ project, we are developing new spectrometers exploiting the bright THz synchrotron radiation extracted by the AILES beamline at SOLEIL. Our spectrometers, based on the heterodyne technique, aim at allowing both broadband and high resolution investigations of molecular spectra in the THz range.

The first instrument, a broadband THz heterodyne spectrometer, associates the broadband synchrotron radiation (multi-bunch operation mode) and a THz molecular laser local oscillator². Ultimately, this spectrometer will enable to cover the 1–4 THz region in 5 GHz windows at Doppler resolution.

The second spectrometer is a dual comb spectrometer exploiting the heterodyne mixing between coherent synchrotron radiation (CSR or low-alpha) and an optical frequency comb. The resulting spectrum is extremely broadband, covering the entire THz range (in a single shot) at a resolution limited by the repetition rate of CSR (846 kHz).

Proof-of-principle of the exploitation of both spectrometers for spectroscopy will be provided and discussed.

REFERENCES

1. ANR-16-CE30-0020-0
2. J.-F. Lampin, O. Pirali, Z. S. Buchanan, S. Eliet, M.-A. Martin-Drumel, J. Turut, P. Roy, F. Hindle and G. Mouret, *Optics Letters* **44**, 4985 (2019)

New Line Positions Analysis of the ν_3 Bands of $^{35}\text{ClNO}_2$ and $^{37}\text{ClNO}_2$ at 370 cm^{-1}

A. Anantharajah^a, F. Kwabia Tchana^a, L. Manceron^{b,c},
J.-M. Flaud^a, and J. Orphal^d

^aLaboratoire Interuniversitaire des Systèmes Atmosphériques (LISA), UMR CNRS 7583, Université de Paris et Université Paris-Est Créteil, Institut Pierre-Simon Laplace, 61 avenue du Général de Gaulle, 94010 Créteil Cedex, France.

^bLigne AILES, Synchrotron SOLEIL, L'Orme des Merisiers, St-Aubin BP48, 91192 Gif-sur-Yvette Cedex, France.

^cSorbonne Université, CNRS, MONARIS, UMR 8233, 4 place Jussieu, 75005 Paris, France.

^dKarlsruhe Institute of Technology (KIT), 76344 Eggenstein-Leopoldshafen, Germany.

ABSTRACT

Nitryl chloride (ClNO_2) is a molecule of great interest for atmospheric chemistry since it is produced by heterogeneous reactions, in the marine troposphere, between NaCl sea-salt aerosols and gaseous N_2O_5 [1,2], and on polar stratospheric clouds, between N_2O_5 and solid HCl [3,4].

Many high-resolution spectroscopic studies in the microwave and mid-infrared regions are available [5 and therein]. However, ClNO_2 presents two fundamentals in the far-infrared region below 600 cm^{-1} , with the lowest corresponding to the Cl-N stretching mode, ν_3 around 370 cm^{-1} . One previous study dealt with the $\nu_3 = 1$ state of ClNO_2 , at a resolution of 0.002 cm^{-1} [6].

Using high resolution (0.00102 cm^{-1}) Fourier transform spectrum recorded at SOLEIL with much improved experimental conditions: (i) the use of synchrotron radiation which resulted in a better signal-to-noise ratio; (ii) the spectrum has been recorded with a resolution twice better than in the previous work [6]; (iii) the spectrum was recorded at low temperature (221 K) with an optical path length of 8.16 m, allowing low pressure (0.025 hPa) compared to the pressure of 3.06 mbar used in the previous work [6], a new investigation of the ν_3 absorption bands of $^{35}\text{ClNO}_2$ and $^{37}\text{ClNO}_2$, located around 370 cm^{-1} was performed. Starting from the results of the previous investigation of the same band [6], the present assigned ν_3 lines involve energy levels of the $\nu_3 = 1$ vibrational state with rotational quantum numbers going up to $K_a = 44$ and $J = 83$, for $^{35}\text{ClNO}_2$ and $^{37}\text{ClNO}_2$. For $^{37}\text{ClNO}_2$, more than 2900 transitions (compared to 968 in the previous work [6]) have been assigned and fitted with an RMS of 0.0002 cm^{-1} , allowing to determine with high accuracy the band center, rotational and centrifugal distortion constants for the $\nu_3 = 1$ vibrational state of $^{37}\text{ClNO}_2$. We have also improved the analysis of the most abundant isotopomer, $^{35}\text{ClNO}_2$.

The spectrum analysis of the second low energy vibration, ν_6 around 408 cm^{-1} is ongoing and will determine the molecular parameters of this spectral region. In turn, this will enable an analysis of the hot bands involving these low energy levels in the mid-infrared region.

REFERENCES

1. B. J. Finlayson-Pitts, M. J. Ezell, and J. N. Pitts Jr, *Nature* **337**, 241-244 (1989).
2. W. Behnke, V. Scheer, and C. Zetzsch, *J. Aerosol Sci.* **24**, 115-116 (1993).
3. M. A. Tolbert, M. J. Rossi, and D. M. Golden, *Science* **240**, 1018-1021 (1988).
4. M. T. Leu, *Geophys. Res. Lett.* **15**, 851-854 (1988).
5. J.-M. Flaud, A. Anantharajah, F. Kwabia Tchana, L. Manceron, J. Orphal, G. Wagner, and M. Birk, *J. Quant. Spectrosc. Radiat. Transf.* **224**, 217-221 (2019).
6. J. Orphal, M. Morillon-Chapey, S. Klee, G. C. Mellau, and M. Winnewisser, *J. Mol. Spectrosc.* **109**, 101-106 (1998).

Lanthanide Oxysulfide Nanoplates: Growth Mechanism and Reactivity from *ex situ* and *in situ* Spectroscopies

S. Carencó

Sorbonne Université, CNRS, Collège de France, LCMCP, 75252 Paris Cedex 05.

ABSTRACT

Metal Oxysulfides ($M_xO_yS_z$), in which the sulfur atoms are reduced (eg. S^{II}), lie at the cross-roads of oxides (M_xO_y) and sulfides (M_xS_y). The quest for efficient nanophosphors, with applications in lightening technologies and nanomedicine, raised the interest for oxysulfide nanoparticles in the 2000's. While bulk oxysulfides are usually prepared from the sulfidation of oxides at high temperature, Ln_2O_2S nanocrystals (Ln = lanthanide, Fig. A) are formed in organic media below 350 °C.^[1]

We produced metal oxysulfide nanoparticles by colloidal synthesis. We obtained unprecedented Ce_2O_2S nanoparticles as well as $(Gd,Ce)_2O_2S$ nanoparticles with Gd:Ce ratio from 0 to 100 %. The interest of cerium lies in its unique electronic properties in the lanthanide series. Ce_2O_2S is indeed the only lanthanide oxysulfide with a low bandgap ($E_g < 2$ eV), while the others are wide-gap semiconductors ($E_g > 3$ eV). Moreover, we evidenced that the 2-nm thick nanoplates showed a direct bandgap, instead of the expected indirect bandgap.^[2]

Using Near-ambient-pressure XPS and XANES at S K-edge, we demonstrated that the nanoparticles were stable in air up to 40 % of cerium.^[3] We then investigated the local structure of the nanoparticles, in relation with the presence of sodium in the reaction medium. At the time, sodium was considered a dopant in the structure.^[1] Thermogravimetric analysis coupled to mass spectrometry was used to identify the surface ligands on the nanoparticles,^[4] while SAXS-WAXS measurements evidenced the formation of a lamellar mesophase during the synthesis. We confirmed by pair-distribution function analysis that Na was not a dopant in the nanoparticles. Lastly, we used μ -XRF and μ -XAS to analyze the interaction of the nanoparticles with macrophage cells, in the context of safer-by-design nanoparticles development.

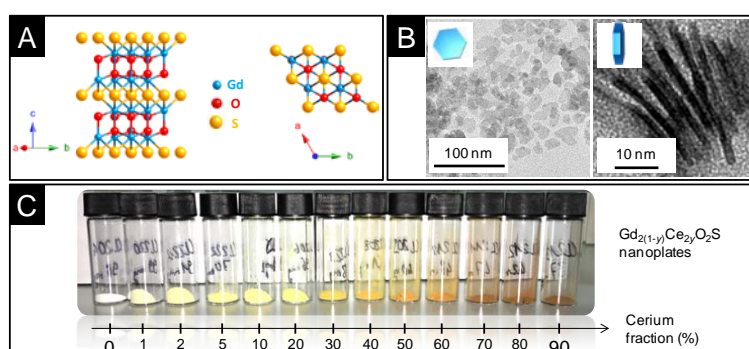


Figure: (A) Gd_2O_2S structure. (B) Hexagonal nanoplates of $Gd_{1.25}Ce_{0.75}O_2S$. (C) Evolution of the powder colors along the series of $(Gd,Ce)_2O_2S$ nanoparticles.

REFERENCES

- [1] Y. Ding, J. Gu, J. Ke, Y.-W. W. Zhang, C.-H. H. Yan, *Angew. Chem. Int. Ed. Engl.* **2011**, *50*, 12330.
- [2] C. Larquet, A.-M. Nguyen, E. Glais, L. Paulatto, C. Sassoie, M. Selmane, P. Lecante, C. Maheu, C. Geantet, L. Cardenas, C. Chanéac, A. Gauzzi, C. Sanchez, S. Carencó, *Chem. Mater.* **2019**, *31*, 5014.
- [3] C. Larquet, A.-M. Nguyen, M. Ávila-Gutiérrez, L. Tinat, B. Lassalle-Kaiser, J.-J. Gallet, F. Bournel, A. Gauzzi, C. Sanchez, S. Carencó, *Inorg. Chem.* **2017**, *56*, 14227.
- [4] C. Larquet, D. Hourlier, A.-M. Nguyen, A. Torres-Pardo, A. Gauzzi, C. Sanchez, S. Carencó, *ChemNanoMat* **2019**, *5*, 539.

Infrared and Terahertz Spectroscopy under Fine-controlled Conditions

B. Langerome^a, T. Souske^a, K. Rader^a, M. Verseils^a, L. Tongtong^a,
S. de Brion^b, L. Manceron^{a,c}, J-B. Brubach^a and P. Roy^a

^a AILES Beamline, Synchrotron SOLEIL, Gif-sur-Yvette Cedex, 91190, France

^b Institut Néel, Université Grenoble Alpes, 38000, France

^c MONARIS, UMR 8233, CNRS - Sorbonne Université, 4 place Jussieu, F-75005 Paris, France,

ABSTRACT

The AILES beamline on the SOLEIL Synchrotron Light Source is an integrated facility for infrared/THz spectroscopy allowing to measure transmission and reflectivity from ambient to GPa pressures or from room temperature down to sub-Kelvin temperatures. Materials that are investigated include both inorganic and organic systems as well as isolated molecules, where temperature and/or pressure effects on rotational, vibrational, electronic and magnetic excitations can be probed using the classical Fourier transform spectroscopy.

An overview of recent examples illustrating the potential of synchrotron radiation for IR/THz spectroscopy will be presented.

Aerosol Synthesis of Thermally Stable Porous Noble Metals and Alloys by using Bi-functional Templates: A Mechanistic Study

M. Odziomek,¹ C. Boissiere,¹ B. Lassalle-Kaiser,² A. Zitolo,²
S. Nowak,³ C. Tard,⁴ M. Giraud,³ M. Faustini¹ and J. Peron³

^{1.} Sorbonne Université, CNRS, Collège de France, PSL Research University, Laboratoire Chimie de la Matière Condensée de Paris, LCMCP, 4 Place Jussieu, Paris, France

^{2.} Synchrotron SOLEIL, L'orme des Merisiers, Saint-Aubin, 91192 Gif-sur-Yvette, France

^{3.} Université de Paris, ITODYS, CNRS, UMR 7086, 15 rue J-A de Baïf, F-75013 Paris, France

^{4.} LCM, CNRS, Ecole Polytechnique, Institut Polytechnique de Paris, France

ABSTRACT

Aerosol-assisted synthesis is a high throughput and waste-free process widely used in the food industry or production of catalysts. Compared to other solution-based syntheses, it is the only approach allowing straightforward and continuous fabrication of sophisticated porous architectures directly from liquid solution. It has been applied for the synthesis of numerous materials including metal oxides, polymers, and biomaterials, but never to porous metallic materials.¹ Despite their importance for a number of applications in catalysis and electrocatalysis, especially in the case of noble metals, aerosol synthesis of porous metals is still a challenge: an additional treatment in a reductive atmosphere is required that typically results in a collapse of the porosity even at moderate temperature. In this contribution, we overcome this issue by using bi-functional polymeric templates acting simultaneously as a templating and reducing agent. Highly porous microspheres made of platinum-group metals and their alloys were prepared. The final materials exhibit outstanding thermal stability up to 800 °C without loss of the porous morphology. We unravel the reduction mechanism at the solid/solid interface at the single-pore level using state-of-the-art *in situ* techniques such as Transmission Electronic Microscopy and X-ray Absorption Spectroscopy. We propose a mechanism based on a radical process thermally triggered by the depolymerization of organic components.² These findings are important for any field exploiting noble metals (e.g. catalysis) with high thermal stability. They also pave the way for the synthesis of intricate porous structures in a simple, cost-effective and green approach, easy for industrial adaptation.

REFERENCES

1. D. P. Debecker, S. Le Bras, C. Boissiere, A. Chaumonnot and C. Sanchez, *Chem. Soc. Rev.*, **47**, 4112-4155 (2018).
2. M. Odziomek, M. Bahri, C. Boissiere, C. Sanchez, B. Lassalle-Kaiser, A. Zitolo, O. Ersen, S. Nowak, C. Tard, M. Giraud, M. Faustini and J. Peron, *Mater. Horiz.*, Advance Article, (2019). doi: 10.1039/C9MH01408J

Monitoring Catalysts at Work: The Advantages of Combined Operando EPR/XAS/ATR-IR/UV-vis Spectroscopy with Multivariate Analysis

J. Rabeah,¹ V. Briois,² S. Adomeit,¹ C. La Fontaine,²
U. Bentrup,¹ A. Brückner¹

1) Leibniz Institute for Catalysis, Albert-Einstein-Str. 29a, 18059 Rostock -Germany

2) Synchrotron SOLEIL, UR1-CNRS, Saint-Aubin, 91192 Gif-sur Yvette, France

ABSTRACT

Combined operando EPR, XANES/EXAFS, ATR-IR and UV-vis spectroscopy has been developed for monitoring a gas-liquid reaction. As a model reaction, the selective aerobic oxidation of benzyl alcohol (BnOH) to benzaldehyde (BA) over Cu^IOTf/2,2-bipyridine/TEMPO/N-methylimidazole catalyst system has been chosen with the aim to precisely unravel the local environment of Cu^{II} and Cu^I intermediates and active sites in solution which have been controversially discussed in literature.¹⁻² The experimental setup (Fig. 1) involves installation of small EPR spectrometer with its modified probe head in the ROCK beamline at SOLEIL. A home-made reactor placed inside the EPR cavity has been equipped with fibre optical probes for UV-vis and ATR-IR measurements.²

EPR provides information on the time-dependent redox behavior of paramagnetic Cu^{II} and TEMPO species during the catalytic reaction, while XANES/EXAFS and UV-vis provide knowledge about all Cu valence and nucleation states, however with less detail due to their spectral overlying. Therefore, Multivariate Curve Resolution with Alternating Least Squares Fitting (MCR-ALS)³ was used to extract the XAS and UV-Vis spectra of pure Cu components involved during the catalytic reaction, together with their evolution profiles. ATR-IR was used to follow the real time conversion of BnOH to BA.

The results indicate that initially formed tetracoordinated (bpy)(NMI)Cu^I complex is able to active molecular O₂ forming EPR-active (bpy)(NMI)Cu^{II}OOH monomer and EPR-silent dinuclear [(bpy)(NMI)Cu^{II} μ-OH]₂. In the presence of TEMPO, both Cu^{II} monomer and dimer are catalytically active in the initial step of the reaction. However, the Cu^{II} dimer is irreversibly cleaved during the course of the reaction forming EPR-silent (bpy)(NMI)(OOH)Cu^{II}-TEMPO. We found that a gradual formation of non-reducible Cu^{II} site is the reason for the slight deactivation of the catalyst. Based on these results a new reaction mechanism is proposed.

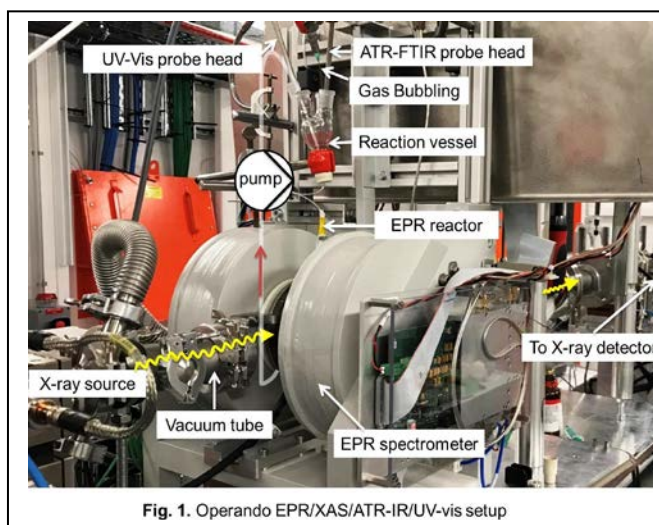


Fig. 1. Operando EPR/XAS/ATR-IR/UV-vis setup

REFERENCES

1. R. C. Walroth, K. C. Miles, J. T. Lukens, S. N. MacMillan, S. S. Stahl, K. M. Lancaster, *J. Am. Chem. Soc.* **139**, 13507-13517 (2017).
2. J. Rabeah, U. Bentrup, R. Stößer, A. Brückner, *Angew. Chem. Int. Ed.* **54**, 11791-11794 (2015).
3. W. H. Cassinelli, L. Martins, A. R. Passos, S. H. Pulcinelli, C. V. Santilli, A. Rochet, V. Briois, *Catal. Today*, **229**, 114-122 (2014).

Ascorbic Acid Directs the Anisotropic Growth of Silver-on-gold Nanoparticles

K. Aliyah¹, J. Lyu¹, C. Goldmann¹, T. Bizien², C. Hamon¹,
D. Alloyeau³ and D. Constantin¹

¹Laboratoire de Physique des Solides, Orsay

²Synchrotron SOLEIL, Saint-Aubin

³Laboratoire Matériaux et Phénomènes Quantiques, Paris

ABSTRACT

Surface plasmon resonances of noble metal nanoparticles can be modulated by tuning the particle morphology (size, anisotropy, edge roundness) or by covering them with a different metal [1]. It is however difficult to follow this complex process, due to the lack of unintrusive *in situ* techniques. An important challenge in the field is to correlate *in situ* single-particle monitoring with other techniques in which the particles are produced in different conditions.

We followed the seeded growth of Au-Ag core-shell noble metal particles by small-angle X-ray scattering, by UV-Vis absorbance spectroscopy and by liquid-cell transmission electron microscopy (ETEM) in liquid cell. The results are correlated with *ex situ* measurements performed on quenched aliquots extracted from the reaction medium.

We will discuss the influence of the various parameters on the kinetics and the final shape of the particles [2]. We will also show that using several complementary methods to follow the same system during its evolution yields a more detailed and reliable picture of the process than any one technique taken separately. Finally, we will conclude that ascorbic acid, widely used for its mild reductive properties, also plays a shape-directing role: it stabilizes the {100} facets of the silver cubic lattice, in synergy with the halide ions.

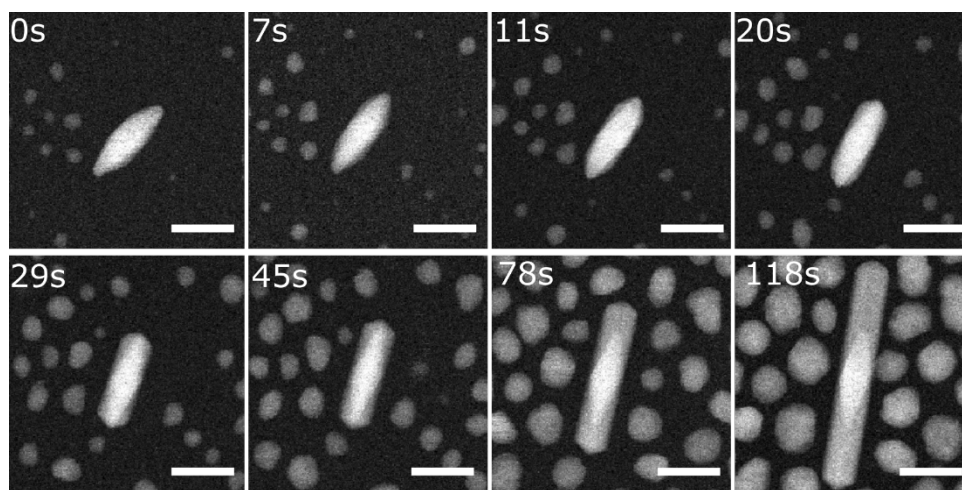


Figure: Time-resolved growth of Au@Ag rods by LCTEM. STEM images showing the anisotropic deposition of silver on a gold bipyramid as well as homonucleation. Scale bar is 50 nm on all images.

REFERENCES

1. C. Hamon, C. Goldmann, and D. Constantin, *Nanoscale* **10**, 18362-18369 (2018).
2. K. Aliyah et al., under revision.

PARALLEL SESSION

Life & Earth Sciences
(Biology / Health & Environment / Geoscience)

SOLEIL Reception Building AUDITORIUM

Thursday, January 16th

Chairpersons:

Benoît Masquida, Rozenn Le Hir and Remi Marsac

- | | |
|-------|--|
| IT-13 | What about collagen in biomaterials?
C. Aimé |
| IT-14 | A. Somogyi |
| OC-17 | 2D mapping bones osteosarcoma with micro-sized X-ray beam
A. Bardouil |
| OC-18 | A BioSAXS study of cubic liquid crystalline nanostructures involving catalase and curcumin in view of therapeutic applications
A. Angelova |
| OC-19 | Light-driven folding of G-quadruplex DNA structures probed by Synchrotron Radiation circular dichroism
K. Laouer |
| IT-15 | Amber fossils revealed by Synchrotron imaging
V. Perrichot |
| IT-16 | Microfluidic chips for crystal growth and serial X-ray analysis
C. Sauter |
| OC-20 | Energy, environment for a sustainable development. Contribution of a 4th generation Synchrotron
D. Vantelon |

PARALLEL SESSION

Life & Earth Sciences
(Biology / Health & Environment / Geoscience)

SOLEIL Reception Building AUDITORIUM

Friday, January 17th

Chairpersons:

Benoît Masquida, Rozenn Le Hir and Remi Marsac

- IT-17 Synchrotron time lapse imaging of lignocellulose biomass hydrolysis
M-F. Devaux ou F. Guillon
- IT-18 ***PX2 - Synchrotron SOLEIL, Gif-sur-Yvette, France***
- OC-21 Cryo-EM structure of an archaeal translation initiation complex at 3.1 Å
resolution
P-D. Coureux
- OC-22 How fluorescence has enlightened antibiotic transport and resistance in
Gram-negative bacteria
M. Masi
- OC-23 Anomalous magnesium: Search for the metal ions in the ribosome
A. Rozov

What about Collagen in Biomaterials?

C. Aimé

UMR Pasteur, Paris, France

A. Somogyi

Synchrotron SOLEIL, Gif-sur-Yvette, France

2D Mapping Bones Osteosarcoma with Micro-sized X-ray Beam

A. Bardouil¹, T. Bizien², I. Almarouk¹, J. Perez², F. Redinil³,
J. Amiaud³, A. Fautrel⁴, N. Nassif⁵, F. Artzner¹

¹Institut de Physique de Rennes, 263 Avenue Général Leclerc, 35700 Rennes

²Synchrotron SOLEIL, L'Orme du Merisier Saint-Aubin, 91192 Gif-sur-Yvette Cedex

³Inserm Nantes, 1 rue Gaston Veil, 44035 Nantes Cedex

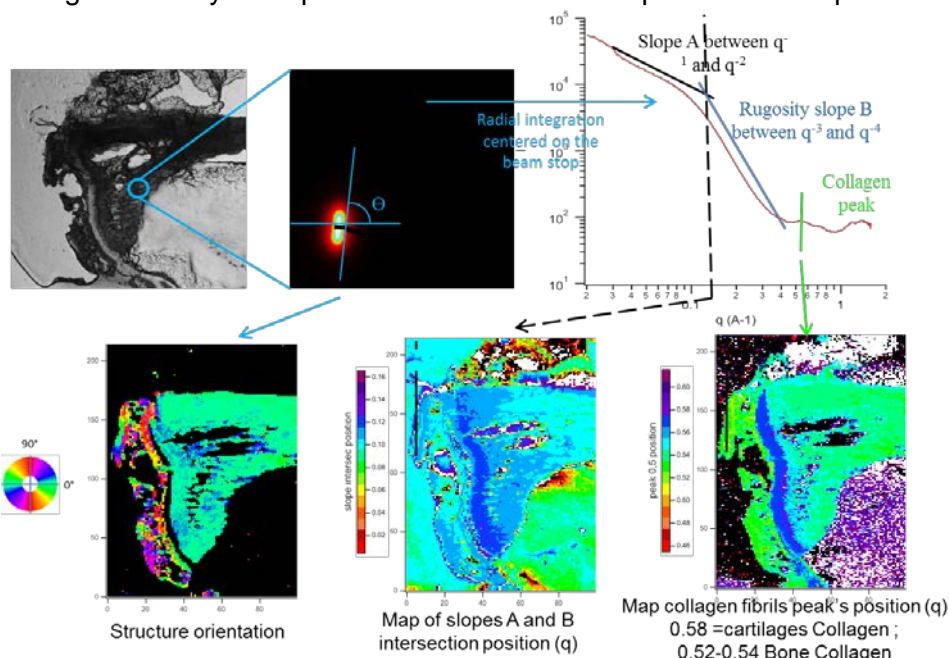
⁴H2P2 Rennes Atalante Villejean, 2 avenue du professeur Léon Bernard, 35043 Rennes Cedex

⁵Laboratoire de chimie de la matière condensée de Paris ; 4 place Jussieu, 75252 Paris Cedex 05

ABSTRACT

Bone tissues exhibit steady-states hierarchical architectures. Osteosarcomas are the most frequent malignant of primary bone tumors. Macroscopically, osteosarcoma looks like a sponge phase of tumor cell and bone. We studied the early stages of tumour invasion in a synergic model of mouse¹.

We scanned, on SWING, mouse femur slices with a 17 μ m microfocus beam to obtain structural maps of a minimum size of 200x100 acquisitions. High throughput data analysis home-made program gives us locally the orientation of the bone structure, the heterogeneity of apatite mineral phase and collagen² superstructure, order and repetition distances are obtained through the analysis of parameters that can be expressed as maps.



The results show abnormal intraperiosteal overproduction of bone with a well defined hierarchical organisations of both apatite crystals and collagen.

REFERENCES

1. Rédini et al, *J. Clin. Med.* 2016, 5(11), 96.
2. Nassif et al, *Nature Materials*. 2012, 11 (8), 724-733.
3. Artzner* et al, *Nature Materials*, 2007, 6, 434-439.

A BioSAXS Study of Cubic Liquid Crystalline Nanostructures Involving Catalase and Curcumin in View of Therapeutic Applications

A. Angelova

*Institut Galien Paris-Sud, CNRS UMR 8612, Univ. Paris-Sud, Université Paris-Saclay,
92290 Châtenay-Malabry cedex, France*

ABSTRACT

Liquid crystalline supramolecular assemblies of non-lamellar structural organization are of interest for development of drug delivery carriers in therapeutic innovation. We report dual-drug loaded monoolein (MO)-based liquid crystalline architectures designed for the encapsulation of a therapeutic protein and a small molecule antioxidant. Catalase is chosen as a metalloprotein, which can provide enzymatic defense against oxidative stress by the decomposition of hydrogen peroxide (H_2O_2). Curcumin, solubilized in fish oil (FO), is co-encapsulated as a chosen drug with multiple therapeutic activities which can recover from the diseased state. The prepared self-assembled biomolecular nanoarchitectures are characterized by biological synchrotron small-angle X-ray scattering (BioSAXS) at multiple compositions of the lipid/co-lipid/water phase diagram. Constant fractions of curcumin and a PEGylated agent are included with regard to the lipid fraction. Stable cubosomal architectures are obtained for several ratios of the main lipid (MO) and the co-lipid (FO) ingredients. The impact of catalase on the structural organization of the cubosome nanocarriers is revealed by the variations of the cubic lattice parameters deduced by BioSAXS. The cellular uptake of the dual drug-loaded nanocarriers is assessed by performing a bioassay of catalase peroxidatic activity in lysates of nanoparticle-treated differentiated SH-SY5Y human cells. The neuroprotective potential of the studied cubosomes is demonstrated *in vitro* in terms of enhanced peroxidatic activity of the catalase enzyme, which enables the inhibition of H_2O_2 accumulation in degenerating neuronal cells.

REFERENCES

1. Rakotoarisoa M, Angelov B, Espinoza S, Khakurel K, Bizien T, Angelova A. *Molecules* **24**(17), 3058 (2019) .
2. Rakotoarisoa, M.; Angelov, B.; Garamus, V.M.; Angelova, A. *ACS Omega*, **4**, 3061–3073 (2019).

Light-driven Folding of G-quadruplex DNA Structures Probed by Synchrotron Radiation Circular Dichroism

K. Laouer¹, F. Wien², B. Nay,³ F. Hache¹ and P. Changenet¹

¹Laboratoire d'Optique et Biosciences (LOB), UMR7645 CNRS - U1182 INSERM - École Polytechnique – Institut Polytechnique de Paris - Route de Saclay 91128 PALAISEAU

²DISCO line, Synchrotron SOLEIL, L'Orme des Merisiers, Saint Aubin BP48, 91192 Gif-sur-Yvette

³Laboratoire de Synthèse Organique (LSO), UMR7652 CNRS –ENSTA - École Polytechnique – Institut Polytechnique de Paris Route de Saclay 91128 PALAISEAU

ABSTRACT

G-quadruplexes (G4) are particular DNA structures resulting from the stacking of several guanine quartets stabilized by metallic cations. G4 are highly polymorphic structures involved in important cellular regulation processes related to their folding mechanism. The ability to control their folding with an external stimulus such as light is therefore a promising strategy for elaboration of new anticancer therapies as well as the construction of smart self-assembled architectures. However, despite the increasing literature devoted to G4, there is still a limited number of studies taking advantage of these DNA structures. One of the main drawback arises from the partial understanding of their folding mechanism. In this context, we undertook a series of SRCD measurements on several biological relevant G4-forming sequences in the presence one non-covalent photo-switch derived from azobenzene (Fig.1.A). We identified three G4-quadruplex forming sequences derived from the human telomeric (Tel21 and Tel22) and the thrombin binding aptamer (TBA) sequences, whose conformational changes can be triggered by photoexcitation. While UV irradiation of the AZO1-Tel21 and AZO1-Tel22 complexes induces a complete unfolding of the DNA scaffold (Fig.1.B), we found that the UV excitation of the AZO1-TBA complexes instead provokes a change of the DNA topology which is consistent with the conversion from a G4 parallel topology to an antiparallel one. We also observed that the reaction is thermally reversible making this complex an ideal system for time-resolved SRCD studies

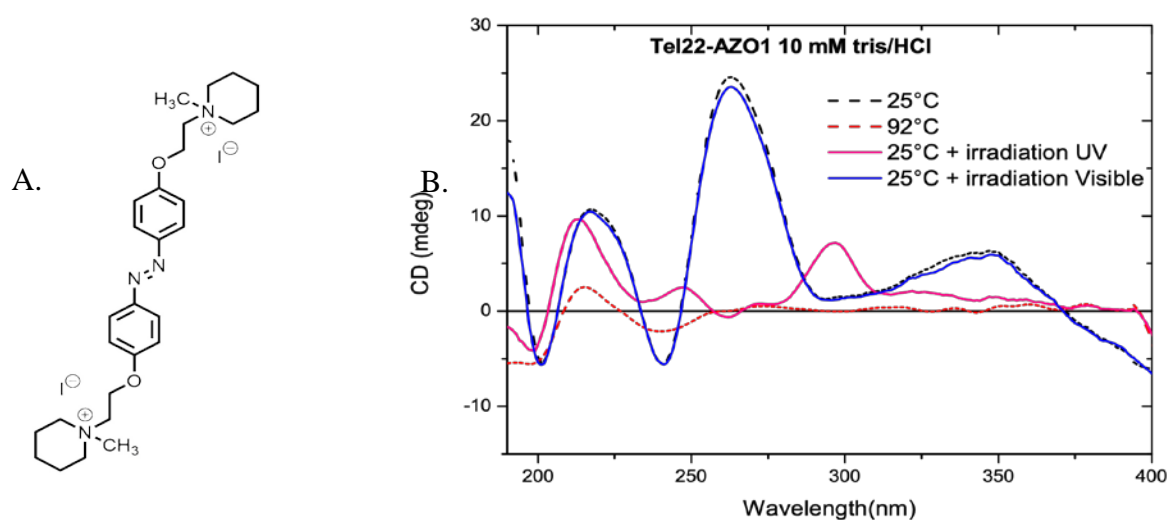


Fig.1 : A. Photosensitive azobenzene derivative (AZO1)
B. Irradiation of Tel 22 sequence in presence of AZO1 at 25°C and comparison with a spectrum obtained at 95 °C.

Amber Fossils Revealed by Synchrotron Imaging

V. Perrichot

Univ Rennes, CNRS, Géosciences Rennes, UMR 6118, 35000 Rennes, France

ABSTRACT

Amber is of great paleontological value because it preserves a diverse array of organisms from different habitats in and close to the amber-producing forests. Terrestrial arthropods are the most commonly preserved inclusions but, in rare instances, amber also contains small mollusks, reptiles, birds, feathers, mammal hairs, plants, and various microbes. Thus, amber discoveries help tracing the evolutionary history of lineages with otherwise poor fossil records, and they also provide insight into the diversity and ecology of terrestrial paleoecosystems.

Inclusions in translucent amber are commonly studied using standard optical microscopes, but the minute size as well as the position of inclusions in an amber piece can prevent the full morphological and anatomical views. Moreover, a significant portion of amber is partly or fully opaque, and biological inclusions in such amber are invisible. Synchrotron imaging techniques are powerful tools to access such poorly exposed and invisible inclusions¹. An optimized imaging protocol has been developed², using propagation phase contrast X-ray synchrotron microradiography to efficiently survey large amounts of opaque amber after immersion in water, followed by phase contrast microtomography for precise characterization of selected organisms.

REFERENCES

1. P. Tafforeau *et al.* 2006. *Appl. Phys. A: Mater.* **83**, 195-202 (2006).
2. M. Lak, D. Néraudeau, A. Nel, P. Cloetens, V. Perrichot and P. Tafforeau, *Microsc. Microanal.* **14**, 251-259 (2008).

Microfluidic Chips for Crystal Growth and Serial Crystallography

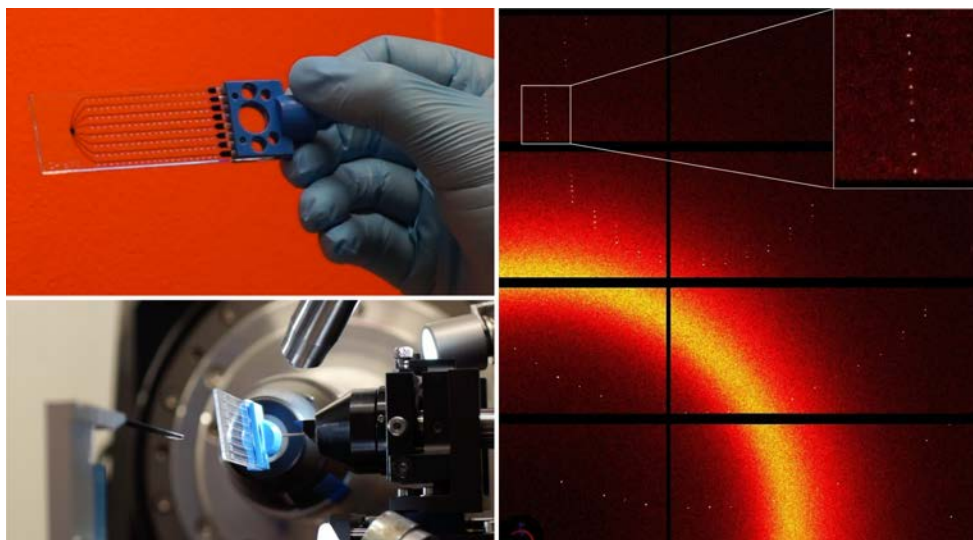
C. Sauter

Architecture et Réactivité de l'ARN, UPR 9002 du CNRS, Institut de Biologie Moléculaire et Cellulaire, Université de Strasbourg, 2 allée Conrad Roentgen, F-67084 Strasbourg, France

ABSTRACT

For about fifteen years, microfluidics has opened up new possibilities and brought many benefits for the crystallization of biomolecules. Indeed, microfluidic systems facilitate the manipulation of nano-volumes of sample solutions, as well as extreme miniaturization and parallelization of crystallization assays. In addition, they provide a convection-free environment that favors the growth of high-quality crystals [1].

As an illustration, a new multifunctional microchip will be presented that combines 1) the search and optimization of crystallization conditions of biomolecules by the counter diffusion method, 2) crystal identification by fluorescence microscopy, 3) microcrystalline seeding, 4) derivatization of crystals by substrate soaking, and 5) *in situ* crystal analysis at room temperature [2]. The concept was tested on a large panel of biomolecules including RNA and various soluble or membrane proteins. Several crystal structures were solved *in situ* by the serial crystallography approach at room temperature under synchrotron radiation.



On-chip crystal analysis by serial crystallography under synchrotron radiation

REFERENCES

1. C. Sauter, K. Dhoub, B. Lorber. *Crystal Growth & Design* **7**, 2247-50 (2007).
2. R. de Wijn, O. Hennig, J. Roche, S. Engilberge, K. Rollet, P. Fernandez-Millan, K. Brillet, H. Betat, M. Mörl, A. Roussel, E. Girard, C. Mueller-Dieckmann, G.C. Fox, V. Oliéric, J.A. Gavira, B. Lorber, C. Sauter. *IUCrJ* **6**: 454–464 (2019).

Energy, Environment for a Sustainable Development.

Contribution of a 4th Generation Synchrotron

V. Briois¹, D. Vantelon²

¹UR1-CNRS, Synchrotron SOLEIL, L'Orme des Merisiers, BP34, 91192 Gif-sur-Yvette

²Synchrotron SOLEIL, L'Orme des Merisiers, BP34, 91192 Gif-sur-Yvette

ABSTRACT

In the frame of the scientific evolution from the current 3rd generation SOLEIL source to a 4th generation one, a series of conferences were held between January 2018 and July 2019 to discuss the opportunities of such a source in the research fields of **Energy and Environmental sciences for a Sustainable Development** [1]. Scientists among the main renowned in France had the opportunity to give their perspectives on the current technical limitations for their research domains. They thus allowed us to identify relevant techniques for which an increase in brightness and coherency as offered by a 4th generation source would be a powerful lever to overcome some of the identified bottle-necks.

Through a few representative examples of issues that could be solved with a 4th generation machine, the purpose of our presentations is to return and discuss with scientists from these communities, the necessary and expected key gains that we identified during these consultations.

REFERENCES

[1] Round Table « **Energy and Environment for a Sustainable Development** ».

Conveners: V. Briois and D. Vantelon,

Themes coordinators: F. Berenguer, C. La Fontaine, S. Belin, B. Lassalle, C. Rivard, G. Landrot.

Synchrotron Time Lapse Imaging of Lignocellulose Biomass Hydrolysis

M-F Devaux¹, F Guillon¹, F Jamme² and C Sandt²

¹ INRA, UR1268 Biopolymères Interactions Assemblages, 44316 Nantes cedex 3, France

² Synchrotron SOLEIL, 91192 Gif-sur-Yvette cedex, France

ABSTRACT

The enzymatic conversion of lignocellulosic materials for the production of chemicals in place of petroleum feedstock is a very promising approach due to high enzyme selectivity and mild use conditions. However, in absence of pretreatment, the efficiency of enzymatic degradation of plant cell walls is low. In the last decade, many efforts have been devoted to the understanding of biomass recalcitrance to enzymatic degradation but no consensus has been reached on which cell wall features are the most important. This is due to the large diversity of biomass and to the fact that it is often considered as a bulk material, not taking into account the diversity and heterogeneity of plant cell walls in general, and the dynamic of enzymatic degradation.

In the present work, the objective was to develop time-lapse imaging to track both enzymes and changes in cell wall composition according to cell types on the course of degradation. Maize stem was considered as a model of grass lignocellulosic biomass and a commercial enzymatic cocktail with both cellulase and xylanase activities was used. The experiments were carried out at synchrotron SOLEIL. The DISCO beam line allowed visualizing both enzyme and cell walls without labelling, by exploiting specific auto-fluorescence properties of enzymatic proteins^{1,2} and of cell wall phenolic compounds. The change in cell wall composition was tracked by FT-IR micro-spectroscopy on the SMIS beam line using a dedicated microfluidic cell². Image analysis and chemometry allowed the quantification of the modifications during degradation and the comparison of cell types.

A contrasted affinity of enzymes according to cell types was evidenced from the beginning of the reaction. Combining the fluorescence and FT-IR information, we demonstrated that enzymes were absent from lignified cell walls and that these cell walls were not modified during the reaction. Enzymes concentrated on non-lignified cell walls. Consistent variations of enzyme concentration were found locally during the degradation with a decrease of the amount of enzyme in cell lumen together with an increased amount of enzymes on the surrounding cell walls. Different rates of polysaccharide degradation were found depending on cell types. In all cases, hemicellulose degradation was found to occur prior to cellulose degradation. An unexpected variability was found in enzyme localisation, initial biochemical composition and degradation pattern highlighting micro-domains in the cell wall of a given cell by fluorescence multiscale imaging and FT-IR microspectroscopy.

REFERENCES

1. G. Tawil, F. Jamme, M. Réfrégiers, A. Viksø-Nielsen, P. Colonna, A. Buléon, *Analytical Chemistry* **83**, 989–993 (2011).
2. M.F. Devaux, F. Jamme, W. André, B. Bouchet, C. Alvarado, S. Durand, P. Robert, L. Saulnier, E. Bonnin, F. Guillon, Synchrotron Time-Lapse Imaging of Lignocellulosic Biomass Hydrolysis: Tracking Enzyme Localization by Protein Autofluorescence and Biochemical Modification of Cell Walls by Microfluidic Infrared Microspectroscopy. *Front.Plant.Sci* **9**, art200 (2018).

PX2

Synchrotron SOLEIL, Gif-sur-Yvette, France

Cryo-EM Structure of an Archaeal Translation Initiation Complex at 3.1 Å Resolution

P-D. Coureux, A. Monestier, C. Lazennec-Schurdevin, R. Kazan,
G. Bourgeois, Y. Mechulam & E. Schmitt

Laboratoire de Biochimie, Ecole polytechnique, CNRS, 91128 Palaiseau cedex, France

E-mail: pierre-damien.coureux@polytechnique.edu

ABSTRACT

Universally, protein biosynthesis begins with accurate selection of the start codon on mRNA and consequently the definition of the open reading frame. In eukaryotes, this process involves many initiation factors and it is therefore the target of many regulations. The most frequent mechanism involves a pre-initiation complex (PIC) made up of the small ribosomal subunit bound to the ternary complex eIF2-GTP-Met-tRNA_i^{Met} (TC), the two small initiation factors eIF1 and eIF1A, as well as two proteins, eIF5 and eIF3, that have a more regulatory function in the process. In the presence of factors belonging to the eIF4 family, the PIC is recruited near the 5'-capped end and scans the mRNA until an AUG codon in a correct context is found. AUG recognition stops scanning, provokes factor release and the assembly of an elongation-proficient 80S complex through large subunit joining, with the help of eIF5B and eIF1A.

In archaea, there is no long-range scanning because mRNAs have Shine-Dalgarno sequences or very short 5' UTR. However, genomic analyses have shown that three initiation factors homologous to their eukaryotic counterparts, aIF1, aIF1A and aIF2 are found. Thus, even if obvious differences between eukaryotes and archaea exist, in particular for the recruitment of the PIC on the mRNA, start codon selection is achieved within a common structural core made up of the small ribosomal subunit, the mRNA, the methionine initiator tRNA (Met-tRNA_i^{Met}) and the three initiation factors e/aIF1, e/aIF1A and e/aIF2.

Previous cryo-electron microscopy structures of the full *Pyrococcus abyssi* PIC led us to propose a spring force model showing how aIF2 controls initiator tRNA pairing to the AUG codon[1]. Then, we used a combination of biochemical experiments and cryo-EM analyses to decipher the molecular mechanisms of start codon selection. In particular the key role of aIF1 was studied[2]. Here, we present the cryo-EM structure of a translation initiation complex obtained in the absence of aIF1 at 3.1 Å resolution. This structure reveals details of full initiator tRNA accommodation in the P site after aIF1 departure. In particular, 30S conformational adjustments and the role of universal ribosomal proteins will be discussed. Finally, we observe for the first time a large set of acetylcytidines along the rRNA sequence likely involved in ribosomal thermostability. This first high-resolution model of the archaeal small ribosomal subunit gives new insights in the molecular evolution of eukaryotic and archaeal translation initiation mechanisms.

Electron density map at 3.1 Å resolution of the archaeal translation initiation complex IC2.

REFERENCES

- [1] Coureux PD, Lazennec-Schurdevin C, Monestier A, Larquet E, Cladière L, Klaholz BP, Schmitt E and Mechulam Y. (2016). Cryo-EM study of start codon selection during archaeal translation initiation. **Nat Commun**, 7:13366.
[2] Monestier A, Lazennec-Schurdevin C, Coureux PD, Mechulam Y, Schmitt E. (2018). Role of aIF1 in *Pyrococcus abyssi* translation initiation. **Nucleic Acids Res.**, 46:11061.

How Fluorescence has Enlightened Antibiotic Transport and Resistance in Gram-negative Bacteria

M. Masi^{1,2}, J-M. Pagès¹ and M. Réfrégiers³

¹ *Membranes and Therapeutic Targets, UMR_MD1 Inserm U1261, Aix-Marseille Université & IRBA, Faculté de Pharmacie, 27 Boulevard Jean Moulin, 13005 Marseille, France*

² *Institute for Integrative Biology of the Cell, UMR9198 Université Paris Saclay CEA-CNRS, Bât21, Avenue de la Terrasse, 91190 Gif-sur-Yvette, France*

³ *DISCO Beamline, Synchrotron SOLEIL, L'Orme des Merisiers Saint-Aubin, BP 48, 91192 Gif-sur-Yvette Cedex, France*³

ABSTRACT

The permeability barrier of Gram-negative cell envelopes is a major obstacle in the discovery and development of new antibiotics. In particular, the synergistic interaction between the low permeability of the outer membrane and active multidrug efflux makes the task all the more difficult. In our work, we use isogenic strains of *Escherichia coli* with controlled permeability barriers, with different influx and/or efflux capacities, to evaluate the specific contribution of each barrier to drug accumulation and activity.

I will illustrate this approach with a recent study on fluoroquinolones, which target the bacterial cytoplasm, to perform Structure to Intracellular Concentration and Activity Relationship (SICAR) analyses. On one hand, the outer membrane of *E. coli* contains about 200,000 copies of OmpF and OmpC porins per cell, which are responsible for the nonspecific diffusion of small polar compounds. Consequently, several antibiotics are active against this species. On the other hand, the inner membrane of *E. coli* contains several multidrug efflux pumps that differ in their structures and mechanisms. Among them, the transmembrane AcrAB-TolC complex is the major efflux pump responsible for the intrinsic resistance of *E. coli* towards a wide variety of antimicrobials. Noteworthy, porin modifications and/or AcrAB overexpression have a significant impact on the emergence of multidrug resistance in clinical strains. Antibacterial activities were examined by using standard minimal inhibitory concentration and resazurin-based real time viability assays. Fluorimetry allowed quantification of intracellular drug concentrations and determination of SICAR coefficients to measure the porin-mediated influx and efflux efficiencies among series of chemically related antibiotics. Together, ratios of drug accumulation and susceptibility were used to rank the importance of antibiotic properties in relation with permeability barriers. Importantly, these experimental data also reflect (favorable or unfavorable) molecular interactions between in transit antibiotics and membrane transporters, which can be confirmed by molecular modelling and molecular dynamics simulations.

I will also present a “tool box”, which has been set up to determine efflux pump activity and inhibition by therapeutic adjuvants.

REFERENCES

1. Vergalli J, Dumont E, Pajović J, Cinquin B, Maigre L, Masi M, Réfrégiers M, Pagès JM. Spectrofluorimetric quantification of antibiotic drug concentration in bacterial cells for the characterization of translocation across bacterial membranes. *Nat Protoc.* 2018, 13:1348-1361.
2. Masi M, Dumont E, Vergalli J, Pajovic J, Réfrégiers M, Pagès JM. Fluorescence enlightens RND pump activity and the intrabacterial concentration of antibiotics. *Res Microbiol.* 2018, 169:432-441.
3. Vergalli J, Dumont E, Cinquin B, Maigre L, Pajovic J, Bacqué E, Mourez M, Réfrégiers M, Pagès JM. Fluoroquinolone structure and translocation flux across bacterial membrane. *Sci Rep.* 2017, 7:9821.
4. Masi M, Réfrégiers M, Pos KM, Pagès JM. Mechanisms of envelope permeability and antibiotic influx and efflux in Gram-negative bacteria. *Nat Microbiol.* 2017, 2:17001.

Anomalous Magnesium: Search for the Metal Ions in the Ribosome

A. Rozov^{1,2}, I. Khusainov², K. El Omari³, R. Duman³, V. Mykhaylyk³,
M. Yusupov², E. Westhof⁴, A. Wagner³ & G. Yusupova²

¹*Urania Therapeutics, 15 rue Neuve, 67540 Ostwald, France.*

²*Institut de Génétique et de Biologie Moléculaire et Cellulaire,
1 rue Laurent Fries, 67404 Illkirch, France.*

³*Diamond Light Source, Harwell Science and Innovation Campus, Chilton, Didcot OX11 0DE, UK.*

⁴*Université de Strasbourg, CNRS, Architecture et Réactivité de l'ARN, UPR 9002,
15 rue René Descartes, F-67000 Strasbourg, France.*

ABSTRACT

The ribosome is the largest and the most abundant RNA-containing macromolecular complex in cells. Ribosomes perform protein synthesis upon subunit association and interaction with mRNA and tRNA ligands. Ribosome structure and function strongly depend on the presence of divalent (mainly Mg^{2+} and Zn^{2+}) and monovalent (mainly K^+ and NH_4^+) cations¹. Of these, magnesium is the most characterized cation, its importance for ribosome activity was investigated in great detail by pioneers of ribosome research. However, magnesium is not the sole component responsible for proper ribosome activity. The highest rate of protein synthesis *in vitro* is achieved in the presence of Mg^{2+} , polyamines and monovalent cations (K^+/NH_4^+) together²⁻⁴.

Despite the vast amount of biochemical data regarding the importance of metal ions for efficient protein synthesis and the increasing number of ribosome structures solved by X-ray crystallography or cryo-electron microscopy, the assignment of metal ions within the ribosome remained elusive due to methodological limitations. Therefore, in the majority of ribosome structural models metal ions are usually assigned as magnesium — the best-known RNA-stabilizing atom.

We have collected extensive experimental data on the potassium composition and environment in structures of functional ribosome complexes obtained by measurement of the potassium anomalous signal at the K-edge, derived from long-wavelength X-ray diffraction data. We elucidate the role of potassium ions in protein synthesis at the three-dimensional level, most notably, in the environment of the ribosome functional decoding and peptidyl transferase centers. Our data expand the fundamental knowledge of the mechanism of ribosome function and structural integrity.

REFERENCES

1. Nierhaus, K. H. J. *Bacteriol.* 196,3817–3819(2014).
2. Jelenc, P. C. & Kurland, C. G. *Proc. Natl Acad. Sci. USA* 76,3174–3178 (1979).
3. Rheinberger, H. J. & Nierhaus, K. H. J. *Biomol. Struct. Dyn.* 5,435–446 (1987).
4. Bartetzko, A. & Nierhaus, K. H. *Methods Enzym.* 164, 650–658 (1988)

POSTERS SESSION

List of Student Posters

- PO-AN-01** Controlling fundamental electronic interactions in SrTiO₃ (100) thin films by Ni doping
F. Alarab
- PO-AN-02** A XAS study of magnetic nanoparticles embedded in ordered mesoporous silica
L. Altenschmidt
- PO-AN-03** Insights on the electrochemical magnesianation of InSb from combined operando X-ray diffraction and X-ray absorption spectroscopy
L. Blondeau
- PO-AN-04** Formation and electronic properties of AuTe surface alloy on Au(111) surface
M. Bouaziz
- PO-AN-05** Probing structure and magnetic ultrafast dynamic profiles by time resolved X-ray resonant magnetic reflectivity
V. Chardonnet
- PO-AN-06** Surface structure investigation of Al₁₃Co₄(010) catalyst using a combination of surface science techniques and ab initio calculations
C. Chatelier
- PO-AN-07** Assessing quantum thermal nuclei fluctuations on multipolar contributions in core level spectroscopy
S. Delhommaye
- PO-AN-08** Investigation of the evolution of the electronic structure at the magnetic transition in layered iridates
P. Foulquier
- PO-AN-09** Synthetic antiferromagnet materials studied by Soft X-ray magnetic resonant scattering
C. Leveillé
- PO-AN-10** Towards the quantification of small structural distortions in bimetallic Prussian Blue Analogs by XMCD at the transition metal K-edge
A. N'Diaye
- PO-DR-11** Photoionization and dissociative photoionization of methylketene and its dimer in the gas phase: Theory and experiment.
I. Derbali
- PO-DR-12** Impacts of the non-classical nucleation mechanism of cerium oxalate
M. Durelle
- PO-DR-13** The single-photon ionisation of C2
O.J. Harper
- PO-DR-14** Quantifying water ionization by soft X-rays using a microfluidic device
L. Huart
- PO-DR-14-bis** Coupling an electron time-of-flight spectrometer and an under vacuum liquid jet for coincidence measurements on solvated biomolecules
L. Huart

- PO-DR-15** Light-driven folding of G-quadruplex DNA structures probed by Synchrotron Radiation circular dichroism
K. Laouer
- PO-DR-16** Excited electronic states in gas-phase thiophene and thiolane molecules using resonant Auger spectroscopy
J.B. Martins
- PO-DR-17** Operando Quick XAS study of oxygen and carbon monoxide activation over bimetallic Pt-Fe catalysts
I. Sadykov
- PO-LH-18** Migration and speciation of anthropogenic uranium in natural soils
S. Bayle
- PO-LH-19** Molecular recognition of a new class of nuclear localization signals by transportin 1
A. Mboukou
- PO-LH-20** Structural and functional insights on the NHEJ network around the Ku-DNA Hub
S. Zahid

Controlling Fundamental Electronic Interactions in SrTiO₃ (100) Thin Films by Ni Doping

F. Alarab^{1,2}, J. Minar², M-C. Richter¹ and K. Hricovini¹

¹ *Université de Cergy-Pontoise, Neuville-sur-Oise 95000, France*

² *New Technologies Research Centre, University of West Bohemia, Plzen, Czech Republic*

ABSTRACT

SrTiO₃ has been a subject of intensive discussions in recent years both experimentally as well as theoretically. Fundamental physical aspects, as for example presence of 2D electron gas on the surface of SrTiO₃, its magnetism, correlation effects and proposed superconductivity meet at the same time with an extensive interest in the development of new materials for solar energy utilization. However, one major constrain in SrTiO₃ is a large band gap (≥ 3 eV), thus it can only harvest sunlight in the UV range. In order to match its absorption spectra to the solar radiation spectrum, SrTiO₃ can be doped with transition metals (TM).

In this study, the main objective is to clarify the electronic structure and the role of electronic correlations in the Ni doped SrTiO₃ (100) thin films using different spectroscopic techniques. Our samples (pure SrTiO₃, 6%Ni:SrTiO₃ and 12%Ni:SrTiO₃) were grown by pulsed laser deposition (PLD) on SrTiO₃ (100) substrate lightly doped with Nb, with a film thickness of about 4 nm. After the growth, all samples were transferred in-situ to the CASSIOPEE beamline (using a vacuum suitcase). Angle-resolved photoemission experiments show very interesting impurity based in-gap states in the doped samples. Ni states contribution in the valence band was confirmed by resonant photoemission near Ni absorption L-edge. The localized nature of these impurity-based states is as well supported by our one-step model calculations using the KKR package.

A XAS Study of Magnetic Nanoparticles Embedded in Ordered Mesoporous Silica

L. Altenschmidt, A. Bordage, G. Fornasieri, A. Bleuzen

ECI, Institut de Chimie Moléculaire et des Matériaux d'Orsay, CNRS, Université Paris-Sud, Université Paris-Saclay, 91400 Orsay, France

ABSTRACT

We are interested in the development of functional magnetic materials based on nanoparticles containing iron and/or cobalt ions embedded in a mesoporous silica matrix. The ordered silica mesoporosity is used for the control of the morphology, the size and the spatial organization of the nanoparticles within.^{1,2} These nanocomposite systems exhibit interesting collective magnetic properties caused by interparticle interactions within the particle assembly.³ These interactions remain even at a strong dilution of the magnetic particles.

Here, we present our recent work on the SAMBA beamline which has been focused on the understanding of the local and electronic structure of the metal ions in oxidized or reduced nanocompounds to correlate them to the observed magnetic behavior. We are focused on understanding the effect of the synthesis conditions, that is the variation of the thermal treatment temperature, the concentration of the metal containing species in regards to the surrounding silica matrix as well as the nature of the used precursor (Prussian blue analogue or nitrate salt).

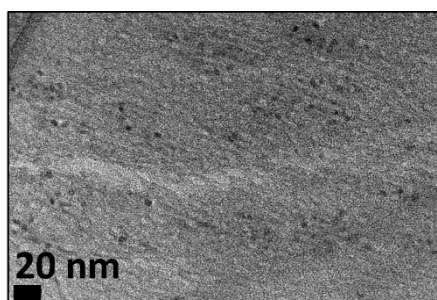


Figure: Magnetic oxide nanoparticles within the mesoporosity of a silica monolith.

REFERENCES

1. E. Delahaye, R. Moulin, M. Aouadi, V. Trannoy, P. Beaunier, G. Fornasieri, A. Bleuzen, *Chemistry* **21**, 16906-16916 (2005).
2. P. Durand, G. Fornasieri, C. Baumier, P. Beaunier, D. Durand, E. Rivière, A. Bleuzen, *J. Mater. Chem.* **20**, 9348-9354 (2010).
3. V. Trannoy, L. Altenschmidt, G. Fornasieri, A. Bordage, E. Rivière, P. Beaunier, A. Bleuzen, *ChemNanoMat* **4**, 1254-1261 (2018).

Insights on the Electrochemical Magnesiumation of InSb from Combined Operando X-ray Diffraction and X-ray Absorption Spectroscopy

L. Blondeau¹, E. Foy¹, S. Belin², S. Surblé¹, F. Testard¹,
H. Khodja¹, M. Gauthier¹

¹ LEEL, NIMBE, CEA, CNRS, Université Paris-Saclay, CEA Saclay 91191 Gif-sur-Yvette France

² Synchrotron SOLEIL, L'Orme des Merisiers, Saint-Aubin 91192 Gif-sur-Yvette, France

ABSTRACT

The continued acceleration of the lithium demand combined with its relatively low abundance and uneven concentration on the Earth's crust might dramatically increase its price in a near future. Mg-batteries are promising candidates to replace Li-ion batteries thanks to Mg abundance, theoretical capacity (2.2Ah/g - 3.8Ah/cm³), low cost and safety. However, metallic Mg reacts with standard electrolytes to form a blocking layer on its surface, preventing cation exchange, and thus dramatically limiting reversible stripping/deposition. An interesting alternative is to substitute Mg metal with another negative electrode made of *p*-block elements as they electrochemically alloy with Mg and possess adequate stability in standard electrolytes [1].

In a recent work, we investigated the InSb alloy as a negative electrode [2] in order to fundamentally understand the electrochemical reactions occurring in alloys in Mg batteries. A strong synergy between In and Sb has been evidenced with the promotion of the electrochemical activity of Sb towards magnesiumation along few cycles, in contrast to what was already reported in other studies.

Using complementary information from *operando* X-Ray diffraction (XRD) and X-Ray Absorption Spectroscopy (XAS), we further characterized in-depth the peculiar electrochemical behavior of InSb. *Operando* XRD measurements demonstrate the formation of the Mg₃Sb₂ phase almost all along the first magnesiumation, accompanied by the extrusion of In metal. While crystalline MgIn has always been detected in the case of pure In or InBi electrodes [3], we observed a kinetically dependent electrochemically-driven amorphization of MgIn. This behavior suggests a possible competition between crystallization and amorphization in the material. EXAFS data, obtained at the In and Sb *K*-edges at the ROCK beamline of synchrotron Soleil, corroborate the formation of Mg₃Sb₂ and In crystalline phases but also the formation of MgIn. It gives us further insights on the atomic environment of In and Sb during the first magnesiumation. Thanks to the evolution of EXAFS spectra as well as the changes in scattering paths, the phase proportions evolution as function of the number of Mg inserted into InSb has been followed. These results are of paramount importance to shed light on synergetic effects between *p*-block elements and to study the relation between *in situ* amorphization and electrochemical behavior.

REFERENCES

- [1] Murgia et al., *Electrochem. Commun.* 60, 56 (2015)
[2] Blondeau et al., *Phys. Chem. C* 123, 1120–1126 (2019)
[3] Murgia et al., *Electrochem. Acta.* 209, 730-736 (2016)

Formation and Electronic Properties of AuTe Surface Alloy on Au(111) Surface

M. Bouaziz^{1,2}, W. Zhang³, Y. Tong¹, Z. Chen¹, Z. Zhang¹, H. Enriquez³,
R. Mlika², H. Korri-Youssoufi⁴, H. Oughaddou³, and A. Bendounan¹

¹*Synchrotron SOLEIL, L'Orme des Merisiers, Saint-Aubin – BP 48,
F-91192, Gif-sur-Yvette Cedex, France*

²*Laboratoire des interfaces et matériaux avancés, Université de Monastir, 5019 Monastir, Tunisie*

³*Institut des Sciences Moléculaires d'Orsay, Université Paris-Sud, 91405 Orsay Cedex, France*

⁴*Institut de Chimie Moléculaire et des Matériaux d'Orsay, Université Paris-Sud,
91400 Orsay Cedex, France*

E-mail: meryem.bouaziz@synchrotron-soleil.fr

ABSTRACT

We report here on the formation and the properties of AuTe alloy monolayer on Au(111) surface. This system presents interesting structural properties as shown in the LEED patterns by the formation of well-ordered and long-range reconstructions, which are confirmed by low-temperature STM results. The XPS measurements indicate the presence of one chemical environment of the Te atoms associated with the Te-Au bonding. In addition, one observes a downward shift of the Shockley surface state, which is the signature of a charge transfer from the Te atoms to the substrate. Moreover, new dispersive bands are observed by Angle-resolved photoemission (ARPES), which originate from a strong hybridization between Te and Au electronic states. These bands are strongly influenced by the surface reconstructions and undergo folding at the boundaries of the reduced surface Brillouin zone. This finding clearly highlights the presence of 2D-type electron system within the AuTe alloy layer. Moreover, ARPES and STS data reveal the existence of a band gap and suggest a semiconductor character of the AuTe monolayer. We will present in this communication the results of systematic investigations using different experimental techniques.

Probing Structure and Magnetic Ultrafast Dynamic Profiles by Time Resolved X-ray Resonant Magnetic Reflectivity

V. Chardonnet¹, M. Hennes¹, R. Jarrier¹, R. Delaunay¹, J. Luning²,
N. Jaouen³, D. Schick⁵, K. Yao⁵, X. Liu³, C. Leveillé³, M. Cammarata⁴
and C. Von Korff Schmising⁵, B. Vodungbo¹ and E. Jal¹

¹*Sorbonne Universités, UPMC Univ. Paris 06, CNRS, Laboratoire de Chimie Physique – Matière et Rayonnement, 75005 Paris, France;*

²*Helmholtz-Zentrum Berlin für Materialien und Energie, 14109 Berlin, Germany;*

³*Synchrotron SOLEIL, Saint-Aubin, Boite Postale 48, 91192 Gif-sur-Yvette Cedex, France;*

⁴*Institut de Physique de Rennes, UMR UR1-CNRS 6251, Université de Rennes 1, F35042, Rennes, France;* ⁵*Institut für Optik und Atomare Physik, Technische Universität Berlin, 10623 Berlin, Germany*

ABSTRACT

Despite more than two decades of research on the ultrafast magnetism dynamics, we are still struggling to get a complete picture of the microscopic mechanism driving ultrafast de-magnetization. Among all the models existing, we can focus on two: Elliott-Yafet spin flip scattering mechanism [1] or the superdiffusive spin transport model [2]. Elliott-Yafet spin flip scattering will reduce the magnetization locally. Its magnetization depth profile will depend directly on the excitation depth profile [3]. While the superdiffusive spin transport model is a non-local process able to transport spin current in no magnetic metal [2]. Thus the de-magnetization depth profile predicted by these two models is different [3]. To distinguish one of both model or a combination of both, the transient magnetization depth profile has to be known and measured.

The X-Ray Resonant Magnetic Reflectivity (XRMR) is one of the few technique to study the magnetization depth profile. It is a non-destructive probing technique with a sub nanometer precision, which combines the layer profile as well as the magnetic depth profile of a specific element [4]. This technique is well mastered at SEXTANT beamline on the RESOXS experiment. Recently, it has been shown using femtoslicing source at BESSY2, that time resolved XRMR (tr-XRMR) experiment can be used to measure simultaneously transient magnetization and structural dynamics. However, this study show that to access a depth resolved magnetization profile, a higher photon flux and/or energy resolution are needed [5].

The only way to get ultra-short photon pulse with more flux is to use a Free Electron Laser (FEL). Here we present the first tr-XRMR experiment which has been performed at a XFEL, namely FLASH 2 in Hamburg. The RESOXS experiment was an essential help for the smooth running of this experiment since it allows us to select our best samples.

Then in order to perform the tr-XRMR experiment we have developed our own reflectometer and we have used the third order radiation of FLASH 2 to reach the Fe L-edge. In a first part, we will present the technical specificities of our tr-XRMR experiment, and the proof that (i) there are enough photons at the third order to measure reflected intensity up to 38 degree and (ii) that it can be well separated from the first order. This has been possible thanks to the comparison of our FLASH data with the SOLEIL measurements performed preliminarily in RESOXS.. In a second part we will show preliminary results demonstrating the capabilities to measure simultaneously transient depth profile of the structure and magnetization.

REFERENCES

- [1] B. Koopmans, et al. Nature materials, 9(3):259, 2010.
- [2] M. Battiato, et al. Physical Review B, 86(2):024404, 2012.
- [3] J. Wieczorek, et al.. Physical Review B, 92(17):174410, 2015.
- [4] S. Macke , et al. .Journal of Physics:Condensed Matter, 26(36):363201, 2014.
- [5] E. Jal, et al. Physical Review B, 95(18):184422, 2017.

Surface Structure Investigation of $\text{Al}_{13}\text{Co}_4(010)$ Catalyst using a Combination of Surface Science Techniques and *ab initio* Calculations

C. Chatelier^{1,2*}, Y. Garreau^{2,3}, A. Vlad², A. Resta², V. Fournée¹,
J. Ledieu¹, M-C. de Weerd¹, A. Coati² and É. Gaudry¹

¹Université de Lorraine, Institut Jean Lamour, CNRS, Campus ARTEM, F-54011 Nancy, France

²Synchrotron SOLEIL, L'Orme des Merisiers Saint-Aubin, F-91192 Gif-sur Yvette, France

³Université de Paris, Laboratoire Matériaux et Phénomènes Quantiques, CNRS, F-75013, Paris, France

ABSTRACT

Substituting noble metal catalysts with inexpensive, environmentally harmless, stable, and selective equivalents is a great challenge for the chemical industry. In this regards, the development of catalysts with a high activity, stability, and selectivity is crucial. Lately [1-2], several transition metal Al-based quasicrystalline approximants – including $\text{Al}_{13}\text{Co}_4$ – were identified as stable, selective and low-cost catalysts for acetylene and butadiene semi-hydrogenations. In depth investigations of their different surface structures and catalytic properties are necessary to provide rational designs of Al-based catalysts.

An investigation of the surface structure of $\text{Al}_{13}\text{Co}_4(010)$ is presented in this work. A combination of Low-Energy Electron Diffraction (LEED), Scanning Tunneling Microscopy (STM), Atomic Force Microscopy (AFM), and Surface X-ray Diffraction (SXRD), together with Density Functional Theory calculations (DFT) provides relevant pieces of information regarding the peculiar surface structure of $\text{Al}_{13}\text{Co}_4(010)$. This surface exhibits a particular faceted and columnar structure similar to the (12110) and (10000) two-fold d-Al-Ni-Co quasicrystalline surfaces [3].

The calculated surface structures and energies of both the terraces and the facets are reported and compared to the experimental results. This work opens up additional perspectives for the comprehension of the catalytic properties of the $\text{Al}_{13}\text{Co}_4(010)$ surface orientation.

REFERENCES

- [1] M. Armbrüster et al., Nat. Mater. 11, 690-693 (2012)
- [2] L. Piccolo et al., Sci. Tech. Adv. Mat. 20:1, 557-567 (2019)
- [3] R. Mäder et al. Phys. Rev. B 80 035433, (2009)

Assessing Quantum Thermal Nuclei Fluctuations on Multipolar Contributions in Core Level Spectroscopy

S. Delhommaye¹, E. de Clermont Gallerande¹, G. Radtke¹, S. Huotari²,
S. P. Collins³, D. Cabaret¹

¹*Sorbonne Université, IMPMC UMR CNRS 7590, Campus Pierre et Marie Curie,
4 place Jussieu, 75005 Paris, France*

²*Department of Physics, P.O. Box 33 (Yliopistonkatu 4) 00014 University of Helsinki, Finland*

³*Diamond Light Source Ltd., Diamond House, Harwell Science and Innovation Campus, Didcot, Oxon
OX11 0DE, United Kingdom*

ABSTRACT

X-ray Absorption spectroscopy (XAS) was recently shown to be sensitive to quantum thermal vibration effects at the K edge of some light (low Z) cations, such as aluminum, in various oxides [1,2], with a noticeable effect on the pre-edge region of the spectrum. At the Al K edge in corundum (α -Al₂O₃), due to vibration-induced on-site hybridization between s and p states of the absorbing Al atom, the pre-edge region presents a peak stemming from these s states even though monopole ($1s \rightarrow s$) transitions are forbidden in XAS. X-Ray Raman Spectroscopy (XRS) is another core-level spectroscopy technique relying on non-resonant inelastic X-ray scattering. It provides information both accessible to XAS in the case of low momentum transfer (\mathbf{q}), where dipole ($1s \rightarrow p$ for a K edge) transitions dominate the spectra, and inaccessible to XAS at high \mathbf{q} value where monopole transition channels may become predominant in the spectra [3]. In this study, the effects of vibrations on the multipolar components were assessed for both techniques: dipole and quadrupole channels for XAS at the K edge of Ti in the rutile phase of TiO₂, and monopole and dipole for XRS at the K edge of Al in corundum.

The XAS and XRS spectra were calculated using the XSpectra module of the QUANTUM Espresso suite of code, relying on pseudopotentials, plane wave basis for wave functions expansion, and periodic boundary conditions, all within a DFT (Density Functional Theory) framework [3,4,5,6]. The quantum thermal vibrations of the nuclei are modeled in the (quasi)-harmonic approximation using the method developed in [1,2]. This allows us to generate temperature-dependent, non-equilibrium configurations of the materials, each one is then used to compute a XAS or XRS spectrum. The final theoretical XAS or XRS spectrum is obtained by averaging the configuration spectra. Results are compared with experimental data obtained at the ID20 beamline at ESRF for the case of the XRS Al K edge, and at the Diamonds Light Source in UK for the case of the XAS Ti K edge. The Al K edge in XRS is at the limit of what could be measured at the time, while the Ti K edge measurement experiment also provides information regarding the temperature influence on the angular dependence of the pre-edge region, allowing the analysis of subtle thermal motion induced effects.

REFERENCES

1. Nemausat et al., 2015 Phys. Rev. B 144310.
2. Nemausat et al., 2017 PCCP 19, 6246-6256.
3. de Clermont Gallerande et al., 2018 Phys. Rev. B 98, 214104.
4. Taillefumier et al., 2002 Phys Rev B 66, 195107.
5. Gougoussis et al., 2009 Phys. Rev. B 80, 075102.
6. Gianozzi et al., 2009 J. Phys.: Cond. Mat 21, 395502.

Investigation of the Evolution of the Electronic Structure at the Magnetic Transition in Layered Iridates

P. Foulquier^{1, 2}, V. Brouet¹, F. Bertran³, P. Le Fèvre³, J. E. Rault³,
A. Forget², D. Colson², J-B. Moussy²

¹Laboratoire de Physique de Solides, CNRS UMR 8502, Univ. Paris Sud, Université Paris Saclay, Orsay, France

²Service de Physique de l'état Condensé, DRF/IRAMIS/SPEC, UMR 3680 CNRS, CEA Saclay, 91191 Gif sur Yvette Cedex, France

³Synchrotron SOLEIL, L'Orme des Merisiers, Saint-Aubin-BP 48, 91192 Gif sur Yvette, France

paul.foulquier@u-psud.fr

ABSTRACT

Ruddlesden-Popper layered perovskite iridates (Sr_2IrO_4 and $\text{Sr}_3\text{Ir}_2\text{O}_7$) are insulators, although they have 5 electrons in the Ir 5d band and would then rather be expected to be metallic. The strong spin-orbit coupling splits the three t_{2g} states into doubly degenerate $J_{\text{eff}}=3/2$ states below E_F , containing 4 electrons, and a narrow half-filled band near the Fermi level of $J_{\text{eff}}=1/2$ character, where correlations could be strong enough to form a Mott insulator [1]. A pending question is to understand the link between the magnetic and insulating states. Indeed, antiferromagnetic order is detected below $T_N=240\text{K}$ for Sr_2IrO_4 and $T_N=280\text{K}$ for $\text{Sr}_3\text{Ir}_2\text{O}_7$, which should be compared to their insulating gaps of 0.6eV and 0.2eV, respectively. These compounds remain insulating above T_N ; in Sr_2IrO_4 there is even hardly any detectable change in resistivity through T_N , while there is a clear drop in $\text{Sr}_3\text{Ir}_2\text{O}_7$. At first sight, this suggests that the insulating character is not directly connected to the AF order. However, optical measurements [2] have confirmed that the gap does not close abruptly at T_N , but there is a small shift and a lot of spectral weight is transferred inside the gap. This behaviour is unusual and not expected in a Mott scenario. Similar behaviour obtained by STM was interpreted as due to a transition between a Slater insulator and a bad metal above T_N , due to strong 2D fluctuations [3].

In Ru doped $\text{Sr}_3\text{Ir}_2\text{O}_7$, we have observed a 0.1eV shift toward Fermi level of the $J_{\text{eff}}=1/2$ band at the X point just above the Neel temperature. We will discuss the origin of this behaviour and contrast it to what is observed in Sr_2IrO_4 and with La doping.

REFERENCES

- [1] B.J. Kim et al., Phys. Rev. Letters **101**, 076402 (2008)
 [2] S.J. Moon et al., Phys. Rev. B **80**, 195110 (2009)
 [3] Q. Li et al., Scientific reports **3**, 3073 (2013)

Synthetic Antiferromagnet Materials Studied by Soft X-ray Magnetic Resonant Scattering

C. Leveillé¹, E. Burgos Parra^{1, 2}, Y. Sassi², W. Legrand², F. Ajejas²,
V. Cros², N. Reyren², and N. Jaouen¹

¹*Synchrotron SOLEIL, Saint-Aubin, Boite Postale 48, 91192 Gif-sur-Yvette Cedex, France.*

²*Unité Mixte de Physique, CNRS, Thales, Univ. Paris-Sud, Université Paris-Saclay,
91767 Palaiseau, France*

ABSTRACT

Antiferromagnetic (AFM) materials are interesting for data storage application because their resilience against external magnetic field and they produce zero stray field due to compensated moments. But exploiting magnetic properties of AFM materials requires larger current density and energy consumption than ferromagnetic (FM) materials. Consequently, the use of Synthetic Antiferromagnetic (SAF) systems, which holds some of AFM advantages, appears as a good compromise. The RKKY AF coupling between the two ferromagnetic films composing a SAF could lead to an enhanced domain wall velocity that is linked with chiral stability [1] or to the stabilization of small AF skyrmions [2].

It has been recently demonstrated that the amplitude and sign of the circular dichroism in X-ray resonant magnetic scattering (XRMS) give direct information on the type (i.e. Néel or Bloch) and on the winding (clockwise or anticlockwise) of the chirality [3-4]. In this contribution, we demonstrate that the same approach is also valid for SAF system and allow extracting the chirality of the spin spiral in these SAF, which is not an easy task with the most of the recently developed approach to investigate chiral magnetic properties in thin films. Temperature dependence of the dichroic signal of XRMS is also reported showing how the evolution in temperature of the different magnetic interactions at play i.e. magnetic anisotropy, interfacial chiral interaction and exchange interaction lead to significant modifications of the properties of the spin textures stabilized in such SAFs.

REFERENCES

- [1] S. Krishnia et al. "Role of RKKY torque on domain wall motion in synthetic antiferromagnetic nanowires with opposite spin Hall angles", *Nat. Sci. Rep.* 7, 11715 (2017).
- [2] W. Legrand et al., "Room-temperature stabilization of antiferromagnetic skyrmions in synthetic antiferromagnets" *Nature Mat.* 19, 34 (2020)
- [3] J.Y. Chauleau et al. "Chirality in magnetic multilayers probed by Symmetry and the amplitude of dichroism in X-ray Resonant Magnetic scattering", *Phys. Rev. Lett.* 120, 037202 (2018).
- [4] W. Legrand et al. "Hybrid chiral domain walls and skyrmions in magnetic multilayers", *Science Adv.* Vol 4, no.7 (2018).

Towards the Quantification of Small Structural Distortions in Bimetallic Prussian Blue Analogs by XMCD at the Transition Metal K-edge

A. N'Diaye, A. Bordage, A. Bleuzen

*Institut de Chimie Moléculaire et des Matériaux d'Orsay, Université Paris Saclay, CNRS
Bât 420, rue du Doyen Georges Poitou, 91 Orsay, France*

ABSTRACT

CoFe Prussian Blue Analogues (PBA) ($X_yCo_4[Fe(CN)_6]_{(8+y)/3} \cdot nH_2O$) exhibit photomagnetic properties due to a photo-induced metal-metal charge transfer when the stoichiometry is well-adjusted. These properties depend on, and therefore can be controlled by, small structural distortions of the A-NC-B linkage (Figure 1) induced by chemical or physical pressure. Nevertheless, these distortions can hardly be characterized by classical structure-characterization techniques because (i) the distortions are very small and (ii) the degree of disorder in PBAs is significant. X-Ray Magnetic Circular Dichroism XMCD at the Transition Metals (TM) K-edge has been found to be sensitive to them, as shown by the significant variations of the Fe and Ni K-edges signals of NiFe PBAs under increasing hydrostatic pressure^{1,2}. However, the information contained in the XMCD signals at the TM K-edge is not well understood. In order to better understand these signals and disentangle the different effects originating them, we are using PBAs as model compounds, in which one parameter at a time can be varied thanks to their versatile chemistry. We initiated this study by the investigation of a series of non-photomagnetic PBAs ($A_4[Fe(CN)_6]_{2.7}$, A = Mn, Co, Ni, Cu) to study the effect of the 3d orbital electronic structure of the A ion on the XMCD signals, with measurements at both the A and Fe K-edges.

We will present our first results on the XMCD signals at the A and Fe K-edge of this series, recorded on the ODE beamline. Furthermore, we combined these data with other XAS experiments from FAME-UHD (French CRG beamline@ESRF) and SAMBA. FAME-UHD offers highly resolved spectra thanks to their crystal analyzer spectrometer, thus bringing information on the electronic structure and site symmetry thanks to the pre-edge analysis. On SAMBA, we measured the EXAFS signal in order to have quantitative information on the local environment of each TMs (coordination number, distance between the TM and its neighbours...).

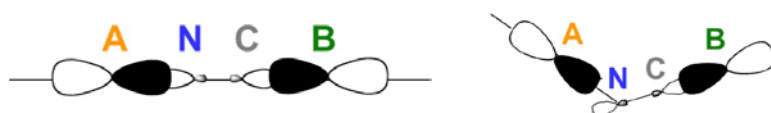


Figure1: Structural distortion of the A-NC-B linkage in PBAs

REFERENCES

1. D. Cafun, J. Lejeune, J-P. Itié, F. Baudelet, A. Bleuzen, *J. Phys. Chem. C* **117**, 19645-19655 (2013)
2. A Bordage, L. Nataf, F. Baudelet and A. Bleuzen, *J. Phys. Conf. Series* **712**, 012109 (2016)

Photoionization and Dissociative Photoionization of Methylketene and its Dimer in the Gas Phase: Theory and Experiment.

I. Derbali¹, H. R. Hrodmarsson², L. Poisson³, M. Hochlaf⁴, M. Schwell⁵,
M-C. Gazeau⁵, J-C. Guillemin⁶, M. E. Alikhani¹, E-L. Zins¹

¹ MONARIS UMR 8233 CNRS, Sorbonne Université,
4 place Jussieu, 75252 Paris Cedex 5, France.

² Synchrotron SOLEIL, L'Orme des Merisiers, 91192 Saint Aubin, Gif-sur-Yvette, France.

³ LIDYL, CEA, CNRS, Université Paris-Saclay, CEA Saclay, 91191 Gif-sur-Yvette, France.

⁴ Université Paris-Est, Laboratoire Modélisation et Simulation Multi Echelle, MSME UMR 8208 CNRS,
5 bd Descartes, 77454 Marne-la-Vallée, France.

⁵ LISA UMR CNRS 7583, Université Paris Est Créteil and Université Paris Diderot, Institut Pierre
Simon Laplace, 61 Avenue du Général de Gaulle, 94010 Créteil, France.

⁶ ISCR UMR 6226 CNRS, École Nationale Supérieure de Chimie de Rennes,
11 Allée de Beaulieu, 35708 Rennes Cedex 7, France.

ABSTRACT

Methylketene, C_3H_4O , as well as some of its isomers¹, have been detected in the interstellar medium in several objects. In order to further understand the observed abundances and chemical reactions that may take place in these dilute media, we investigated the single photon ionization of the C_3H_4O molecule and of its dimer, $(C_3H_4O)_2$, in the gas-phase, in the 8.7-15.5 eV energy range. Experiments have been carried out using the DELICIOUS3 spectrometer², in connection with the DESIRS beamline at SOLEIL. We measured the Slow Photoelectron spectra (SPES) of these molecular species and of their fragments in coincidence. In an effort to provide an accurate structural and spectroscopic characterization of C_3H_4O and $(C_3H_4O)_2$ molecules and the corresponding cationic species, state-of-the-art computations have been carried out.³⁻⁶ The ionic fragmentation mechanisms of C_3H_4O and $(C_3H_4O)_2$ have been also studied. The calculated appearance energies of the fragments are in excellent agreement with the experimental data. The theoretical characterization of the electronic excited states of the cationic monomer was used to assign the SPES spectra. We are therefore confident that the highly accurate spectroscopic data provided herein can be useful to interpret astrophysical abundances of C_3H_4O , its non-covalent dimer and their cations in the various interstellar environments where they may be detected.

REFERENCES

- ¹ Bermúdez, C., Tercero, B., Motiyenko, R. A., Margulès, L., Cernicharo, J., Ellinger, Y., and Guillemin, J. C. 2018, 619, A92.
- ² G. A. Garcia, B. K. Cunha de Miranda, M. Tia, S. Daly, L. Nahon, Rev. Sci. Instr., 2013, 84, 053112.
- ³ Mahjoub, A., Hochlaf, M., Garcia, G. A., Nahon, L., & Poisson, L. (2012), J. P. C. 2012, 116(34), 8706-8712.
- ⁴ Bellili, A., Gouid, Z., Gazeau, M. C., Bénilan, Y., Fray, N., Guillemin, J. C., ... & Schwell, M., PCCP. 2019, 21(47), 26017-26026.
- ⁵ Mahjoub, A., Hochlaf, M., Poisson, L., Nieuwjaer, N., Lecomte, F., Schermann, J. P., Grégoire, G., Manil, B., and Nahon, L., C. P. C. 2011, 12(10), 1822-1832.
- ⁶ I. Derbali, H. R. Hrodmarsson, Z. Gouid, M. Schwell, M. C. Gazeau, J.-C. Guillemin, M. Hochlaf, M. E. Alikhani and E.-L. Zins. PCCP. 2019, 21, 14053–14062.

Impacts of the Non-classical Nucleation Mechanism of Cerium Oxalate

M. Durelle^{1,2}, S. Charton², D. Carrière¹

1. NIMBE, CEA Saclay, 91191 Gif sur Yvette cedex, France

2. CEA, DEN, DMRC, Univ. Montpellier, Marcoule, France

ABSTRACT

Crystal precipitation in solution is a common process in industry which remains ill-understood. In the last decades, many efforts were made to design precipitation reactors using numerical simulations[1] in order to avoid using trial and error methods, especially for the precipitation of radioactive compounds like the plutonium oxalate. But all the process models are built on the classical view of crystallization, where thermal fluctuations of the reactive solution lead to the formation of some “clusters” of monomers with the same symmetry as the crystal[2]. In other words, the classical nucleation theories (CNT) overlook by construction any possible amorphous intermediate between the ions in solution and the final crystals.

This strong hypothesis of the CNT is more and more questioned. For many systems, including cerium oxalate[3], the nucleation occurs through amorphous states which are currently ignored by the CNT and which lead in some cases to a misestimation of the nucleation rate up to 400 orders of magnitude[4]. The strong mismatch between experimental observations and the CNT potentially impacts deeply the process models; but the implications have not been assessed yet. Progress is hampered by the lack of structural data on the elusive intermediate states, because of their short formation time ($\ll s$) and their characteristic sizes ranging from the Angstrom scale to the micron scale.

Here, we tackle this challenge by studying the nucleation of cerium oxalate using a new “plug and play” apparatus which allow the analysis by SAXS from 250ms to 5min. We show crystallization of cerium oxalate involves transient disordered states which increase the induction time of at least one order of magnitude in comparison with the one measured with the classical view of nucleation. This finding implies that the industrial process models misestimate strongly the driving force of nucleation (supersaturation), because they overlook a pseudo-equilibria between the transient disordered states, the solution and/or the crystal.

REFERENCES

- [1] M. Bertrand, E. Plasari, O. Lebaigue, P. Baron, N. Lamarque, et F. Ducros, « Hybrid LES–multizonal modelling of the uranium oxalate precipitation », *Chem. Eng. Sci.*, vol. 77, p. 95–104, 2012.
- [2] K. F. Kelton et A. L. Greer, *Nucleation in condensed matter applications in materials and biology*. Oxford, U.K.: Pergamon, 2010.
- [3] I. Rodríguez-Ruiz, S. Charton, D. Radajewski, T. Bizien, et S. Teychené, « Ultra-fast precipitation of transient amorphous cerium oxalate in concentrated nitric acid media », *CrystEngComm*, vol. 20, n° 24, p. 3302–3307, 2018.
- [4] W. J. E. M. Habraken *et al.*, « Ion-association complexes unite classical and non-classical theories for the biomimetic nucleation of calcium phosphate », *Nat. Commun.*, vol. 4, n° 1, déc. 2013.

The Single-photon Ionisation of C₂

O.J. Harper¹, S. Boyé-Péronne¹, G.A. Garcia², H.R. Hrodmarsson²,
J-C. Loison³ and B. Gans¹

¹ Institut des Sciences Moléculaires d'Orsay, Université Paris-Saclay, CNRS

² Synchrotron SOLEIL, L'Orme des Merisiers, Saint Aubin

³ Institut des Sciences Moléculaires, Université de Bordeaux, CNRS

ABSTRACT

The C₂ carbon dimer can be found in many different environments such as flames¹, plasmas and various astrophysical media². In particular, it was the first reactive species to have been observed in a comet's coma and it lends its name to some Diffuse Interstellar Bands containing high C₂ column densities: C₂-DIBs³. Owing to the intense UV radiation in these environments, it is important to quantify the photoionisation of C₂, an important source of C₂⁺ which is more reactive with H₂ than the neutral form. However, photoionisation studies are scarce and, until now, have employed multi-photon techniques⁴.

For spin-selection reasons, it is impossible to reach the cation ground state ($X^+ \ ^4\Sigma_g^-$) from the neutral ground state ($X \ ^1\Sigma_g^+$). There are many low-lying electronic states in the cation which adds to the difficulty of studying C₂⁺. The investigation of these states and their vibronic structure of this work constitutes the first single-photon ionisation study of C₂.

The novel experimental setup is based on a flow-tube reactor coupled with the DELICIOUS III spectrometer of the DESIRS beamline⁵. F atoms produced upstream in a microwave discharge are fed into the reactor containing CH₄ where H-abstraction reactions yielding radicals can take place. Subsequent radical – radical reactions produce C₂ which is then ionised by the synchrotron radiation in the Vacuum Ultra-Violet spectral domain. C₂ is produced in both its ground state ($X \ ^1\Sigma_g^+$) and metastable state ($a \ ^3\Pi_u$) giving access to states of all spin multiplicity in the cation following photoionisation.

In this poster, I will illustrate the results of this spectroscopic study [6] including the adiabatic ionisation potential for the two lowest electronic states in C₂⁺ which are in good agreement with the recent work by Krechkivska *et al.*⁴. There is also an excellent agreement between these experimental results and theoretical results which were obtained using *ab initio* calculations and Frank-Condon simulations

REFERENCES

1. W. H. Wollaston, *Philosophical Transactions of the Royal Society of London* **92**, 365-380 (1802)
2. R. C. Hupe *et al.*, *The Astrophysical Journal* **761**, 38 (2012)
3. M. Elyajouri *et al.*, *Astrophysics and Astronomy* **616**, A143 (2018)
4. O. Krechkivska *et al.*, *The Journal of Chemical Physics* **120**, 6010-6018 (2004)
5. G.A. Garcia *et al.*, *Journal of Chemical Physics* **142**, 164201 (2015).
6. O.J. Harper *et al.*, submitted to *Journal of Chemical Physics*

Quantifying Water Ionization by Soft X-rays using a Microfluidic Device

L. Huart^{1;2;3}, C. Chevallard¹, C. Nicolas², J. Kaddissy¹,
A. Touati³, J-M. Guigner³, M.-F. Politis⁴, P. Mercere²,
J-P. Renault¹, M-A. Hervé du Penhoat³

¹NIMBE UMR CEA-CNRS 3685, Saclay, France,

²Synchrotron SOLEIL, Saint Aubin, France,

³IMPMC, Sorbonne Université, UMR CNRS 7590, MNHN, 75005 Paris, France

⁴LAMBE UMR 8587, Université d'Evry val d'Essonne & Université Paris-Saclay, 91025 Evry, France

ABSTRACT

The description of the biological effects of ionizing radiation requires a good knowledge of the dose deposition processes at both the cellular and molecular scales. However, the specific behavior of subkeV electrons which deposit their energy in nanometric volumes, remains poorly described [1]. Moreover, theoretical calculations have shown that ionizing the K-shell electrons of metal ions in solution can lead to large local production of radical and slow electron species [2]. Irradiating solutions containing metal ions, such as Mg²⁺, with monochromatic X-rays around their K edges could thus allow to investigate this process.

Liquid water samples were first irradiated in a static cell with monochromatic soft X-rays (0.2-1.4 keV) at the Metrologie beamline (SOLEIL synchrotron, France). Hydroxyl radical quantification was conducted through OH scavenging by benzoate to form the fluorescent hydroxybenzoate [3]. Yields of OH radicals exhibit a minimum around 1.5 keV, in good agreement with the literature [4, 5]. This minimum may be attributed to an increased ionization density in the photo- and Auger electrons tracks. Moreover, OH yields are found relatively independent of the benzoate concentration in the investigated range, which correspond to scavenging times from 170 ns to 170 ps.

Implementation of a new microfluidic cell in the setup has permitted to drastically increase the signal/noise ratio and our detection sensitivity. Therefore, the OH scavenging method was also applied to solutions containing or not Mg ions. By varying the X-ray energy below and above the K-shell of Mg atoms (1317 eV), the OH radicals production was measured in order to probe a threshold effect. Our results will be compared with standard gamma-rays expositions and differences will be highlighted.

REFERENCES

1. D.T. Goodhead and J. Thacker. *Int. J. Radiat. Biol. Relat. Stud. Phys. Chem. Med.* 31: 541 (1977).
2. V. Stumpf, K. Gokhberg, L. S. Cederbaum, *Nature Chemistry* 8: 237 (2016).
3. G. Louit, S. Foley, J. Cabillic, H. Coffigny, F. Taran, A. Valleix, J.-P. Renault, S. Pin. *Radiat. Phys. Chem.* 72: 119 (2005).
4. J. Fulford, P. Bonner, D. T. Goodhead, M.A. Hill, P. O'Neill. *J. Phys. Chem. A* 103: 11345 (1999).
5. J.A. LaVerne and S.M. Pimblott, *J. Phys. Chem.* 95: 3196 (1991).

Coupling an Electron Time-of-flight Spectrometer and an under Vacuum Liquid Jet for Coincidence Measurements on Solvated Biomolecules

L.Huart^{1;2;3}, A.Kumar³, F.Penent¹, I.Ismail⁴, P.Lablanquie⁴, J-P.Renault¹, M-A.Hervé du Penhoat³, C.Nicolas², J. Palaudoux⁴

¹NIMBE UMR CEA-CNRS 3685, Saclay, France,

²Synchrotron SOLEIL, Saint Aubin, France,

³IMPMC, Sorbonne Université - UPMC, UMR CNRS 7590, Paris, France

⁴LCPMR, Sorbonne Université - UPMC, UMR CNRS 7614, Paris, France

ABSTRACT

Radiation damage of biological systems is a complex multi-scale problem, not only in the spatial domain but also in the temporal domain. While interactions start at the atomic level (from atto- to femto-second), they can impact the molecular level (femto- to pico-second) and ultimately affect a cell's behavior over hours or days, culminating, in the worst case, in a full breakdown of a living organism over months to years. Photoelectron spectroscopy constitutes one of the basic experimental methods to study processes initiated by interaction of light with matter. It is widely applied in experiments or photoionization of gaseous, solid, and more recently, in liquid media [1].

The Magnetic Bottle Time-Of-Flight (MB-TOF) is specially designed to study multi-electron processes [2]. Indeed, due to its almost 4π electron collection efficiency, it is well suited to studying the early stages of an inner-shell photoionization, via coincidence techniques between the photoelectron and the resulting Auger electrons. Thus, coupled with an under vacuum liquid jet, it allows to investigate the different relaxation pathways of biomolecules in an aqueous media, after being irradiated by soft X-ray radiation [3].

We will present the first results obtained on different solutes and highlight how it is possible to clearly disentangle the liquid phase signal from the signal arising from the surrounding gas phase water [4]. Particular attention will be drawn to non-local energy transfers (between the solute and water molecules) such as interatomic coulombic decay or electron transfer mediated decay [5].

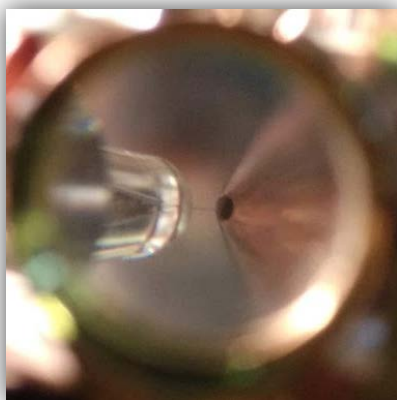


Fig 1 : Photography of the liquid jet

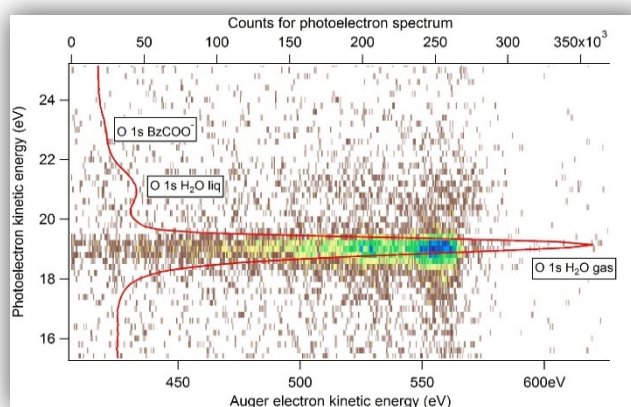


Fig. 2: 2D map representing coincidence between two electrons. O1s photoelectron spectrum (in red) recorded at 580 eV.

REFERENCES

1. G. Kumar et al., Faraday Discuss., 212, 359–381 (2018).
2. P. Lablanquie et al., J. Phys. B: At. Mol. Opt. Phys., 49, 182002 (2016).
3. H. L. Williams et al., J. Phys. Chem., 148, 194303 (2018).
4. S. Thürmer et al., Physical Review Letter, 111, 173005 (2013).
5. I. Unger et al., Nature Chemistry, 9(7), 708–714 (2017).

Light-driven Folding of G-quadruplex DNA Structures Probed by Synchrotron Radiation Circular Dichroism

K. Laouer¹, F.Wien², B.Nay,³ F.Hache¹ and P.Changenet¹

¹Laboratoire d'Optique et Biosciences (LOB), UMR7645 CNRS - U1182 INSERM - École Polytechnique – Institut Polytechnique de Paris - Route de Saclay 91128 PALAISEAU

²DISCO line, Synchrotron SOLEIL, L'Orme des Merisiers, Saint Aubin BP48, 91192 Gif-sur-Yvette

³Laboratoire de Synthèse Organique (LSO), UMR7652 CNRS –ENSTA - École Polytechnique – Institut Polytechnique de Paris Route de Saclay 91128 PALAISEAU

ABSTRACT

G-quadruplexes (G4) are particular DNA structures resulting from the stacking of several guanine quartets stabilized by metallic cations. G4 are highly polymorphic structures involved in important cellular regulation processes related to their folding mechanism. The ability to control their folding with an external stimulus such as light is therefore a promising strategy for elaboration of new anticancer therapies as well as the construction of smart self-assembled architectures. However, despite the increasing literature devoted to G4, there is still a limited number of studies taking advantage of these DNA structures. One of the main drawback arises from the partial understanding of their folding mechanism. In this context, we undertook a series of SRCD measurements on several biological relevant G4-forming sequences in the presence one non-covalent photo-switch derived from azobenzene (Fig.1.A). We identified three G4-quadruplex forming sequences derived from the human telomeric (Tel21 and Tel22) and the thrombin binding aptamer (TBA) sequences, whose conformational changes can be triggered by photoexcitation. While UV irradiation of the AZO1-Tel21 and AZO1-Tel22 complexes induces a complete unfolding of the DNA scaffold (Fig.1.B), we found that the UV excitation of the AZO1-TBA complexes instead provokes a change of the DNA topology which is consistent with the conversion from a G4 parallel topology to an antiparallel one. We also observed that the reaction is thermally reversible making this complex an ideal system for time-resolved SRCD studies

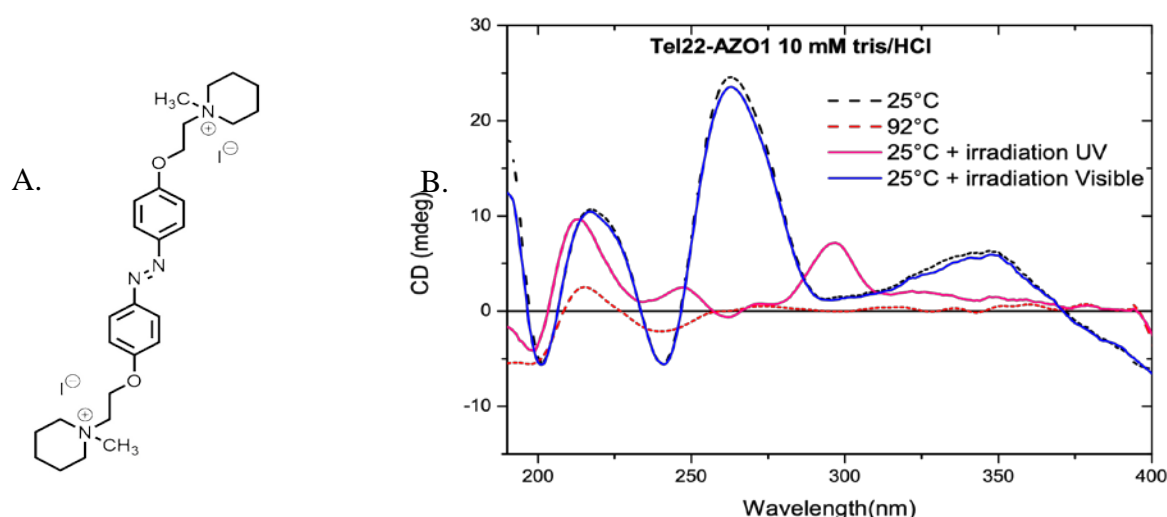


Fig.1 : A. Photosensitive azobenzene derivative (AZO1)
B. Irradiation of Tel 22 sequence in presence of AZO1 at 25°C and comparison with a spectrum obtained at 95 °C.

Excited Electronic States in Gas-phase Thiophene and Thiolane Molecules using Resonant Auger Spectroscopy

J.B. Martins¹, C.E.V. de Moura², G. Goldsztejn³, N. Sisourat¹, R. Püttner⁴, O. Travnikova^{1,5}, L. Journal^{1,5}, R. Guillemin^{1,5}, I. Ismail¹, D. Koulentianos^{1,6}, M.L. Rocco⁷, M. N. Piancastelli^{1,8}, M. Simon^{1,5} and T. Marchenko^{1,5}

¹Laboratoire de Chimie Physique-Matière et Rayonnement, Sorbonne Université, 75005, Paris, France

²Institute de Chimie Radicalaire, Aix-Marseille Université, 13013, Marseille, France

³ILIDYL, CEA, CNRS, Université Paris-Saclay, bât. 522, CEA Paris-Saclay, 91191 Gif-sur-Yvette, France

⁴Freie Universität Berlin, 14195, Berlin, Germany

⁵Synchrotron SOLEIL, 91190, Saint-Aubin, France

⁶Göteborg Universitet, 41296, Göteborg, Sweden

⁷Universidade Federal do Rio de Janeiro, 21941-485, Rio de Janeiro, Brazil

⁸Uppsala Universitet, 751-20, Uppsala, Sweden

ABSTRACT

In this work, we present an experimental and theoretical study of thiophene and thiolane gas-phase molecules around the resonant excitation in the sulfur *K*-shell to the lowest unoccupied molecular orbital (LUMO) and further beyond the ionization threshold through high-resolution high-energy resonant Auger spectroscopy. This experimental method enables the build of a two-dimensional (2D) Auger map, which gives a progressive evolution of the Auger spectra, and highlights the qualitative differences in the spectral lines behavior. The Auger 2D maps enable the detailed analysis of the first two excited states obtained from the promotion of the *S* 1*s* electrons to the LUMO π_{C-C}^* and (LUMO+1) σ_{S-C}^* . Comparing the excited state (*S* 1*s*⁻¹) and the final state (*S* 2*p*⁻²) for the thiophene molecule, an unexpected change in the energy order of resonantly excited orbitals is observed. The study of pyrrole in the N *K*-shell do not show such change in the energy order of resonantly excited orbitals.¹ Furthermore, a theoretical study shows the same change in the energy order of the two first unoccupied orbitals by decreasing the π_{C-C}^* energy when the relaxation effects are included.²

To understand this feature in the Auger maps, we applied quantum chemistry theoretical calculations. We choose a multi-configurational wave function method, applying a specific routine for inner-shell states (IS-CASSCF)³, in which high energy states can be obtained by constraining the occupation of the core orbitals and optimizing them during an isolated SCF step. The quality of our description for this spectroscopic problem is demonstrated by the calculation of the *K*-shell vertical transitions, which provides a good agreement with our measured absorption spectra. Electronic relaxation effects are taken into account and are shown to be essential for the accurate description of the core excitations. Preliminary results from second-order perturbation analysis of natural bond orbitals show that stabilization of the π_{C-C}^* orbital by the electron lone pairs of the sulfur atom plays an important role in the energy order of the orbitals involved in the excitation and Auger decay of thiophene excited at the *S* 1*s* shell. This effect of energy inversion observed in thiophene is expected to be general for aromatic molecules excited at the deep core shells.

REFERENCES

1. M. Mauerer et al, *J. Chem. Phys.* **99**, 3343 - 3352 (1993)
2. G. de Alti et al, *J. Chem. Phys.* **90**, 231 - 242 (1984)
3. A. B. Rocha, *J. Chem. Phys.* **134**, 024107 (2011)

Operando Quick XAS Study of Oxygen and Carbon Monoxide Activation over Bimetallic Pt-Fe Catalysts

I. Sadykov¹, A.H. Clark¹, M. Zabilskiy¹, J.A. van Bokhoven^{1,2},
O.V. Safonova^{1*}

¹Paul Scherrer Institute, CH-5232 Villigen, Switzerland;

²Department of Chemistry and Bioengineering, ETH Zurich, CH-8093 Zurich, Switzerland.

ABSTRACT

We studied carbon monoxide oxidation over Pt-Fe bimetallic catalyst supported on γ - Al_2O_3 using the operando Quick X-ray absorption spectroscopy in the dedicated cell¹. This element specific time-resolved method helped us to demonstrate that under steady-state conditions Pt-Fe catalyst consists of a Fe^{2+} and Fe^{3+} species mixture coexisting with fully reduced Pt nanoparticles covered by carbon monoxide. Transient experiments at Fe K-edge consisting of periodic switches between carbon monoxide and carbon dioxide / oxygen gas mixtures helped us to correlate the changes in the Fe^{2+} and Fe^{3+} concentrations with the carbon dioxide conversion (Fig. 1). During the same experiments, Pt L_3 edge XAS demonstrated no changes in Pt coverage by carbon monoxide. Therefore, we propose that oxygen activation over Pt-Fe catalysts is mediated by $\text{Fe}^{3+}/\text{Fe}^{2+}$ redox couple. Our results suggest that during carbon monoxide oxidation, Fe^{2+} sites activate oxygen in a close vicinity of Pt nanoparticles supplying carbon monoxide. These sites can be found with higher probability in Fe^{2+} state. This is because oxygen activation, resulting in oxidation of Fe^{2+} into Fe^{3+} state, is slower than the Fe^{3+} reduction taking place during carbon monoxide oxidation completing the catalytic cycle.

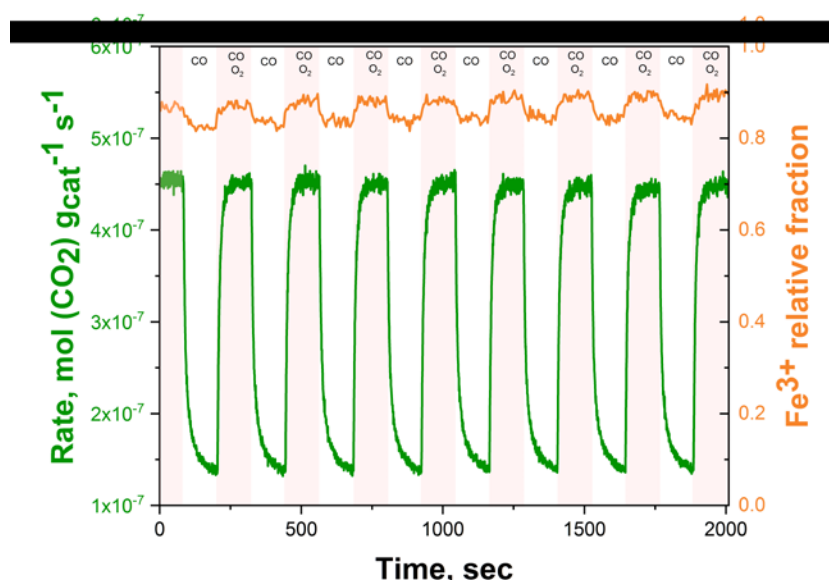


Figure 1. Transient oxygen cut-off experiment for the 1:1 Pt-Fe / γ - Al_2O_3 catalyst at 373 K.

REFERENCES

1. G. L. Chiarello, M. Nachtegaal, V. Marchionni, L. Quaroni and D. Ferri, Rev. Sci. Instr. **85**, 074102 (2014).

Migration and Speciation of Anthropogenic Uranium in Natural Soils

S. Bayle^{*(1,2,3)}, P-L. Solari⁽²⁾, P. Crançon⁽³⁾, M-R. Beccia⁽¹⁾,
C. Den Auwer⁽¹⁾

(1) *Institut de Chimie de Nice, UMR 7272, Université Côte d'Azur, 06108 Nice, France*

(2) *Synchrotron Soleil L'Orme des Merisiers, Saint-Aubin, BP 48,
F-91192 Gif-sur-Yvette Cedex, France*

(3) *CEA, DAM, DIF, F-92297 Arpajon, France*

ABSTRACT

Uranium is a radioelement of the actinide family. The half-life of ^{238}U is 4.5 billion years and it is the major isotope of natural uranium. As a consequence, ^{238}U has a very low radiotoxicity. But the health risk associated with ^{238}U is mainly due to its chemical toxicity.

During last decades, several events have caused significant uranium contamination in the environment. In addition to nuclear accidents and weapon tests, uranium metal (U(0)) has been used extensively in wars (First Gulf War, Iraq War, Kosovo War, etc.) as an anti-armour weapon, resulting in significant pollution of the environment.

Long-term studies of uranium behavior in soils have been conducted since the 1950s (particularly at the Hanford site in the USA)⁽¹⁻²⁾. The mechanisms governing its speciation and migration are shown to be highly sensitive to chemical conditions such as pH, redox and ionic strength, and this strongly site-dependent. Forecasting migration models that take speciation into account are therefore difficult to implement, making health risk assessment complicated.

The objective of my research project is to understand, at several spatial scales (ranging from micrometers to meters) the mechanisms governing the migration of uranium particles deposited on the soil surface as U(0) and its evolution over time. In order to achieve this, two strategies of research have been privileged:

- a field study of contaminated area, where the distribution and speciation of anthropogenic uranium was determined by XAFS and TLRFS spectroscopies as a function of soil depth.

- a laboratory study, where columns composed of a model soil and a solid uranium source term are leached to simulate the conditions of dissolution and subsurface uranium migration. The objective of this approach using micro XAS imaging is to observe at the micrometer scale the first changes in uranium speciation.

The combination of those data (field study and model columns) is necessary to extrapolate the migration modelling to larger environmental scales.

REFERENCES

- 1- NEWCOMB, Reuben Clair, STRAND, Jesse Richard, et FRANK, F. J. *Geology and ground-water characteristics of the Hanford Reservation of the US Atomic Energy Commission, Washington*. US Govt. Print. Off., 1972.
- 2- FRESHLEY, M. D. et THORNE, P. D. *Ground-water contribution to dose from past Hanford Operations*. Pacific Northwest National Lab.(PNNL), Richland, WA (United States), 1992.

* contact: simon.bayle@univ-cotedazur.fr

Molecular Recognition of a New Class of Nuclear Localization Signals by Transportin 1

A. Mboukou, M. Catala, C. Tisné & P. Barraud

*Laboratoire d'Expression Génétique Microbienne, Institut de Biologie Physico-Chimique, IBPC, CNRS, Université de Paris, 75005, Paris, France.
E-mail : allegra.mboukou@ibpc.fr*

ABSTRACT

A hallmark of eukaryotic cells is the physical separation of the genetic material and its associated proteins in the nucleus from the translational machinery located in the cytoplasm. Trafficking of macromolecules between the nucleus and cytoplasm through nuclear pore complexes (NPCs) is a selective and efficient process orchestrated by transport receptors [1]. Transportin 1 (Trn1), a transport receptor involved in nuclear import, binds directly to its cargos without adaptors in the cytoplasm, targets them to the nucleus through the NPC and releases them in the nucleus. Trn1 recognizes a well-characterized group of nuclear localization signals (NLSs) called PY-NLSs [2]. In addition, Trn1 also mediates the import of multiple proteins lacking a PY-NLS (non PY-NLSs), including some ribosomal proteins, histones and viral proteins [3]. Although it is clear that Trn1 must adapt to recognize different classes of NLSs, the molecular mechanisms controlling the recognition of non PY-NLSs by Trn1 are poorly characterized. With the help of X-ray crystallography and other biophysical methods, we want to characterize the interaction between Trn1 and a set of non PY-NLSs. We also aim at defining a set of rules governing the recognition of non PY-NLSs by Trn1. Our latest results on this topic will be presented.

REFERENCES

- [1] A. Cook, F. Bono, M. Jinek and E. Conti. (2007). Structural Biology of Nucleocytoplasmic Transport. **Annual Review of Biochemistry** 76:647-671
- [2] B. Lee, A. Cansizoglu, K. Suel, T. Louis, Z. Zhang and Chook. (2006). Rules for Nuclear Localization Sequence Recognition by Karyopherin β 2. **Cell** 126:543-558
- [3] L. Twyffels, C. Gueydan and V. Kruys. (2014). Transportin-1 and Transportin-2: Protein nuclear import and beyond. **FEBS Letters** 588:1857-1868

Structural and Functional Insights on the NHEJ Network around the Ku-DNA Hub

S. Zahid^{a,b,c,d}, V. Ropars^a, C. Nemoz^a, A. Gontier^a, S. Combet^b,
L.M.G. Chavas^c, J-B. Charbonnier^a

(a) *Institute for Integrative Biology of the Cell (I2BC), Institute Joliot, CEA, CNRS, Univ.Paris-Sud, Université Paris-Saclay, 91191, Gif-sur-Yvette cedex, France;*

(b) *Laboratoire Léon-Brillouin (LLB), CEA-Saclay, UMR 12 CNRS, 91191, Gif-sur-Yvette cedex, France ;*

(c) *Synchrotron SOLEIL, L'Orme des Merisiers, Saint-Aubin – BP 48, 91192 Gif-sur-Yvette Cedex, France ;*

(d) *Fellowship LLB-SOLEIL/CNRS*

ABSTRACT

Chemotherapy or radiotherapy treatments aim at generating DNA double-strand breaks (DSBs). Tumor cells are more sensitive to DSBs than healthy cells due to their phenotype and genotype [1]. One important axis in radiobiology is to combine radiation therapy with inhibitors of the DNA repair pathways to increase radio-sensitivity and overcome radiation resistance of some cancer cells [2]. Our objectives is to unveil the molecular mechanism off the NHEJ pathway (Non Homologue End Joining) and to characterize new specific inhibitors of this pathway. Several recent studies showed a central role of Ku70-Ku80 (Ku) heterodimer in the NHEJ for DSB recognition and in downstream DNA events (processing and ligation steps). Ku can recruit several enzymes of the NHEJ pathway through direct interactions and thus acts as a hub that coordinates the whole NHEJ pathway [3]. Many interactions involve motifs called KBM (Ku Binding Motif).

Our laboratory recently determined the first crystal structures of Ku-DNA complexes in interaction with peptides containing the KBM. We thus determined the structure of Ku-DNA with the KBM of the ligation factor XLF and of the processing factor APLF [4]. Our objectives is now to further characterize the interaction network mediated by Ku in the NHEJ. The poster presents our recent progress on the interactions between Ku and the NHEJ factors (peptides or domains) containing a KBM: the ligation factor PAXX and the WRN helicase [5]. We characterized the affinity of several PAXX and WRN KBMs with Ku by ITC. We also present our progress on the analyses of Ku-DNA-KBMs complexes by combining SAXS, Crystallography and Electron microscopy.

REFERENCES

1. Luo et al., "Principles of cancer therapy: oncogene and non-oncogene addiction", *Cell* 136, 823-837 (2009).
2. Morgan and Lawrence, "Overcoming Radiation Resistance by Targeting DNA Damage Response Pathways", *Clin. Cancer Res.* 21, 2898-2904 (2015).
3. Frit et al., "Plugged into the Ku-DNA hub: The NHEJ network", *Prog. Biophys. Mol. Biol.* S0079-6107, 30251-7 (2019).
4. Nemoz et al., "XLF and APLF bind Ku80 at two remote sites to ensure DNA repair by non-homologous end joining", *Nat. Struc. Mol. Bio.* 25, 971-980 (2018).
5. Tadi et al., "PAXX is an Accessory c-NHEJ Factor that Associates with Ku70 and Has Overlapping Functions with XLF", *Cell Rep.* 17, 541-555 (2016).

List of Other Posters

- PO-01** Deformation measurement of a young wheat grain using a multi-photon microscope
H. Chauvet
- PO-02** Phase transition in a colloidal membrane: Where is the hexatic phase ?
D. Constantin
- PO-03** HR X-ray tomography of calcareous biocrystals grown on genetically controlled organic substrates
Y. Dauphin
- PO-04** Electron radiation effects on crystal structure of brucite and portlandite
E. Garcia-Caurel
- PO-05** Self-assembly of faceted nanocrystals
C. Hamon
- PO-06** Kinetics of dynamics processes and live imaging
F. Jamme
- PO-07** U Migration Processes in U Mine Waste Rocks: Impact of the Weathering Conditions on the Main U-bearing Phases
F. Lahrouch
- PO-08** Real-case applications at SAMBA beamline of FASTOSH, a new program to treat XAFS data relevant to geochemical & environmental studies
G. Landrot
- PO-09** Safe(r) by design of nanomaterials: The role of speciation
A. Masion
- PO-10** MAGELEC: A unique sample environment for performing RIXS under electric and magnetic field
A. Nicolaou
- PO-11** Unravelling the thermal phase transformation of alumino-germanate nanotubes
E. Paineau
- PO-12** X-ray absorption study on the origin of the deviation from Vegard's law for $U(Al_{1-x}Ge_x)_3$ solid solution
M. Pasturel
- PO-13** Structural Properties of $TbMgNi_{4-x}Co_x$ Hydrides and Deuterides
V. Paul-Boncour
- PO-14** Operando XAS investigations on Mg-based complex hydrides as anodes of solid-state Li-ion batteries
K. Provost
- PO-15** Formation of CoRu nanoalloys: A comprehensive study by UV-visible and X-ray absorption spectrometries
L. Sicard
- PO-16** Sinogram correction method for monochromatic beam of a Synchrotron X-ray source
D. N. Trinca
- PO-17** Significant band offset in 2D MoS_2 /black phosphorus heterostructure
Z. Zhang

Deformation Measurement of a Young Wheat Grain using a Multi-photon Microscope

H. Chauvet¹, C. Girousse², E. Badel³, V. Legué³
and F. Jamme¹

¹Synchrotron Soleil, ligne DISCO, Gif-sur-Yvette.

²UMR GDEC INRA/UCA, Clermont-Ferrand.

³UMR PIAF INRA/UCA, Clermont-Ferrand.

ABSTRACT

The size of grains determine the wheat yields and understanding the mechanisms which controls the growth remains a major issue. The perception of mechanical signals during early stage of grain development could be one of the growth regulator as suggested by some studies on the development of seeds of *Arabidopsis* [1, 2]. A challenge to tackle this question remains in the difficulty to image the same grain during its growth at the cellular level to study the dynamic of its shaping. Here we present preliminary results that shows: I) the possibility to follow for several hours the growth of the external cell envelopes of the same grain using a multi-photon microscope, and II) a computational method to estimate the displacement field from the images (3D + time evolution) at the surface of the grain (Figure 1).

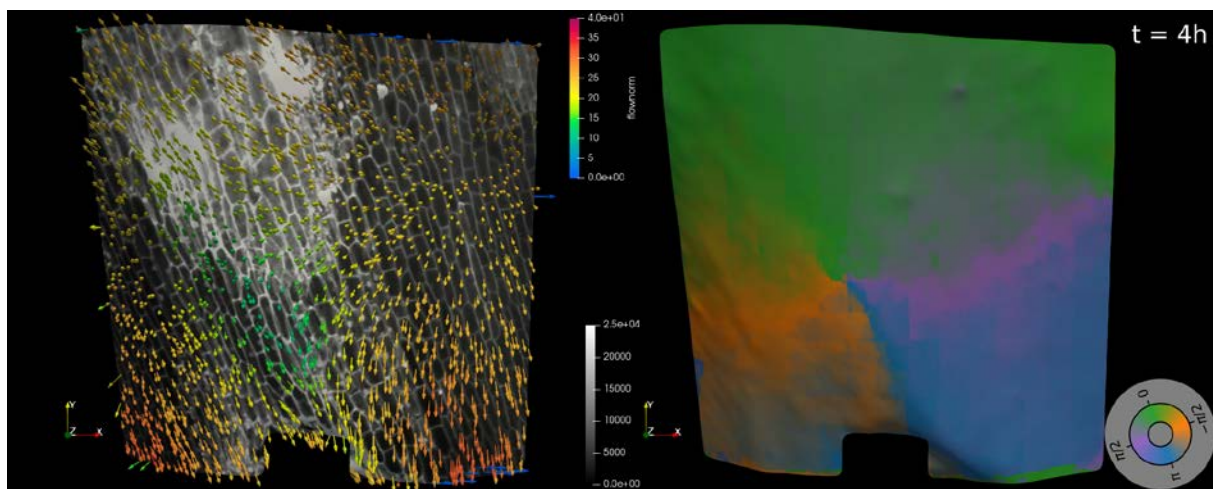


Figure 1: Estimation of the displacement field at the surface of a young grain of wheat (4h after the beginning of the experiment). **On the left**, displacement vector field showing a stretching zone with an upper part of the grain moving upward and a bottom part moving downward. **On the right**, the orientation of the same displacement field.

REFERENCES

1. Creff A, Brocard L, Ingram G (2015) A mechanically sensitive cell layer regulates the physical properties of the Arabidopsis seed coat. Nat Commun.
2. Garcia D, Fitz Gerald JN, Berger F (2005) Maternal Control of Integument Cell Elongation and Zygotic Control of Endosperm Growth Are Coordinated to Determine Seed Size in Arabidopsis. The Plant Cell 17: 52-60.

Phase Transition in a Colloidal Membrane: Where is the Hexatic Phase?

T. Gibaud¹, D. Constantin²

¹Laboratoire de Physique, Ecole Normale Supérieure de Lyon

²Laboratoire de Physique des Solides, Orsay

ABSTRACT

Using synchrotron-based small angle x-ray scattering, we study rigid *fd* viruses assembled into isolated monolayers from mixtures with a non-absorbing polymer, which acts as osmotic agent. As the polymer concentration increases we observe a direct liquid to crystal transition, without an intermediate hexatic phase, in contrast with many other similar systems, such as concentrated DNA phases or packings of surfactant micelles. We tentatively attribute this effect to the difference in stiffness. The liquid phase can be well described by a hard-disk fluid, while we model the crystalline one as a hexagonal harmonic lattice and we evaluate its elastic constants [1].

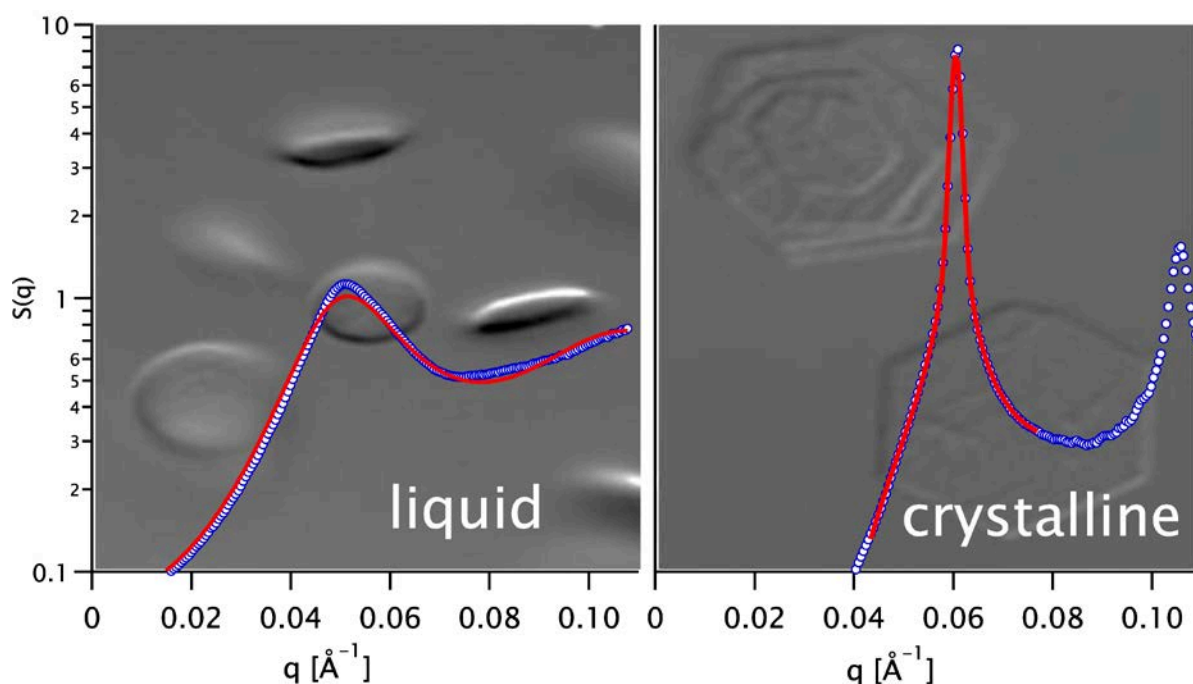


Figure: Structure factors in the liquid and crystalline phases. The structure factors $S(q)$ in the liquid (left) and crystalline (right) phases: experimental values (symbols) and fits (solid red lines). The background for each graph is an optical microscopy image of the corresponding phase.

REFERENCES

1. T. Gibaud and D. Constantin, *J. Phys. Chem. Lett.* **9**, 4302-4307 (2018).

HR X-ray Tomography of Calcareous Biocrystals Grown on Genetically Controlled Organic Substrates

J.P. Cuif¹, Y. Dauphin¹, K. Medjoubi², A. Somogyi²,
C. Lo³, D. Saulnier D.⁴

¹ *Museum National Histoire Naturelle 57 rue Cuvier 75005 Paris;*

² *Synchrotron SOLEIL Saint Aubin;*

³ *DRM Papeete, Polynesia ;*

⁴ *IFREMER Vairao Polynesia*

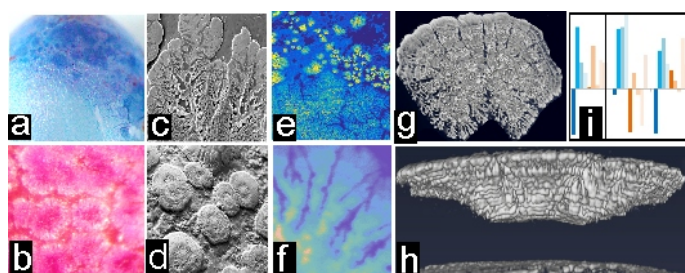
ABSTRACT

During the last century many attempts were made to produce synthetic calcareous units with morphological patterns and physical properties similar to those that living organisms produce with precisely controlled structure and mineralogy. Among them, the aragonite tablets of the nacre (the pearl forming unit) is the best known. To date none of these attempts succeeded in producing acceptable copy of the natural “bio-crystals” that are actually three-dimensional molecular architectures.

Complexity of the biochemical blends that drive the formation of these calcareous crystal-like units contributes to explain these repeated failures. Another cause is rooted in the fact that none of these natural biocrystals follows the crystallographic growth rules. Instead of being formed by a one-step crystallization (as expected in the experiments) they are produced through a sequential process, each step of which being driven by a specific group of genes producing the appropriate molecular assemblage.

Pearl cultivation offers a remarkable experimental field to overcome this complexity: the proposed poster aims at explaining how NANOSCOPIUM takes place in the ongoing three-partner collaboration with Polynesian Institutions dedicated to pearl cultivation and the Museum National d'Histoire Naturelle.

Pearls are produced by cutting a small piece of the nacre-producing epithelium of a pearl-oyster and placing it within the body of another animal of the same species. Actually long and various mineralization trajectories are often needed before returning to production of nacre: studying this process offers an exceptional opportunity to establish a direct relationship between gene activity, biochemistry of the organic secretions by the mineralizing tissue and microstructure of the resulting minerals.



a-b: Biochemical characterizations of pearl surfaces; a: Coomassie blue, b: Schiff dye. **c-d:** SEM views of “pre-nacre” mineral units. **e-f:** NANOSCOPIUM maps. e: Sr, f: Ca

g-h: NANOSCOPIUM tomography.
i: Diversity in expression of the calcifying genes.

With essential analytical advantage of an infra-micrometric resolution, NANOSCOPIUM provides relevant structural and compositional data ensuring the link between biochemical characterization of the mineralizing secretions (a, b), the optical and SEM views of the earliest mineral production (c, d) and diversity of the gene expressions (i).

Recent papers [1, 2] illustrate the ability of the NANOSCOPIUM beamline to contribute to this bio-crystallographic investigation.

REFERENCES

1. Cuif, Dauphin, Luquet, Medjoubi, Somogyi, 2018 *Minerals*, 8, 370; doi:10.3390/min8090370
2. Cuif, Dauphin, Lo, Luquet, Medjoubi, Somogyi et al. *Aquaculture Research*, doi: 10.1111./ARE.1439

Electron Radiation Effects on Crystal Structure of Brucite and Portlandite

E. Garcia-Caurel¹, M.-N. de Noirfontaine², M. Courtail²,
S. Tusseau-Nenez³, O. Cavani², B. Boizot², F. Dunstetter²,
F. Borondics⁴, D. Gorse-Pomonti²

¹LPICM, CNRS, Ecole Polytechnique, IP Paris, F-91128, Palaiseau France,

²LSI, CEA/DRF/IRAMIS CNRS, Ecole Polytechnique, IP Paris, F-91128, Palaiseau France,

³PMC, CNRS, Ecole Polytechnique, IP Paris, F-91128, Palaiseau France,

⁴SMIS beam line, Synchrotron SOLEIL, Saint-Aubin, 91192, Gif-sur-Yvette France

ABSTRACT

Brucite $\text{Mg}(\text{OH})_2$ and portlandite $\text{Ca}(\text{OH})_2$ are isomorphous layered hydroxide compounds. Brucite is known to be stable under pressure up to 78 GPa whereas portlandite exhibits a reversible pressure-induced crystalline-amorphous transition at 12 GPa. But decomposition on heating of portlandite occurs at higher temperature than for brucite. Here we study their stability under irradiation by associating IR microscopy and X-ray diffraction. Commercial powders are electron-irradiated at 2.5 MeV, room temperature and high dose rate ($\sim 10^8$ Gy/h) using the accelerator NEC Pelletron of the SIRIUS platform (Ecole Polytechnique, Palaiseau) [1]. Both compounds are radiation resistant up to the highest dose (~ 15 GGy for brucite, ~ 8.5 GGy for portlandite). Only minor radiation effects are detected, essentially in brucite. Radiation damages in portlandite are found to be comparable to the ones observed by heating the powder, at least up to 3.5 GGy for which an effective temperature of 130°C is observed. This is definitely not the case in brucite for which the XRD study reveals i) a net dilatation along the c-axis but at the same time a contraction in the basal plane, ii) some diffuse scattering over a wide angular range compatible with some disorder in the H-sublattice, a result confirmed by the IR study revealing also that the onset of dehydroxylation should be attained at 15 GGy [2]. The results of the XRD and IR microscopy study are detailed. Hypotheses regarding the underlying damage mechanisms are formulated.

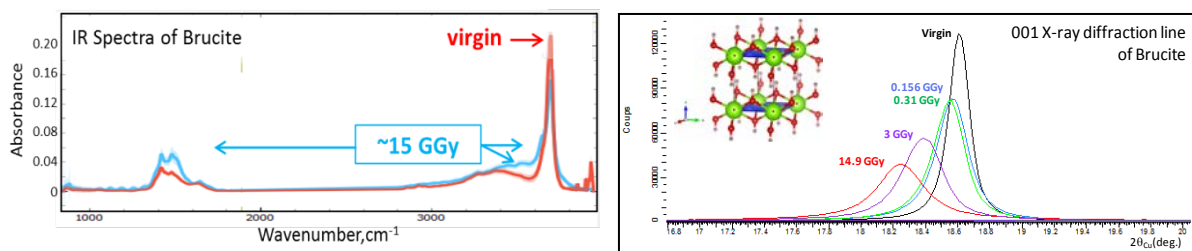


Figure.; Left: IR spectra of a non-irradiated and an electron irradiated brucite sample to a very high dose; Right: Evolution of the 001 X-ray diffraction line of a brucite sample with the absorbed dose.

REFERENCES

1. M.-N. de Noirfontaine et al. J. Nucl. Mater. 509 (2018) 78-93.
2. M.-N. de Noirfontaine et al. Submitted to Appl. Clay Sci.

Self-assembly of Faceted Nanocrystals

J. Lyu, C. Goldmann, D. Constantin, C. Hamon

MATRIX Team, CNRS, Laboratoire de Physique des Solides, UMR 8502,
Université Paris Sud, 91405 Orsay

ABSTRACT

Tailoring the crystal structure of plasmonic nanoparticle superlattices is a crucial step in controlling the collective physical response of these nanostructured materials. Various strategies can achieve this goal for isotropic nanoparticles, but few of them have been successful with anisotropic building blocks. In this work we use hybrid particles,¹ consisting of gold nanorods encased in silver shells with a thickness that can be controlled from a few atomic layers to tens of nanometers. The particles were synthesized, characterized by a combination of techniques and assembled into supercrystals with a smectic B configuration, i.e. a 2D in-plane periodic order without interplane lateral correlations. We showed that, by tuning the silver shell thickness, the in-plane order can be changed from hexagonal to square and the lattice parameters can be adjusted. The spatial distribution of the supercrystal was systematically studied by optical and electron microscopy and by small-angle X-ray scattering. Through optimized surface chemistry, we obtain homogeneous, millimeter-size films of standing nanoparticles, which hold promise for all applications using plasmon-enhanced technologies.

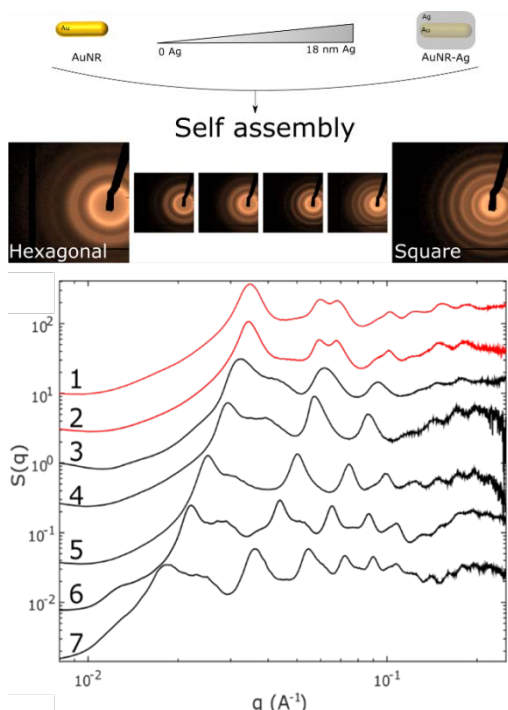


Figure 1. Gold nanorods are prepared by colloidal chemistry and coated with an Ag shell. This transform the morphology of the nanoparticles which evolves from an octagonal cross section to a square cross section. This allow to tune the lattice symmetry and core to core-distances.

REFERENCES

- ¹ Hamon, C., C. Goldmann, et al. (2018). "Controlling the symmetry of supercrystals formed by plasmonic core-shell nanorods with tunable cross-section." *Nanoscale* 10(38): 18362-18369.

Kinetics of Dynamics Processes and Live Imaging

F. Jamme¹, H. Chauvet¹, P. Montaville¹, A. Giuliani^{1,2},
V. Rouam¹, F. Wien¹, M. Réfrégiers¹

¹Synchrotron SOLEIL, DISCO beamline, L'Orme des Merisiers, 91192 Gif-sur-Yvette, France

²UAR 1008 CEPIA, INRA, Nantes 44316, France

ABSTRACT

Synchrotron Deep-UV (DUV) fluorescence opens up new possibilities because it does not need external specific probes or labelling but instead allows use of the intrinsic fluorescence that exists for many biomolecules when excited in this wavelength range. Label free autofluorescence detection is of particular interest in analytical chemistry and biology because it does not need chemical linking of a probe to the molecule of interest.

DUV live imaging, provides a window into the spatially complex, rapidly evolving physiology of the cell that structural imaging alone cannot. Observing this physiology directly involves inevitable trade-offs of spatial resolution, temporal resolution, and phototoxicity. This is especially true when imaging in three dimensions, which is essential to obtain a complete picture of many dynamic subcellular processes.

DISCO team has worked for better integration of experiments on multi-beamlines. It started with Synchrotron Infrared (SMIS) and multimodal imaging, supported with the development of dedicated registration algorithms. Some imaging projects were also possible only by coupling analysis with hard X-Ray imaging at DIFFABS. Since a couple of years, more and more links appear with the two crystallography beamlines, it was obvious for SRCD but with the possibility to image microcrystals in DUV, new projects are built jointly.

UV SIM light-sheet microscopy will allow rapid, super-resolution imaging of dynamics processes with negligible photobleaching and photo-toxicity. Coupled to complementary techniques, integrative biology at SOLEIL will provide a crucial window into the physiology of living samples and many biological processes.

REFERENCES

1. J. Vergalli, E. Dumont, J. Pajović, B. Cinquin, L. Maigre, M. Masi, M. Réfrégiers, J-M. Pagès (2018) Quantification of antibiotic fluorescence in intact cells for the characterization of translocation across bacterial membranes. *Nature Protocols*, 13, 1348
2. M. Masi, M. Réfrégiers, K.M. Pos, J-M. Pagès (2017) New insights in antibiotic resistance associated to membrane permeability *Nature Microbiology* 2: 17001
3. Dumont, E.; Vergalli, J.; Conraux, L.; Taillier, C.; Vassort, A.; Pajović, J.; Réfrégiers, M.; Mourez, M.; J-M., Pages (2018) Antibiotic and efflux: Combined spectrofluorimetry and mass spectrometry to evaluate the involvement of concentration and efflux activity in antibiotic intracellular accumulation *Journal of Antimicrobials Chemotherapy*,
4. Dumont, E., Vergalli, J., Pajovic, J., Bhamidimarri, S.P., Morante, K., Wang, J., Lubriks, D., Suna, E., Stavenger, R.A., Winterhalter, M., Réfrégiers, M., Pagès, J.M. (2019) "Mechanistic aspects of maltotriose-conjugate translocation to the Gram-negative bacteria cytoplasm" *Life Science Alliance.*, 2(1): art.n° e201800242
5. Devaux, M.F., Jamme, F., André, W., Bouchet, B., Alvarado, C., Durand, S., Robert, P., Saulnier, L., Bonnin, E., Guillon, F. "Synchrotron Time-Lapse Imaging of Lignocellulosic Biomass Hydrolysis: Tracking Enzyme Localization by Protein Autofluorescence and Biochemical Modification of Cell Walls by Microfluidic Infrared Microspectroscopy" *Frontiers in Plant Science.*, 9: art.n° 200. (2018).
6. Chabbert, B., Habrant, A., Herbaut, M., Foulon, L., Aguié-Béghin, V., Garajova, S., Grisel, S., Bennati-Granier, C., Gimbert-Herpoël, I., Jamme, F., Réfrégiers, M., Sandt, C., Berrin, J.G., Paës, G. "Action of lytic polysaccharide monooxygenase on plant tissue is governed by cellular type" *Scientific Reports.*, 7: art.n° 17792. (2017).
7. Flourey, J., Bianchi, T., Thévenot, J., Dupont, D., Jamme, F., Lutton, E., Panouillé, M., Boué, F., Le Feunteun, S. "Exploring the breakdown of dairy protein gels during in vitro gastric

U Migration Processes in U Mine Waste Rocks: Impact of the Weathering Conditions on the Main U-bearing Phases

F. Lahrouch⁽¹⁾, A. Tayal^(1,Δ), A. Kanzari^(1,‡), M. Hunault⁽²⁾, P-L. Solari⁽²⁾,
M. Descostes⁽³⁾, M. Gérard⁽¹⁾

¹Sorbonne Université, IRD, UMR CNRS 759, MNHM, IMPMC, 75005 Paris, France

^ΔPresent address: Deutsches Elektronen-Synchrotron, Notkestraße 85, 22607 Hamburg

[‡]Present address: ERAMET Research, 78193 Trappes France

²Synchrotron Soleil, L'Orme des Merisiers, BP 48, Saint-Aubin, F-91192 Gif-sur-Yvette Cedex, France

³ORANO Mining, R & D Department., Paris, France

ABSTRACT

Five decades of uranium ore extraction in France produced hundreds of millions of tons of waste rocks (essentially granitic overburden waste rocks with U-concentration below than 100 ppm). Despite of a low uranium concentration, the large volume of rocks involved and the conditions of repository require environmental monitoring to understand the long-term reactivity of the waste rocks. Indeed, weathering conditions and pedogenesis modify the mineral paragenesis by hydrolysis of primary minerals and/or by neoformation of secondary U rich minerals. The comprehension of the uranium migration mechanisms related to the arenisation and soil formation is essential to predict or prevent any pollution risk.

In natural settings, U occurs in the tetravalent [U(IV)] or hexavalent [U(VI)] oxidation states. U(IV) form, which composes the uranium ore (uraninite ($U^{IV}O_2$) or coffinite ($U^{IV}(SiO_4)_{1-x}(OH)_{4x}$), is stable in reduced media and has a low solubility. U(VI) form, named uranyl, is a di-oxo cation highly soluble and possessing affinities for metallic oxides, phosphates, carbonates or hydroxides. In the post-mining context, the uranium migration is not only ruled by the U(IV)/U(VI) equilibrium but also by the mineralogical and geochemical environment. Thus, weathering degree and hydrolyzing conditions played a primary role in the U-mineral neoformation and/or the uranyl sorption [1].

X-ray absorption spectroscopy is a powerful tool to probe the uranium speciation in the natural environment. Combined to mineralogical and geochemical studies by SEM and EDS/WDS microprobe it contributes to determine the processes of U migration and reconcentration. XANES and EXAFS analysis on powder samples of weathered waste rocks and soil samples showed that the uranium is present as uranyl form mainly associated to phosphate aggregates and/or to hydrous ferric oxyhydroxide phases. Additionally, XANES and EXAFS on petrographic thin sections of soil samples (Fig1, 2) provide in situ information of U reconcentration. Finally, this multiple approach using samples under powder and petrographic thin section show that the uranium is trapped and concentrated in secondary sub-micrometric phosphates sorbed on ferric oxides phases.

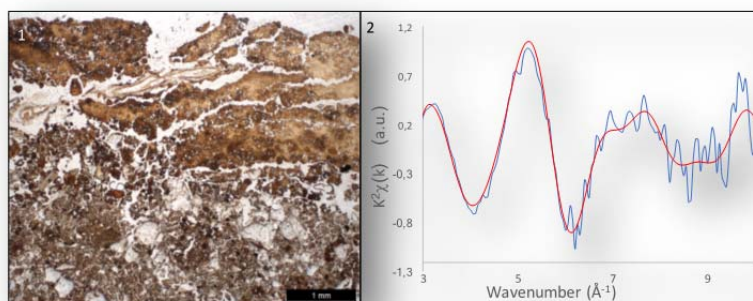


Figure 1. Petrographic thin section of a rich ferrihydrite soil sample (PPL optical photograph)

2. EXAFS spectra of a U-hotspot located on the petrographic thin section. (blue: experimental; red: fitted)

REFERENCES

[1] Allard T., Ildefonse P., Beaucaire C., Calas G. (1999) "Structural chemistry of uranium associated with Si, Al, Fe gels in a granitic uranium mine" *Chem. Geol.* 158: 81–103

Real-case Applications at SAMBA Beamline of FASTOSH, a New Program to Treat XAFS Data Relevant to Geochemical & Environmental Studies

G. Landrot

Synchrotron SOLEIL, L'Orme des Merisiers, Saint-Aubin, BP 48 91192, Gif-sur-Yvette, France

ABSTRACT

FASTOSH is a new standalone program to process X-ray Absorption Fine Structure (XAFS) spectroscopy data [1]. In addition to providing basic tools for pre-treating XAFS data that utilize imported functions from Larch [2], it features unique functionalities, including an automatic data viewer that allows to display in real-time XAFS data in 2D or 3D and progressive improvement of its signal-to-noise ratio, an interactive background-subtraction tool for Multi-Channel Analyzer (MCA) patterns collected by multi-pixel fluorescence detectors, two different auto-deglitching tools, a PCA/Target Transformation module, and a tool to post-treat data processed by the MCR-ALS Matlab Toolbox of Jaumot *et al* [3].

This program was recently deployed and tested for the first time at SAMBA beamline. The outcomes of these trials will be presented in this talk. It will be demonstrated, using real-case studies involving XAFS data collected at SAMBA beamline, how the functionalities of this program represent useful assets for research applications where the XAFS method is employed, including Geochemical and Environmental studies.

REFERENCES

1. Landrot G (2018) *Goldschmidt Abstracts*, 2018 1402
2. M. Newville, (2013) *Journal of Physics: Conference Series*.430(1), 012007.
3. Jaumot *et al.* (2005) *Chemometrics and Intelligent Laboratory Systems*, 76, 101–110

Safe(r) by Design of Nanomaterials: The Role of Speciation

A. Masion, M. Auffan, J. Rose

*CNRS CEREGE, Europole Arbois, BP 80, 13545 Aix en Provence, France
LabEx SERENADE, Europole Arbois, BP 80, 13545 Aix en Provence, France*

ABSTRACT

To address concerns about the safety of nanomaterials, the use of the safe(r) by design is attracting increasing interest in the development of these materials. Indeed, to reduce the risk associated with nanomaterials, the strategy consists in reducing the hazard or the exposure or both. While lowering the hazard may not be an option without comprising the functionality, reducing the exposure is usually easier to achieve. This often translates to design materials in which the active (and potentially hazardous) nanoparticle is surrounded by a shell /embedded in a matrix to protect against harmful effects and/or prevent release from the material.

The effectiveness of this strategy rest on the stability of the composite, i.e. the strength of the bond between the nanoparticle and its shells as well as the resistance of the shell(s)/matrix during the use and end-of-life phases of the nano-enabled products. The material stability is examined after real/simulated aging with element specific probes. Here we present some examples taken from case studies using off the shelf products on how surface speciation informs about the efficiency of the product formulation in a safe(r) by design perspective.

MAGELEC: A Unique Sample Environment for Performing RIXS under Electric and Magnetic Field

A. Nicolaou^{*1}, V. Pinty¹, F. Marteau¹, J-M. Dubuisson¹, P. Rommeluere¹,
E. Dupuy¹, F. Bouvet¹, D. Corruble¹, C. S  the², M. Ag  ker³,
J-E. Rubensson³, M. Nouna¹, P. Goy¹, S. Lorcy¹, C. Herbeaux¹

¹ Synchrotron SOLEIL, L'Orme des Merisiers, Saint-Aubin, BP 48, 91192 Gif-sur-Yvette, France

² MAX IV Laboratory, Lund University, Box 118, SE-221 00 Lund, Sweden¹ Uppsala University

³ Department of Physics and Astronomy, Uppsala University, Box 516,
SE-751 20 Uppsala, Sweden

ABSTRACT

Resonant-inelastic X-ray scattering (RIXS) is a photon-in photon-out technique where the system is resonantly excited at an absorption threshold and the scattered photons are measured in order to probe the energy and momentum transfer of the intrinsic excitations of the system, such as electronic, magnetic or lattice excitations. This spectroscopy has been subject of a remarkable progress in the last years for its capability of extracting information of fundamental interest for the description of the physical properties of correlated systems [1].

Thanks to the collaboration between SOLEIL and MAX IV synchrotrons we have developed a unique sample environment for performing high-resolution RIXS experiments in presence of electric and/or magnetic fields. We have equipped the soft X-rays end-station of the SEXTANTS beamline with a quadrupolar magnet delivering a rotatable magnetic field with a maximum strength of 0.45 T. Thanks to its particular design the whole scattering plane remains available for magnetic circular dichroism RIXS experiments (RIXS-MCD).

I will start by presenting the layout of the quadrupolar magnet now available for RIXS-MCD at the SEXTANTS beamline and the sample holder equipped by 12 electrical contacts. I will then show the first RIXS-MCD map obtained at SEXTANTS on a ferromagnetic transition metal oxide where clear dichroic contrast is observable in the energy loss range corresponding to interband *dd* transitions.

This experimental setup, in connection with the recent ability to control thin film growth at the atomic level to produce epitaxial hetero-structures, will open new perspectives in fundamental research on magnetic materials, where macroscopic properties arise from a fine tuning charge, spin and lattice degrees of freedom [2]. In this context, RIXS is indeed one of the most powerful spectroscopies for measuring operating devices, through the measure of electronic, structural and magnetic properties in *operando* conditions. Actually, its element sensitivity would allow decoupling the contribution of the different chemical species constituting the system and its bulk sensitivity accessing to buried layers.

In conclusion, the MAGELEC experimental setup will open new perspectives at the SEXTANTS beamline thanks to the possibility to tackle several kinds of open questions in the field of transition metal compounds beyond the accuracy obtained by the widely used X-ray magnetic circular dichroism [3] and in *operando* conditions.

REFERENCES

[1] L.J.P. Ament et al. Rev. Mod. Phys. **83**, 705

[2] S. M. Wu et al. Nature Mat. 2010

[3] J. Miyawaki et al. PRB 96, 214420 (2017); J. of Synchrotron Rad. (2017) 24

Unravelling the Thermal Phase Transformation of Alumino-germanate Nanotubes

G. Monet^a, P. Launois^a, S. Rouzière^a, D. Vantelon^b,
D. Thiaudière^b, and E. Paineau^a

*a. Laboratoire de Physique des Solides, Université Paris Saclay, CNRS,
91405 Orsay Cedex, France*

b. Synchrotron SOLEIL, L'Orme des Merisiers, 91190 Saint-Aubin, France

ABSTRACT

Metal oxide aluminosilicate and aluminogermanate nanotubes, called imogolite nanotubes (INT), are fascinating nanotubes, easily synthesized with well-controlled diameter and with different morphologies and organization [1,2]. These nanotubes undergo major structural changes at high temperatures, including the transformation from one-dimensional (1-D) nanochannels into a structure which is supposed to be lamellar [2,3], but which had not been studied in details in the literature.

Here, we report a complete analysis of the structural transformation of single or double-walled aluminogermanate nanotubes, up to 900°C. We applied an original approach combining in-situ X-ray absorption spectroscopy measurements (LUCIA & DiffAbs beamlines), allowing us to investigate the evolution of both Al and Ge atoms coordination during the transformation process. Quantitative analysis of XANES spectra (Figure) reveals that the dehydroxylation of nanotubes does not lead to a lamellar phase but rather to metastable intermediate states (“meta-imogolite”). Above 600°C, we observed a progressive atomic reorganization of this phase towards a mullite structure. The understanding of the structural modifications of these nanomaterials at high temperatures represents a benchmark for further studies concerning the properties of these transformed INT-based compounds, for instance with respect to the topical issue of geopolymers.

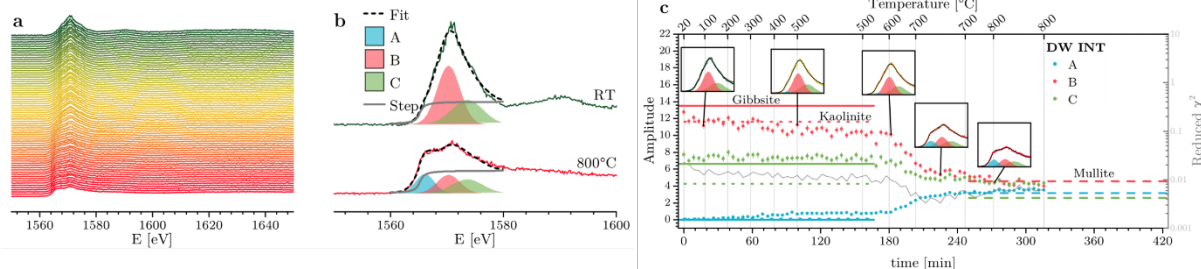


Figure: (a) Al K-edge XANES spectra series measured for a DW imogolite nanotube powder heated in-situ from room temperature (RT, green curve) to 800°C (red curve). (b) Refinement procedure of the absorption edge by 3 Gaussian components. (c) Amplitude of the fitting Gaussians over heat treatment.

REFERENCES

1. E. Paineau and P. Launois, “Nanomaterials from imogolite: structure, properties and functional materials” in *Nanomaterials from clay minerals*, edited by A. Wang and W. Wang, Amsterdam: Elsevier, 2019, pp. 257-284.
2. G. Monet, M. S. Amara, S. Rouzière, E. Paineau, Z. Chai, J. D. Elliott, E. Poli, L.-M. Liu, G. Teobaldi, and P. Launois, *Nat. Comm.* **9**, 2033 (2018).
3. K. J. D. MacKenzie, M. E. Bowden, I. W. M. Brown, R. H. Meinhold, *Clays Clay Miner.* **37**, 317-324 (1989).
4. C. Zanzottera, A. Vicente, M. Armandi, C. Fernandez, E. Garrone, B. Bonelli, *J. Phys. Chem. C* **116**, 23577-23584 (2012).

X-ray Absorption Study on the Origin of the Deviation from Vegard's Law for $U(Al_{1-x}Ge_x)_3$ Solid Solution

M. Pasturel^a, S. Le Tonquesse^a, V. Demange^a, A. Tayal^b,
P. L. Solari^b, C. Prestipino^a

^a Univ Rennes, CNRS, ISCR-UMR6226, F-35000, Rennes, France

^b Synchrotron SOLEIL, L'Orme des Merisiers, BP 48, St Aubin, 91192, Gif sur Yvette, France

ABSTRACT

Similarly to silicon, germanium added to the nuclear material UAl_3 was shown to efficiently block the formation of the undesired UAl_4 during the fabrication process or under irradiation by the reaction of the former with the aluminium matrix in fuel plates or irradiation targets [1]. However differently from $U(Al,Si)_3$ for which numerous data are available in literature [2-4], scarce reports are available for the $U(Al,Ge)_3$ solid solution [5,6]. In particular, it is very interesting that contrary to similar USn_3-UGa_3 , USn_3-UAl_3 and UAl_2-UCo_2 [7] solid solutions, $U(Al,Ge)_3$ presents an evolution of lattice parameter that deviates strongly from the Vegard's law (Figure 1).

For such reasons, we performed a study on the local structure of $U(Al_{1-x}Ge_x)_3$ intermetallics with $x = 0, 0.25, 0.5, 0.75$ and 1 using EXAFS and XANES measurements at U L_3 and Ge K-edges at the Mars beamline in order to better understand the structural origin of such deviation and improve the comprehension of chemical bonding in this potential nuclear material. From the analysis of bond evolution (obtained by diffraction and EXAFS) and HERFD XANES and specific heat measurements we were able to explain the origin of the deviation from the Vegard's law for $U(Al_{1-x}Ge_x)_3$. The deviation has been proven to be based on actual bond length variation while the possible long-range ordering phenomena as UAl_3-USi_3 have been excluded by the absence of superstructures or diffuse scattering in electron diffraction. Indeed the deviation is mainly related to a decrease of U-Ge bond length induced by the increase of Al concentration in the solid solution, related to the depopulation of the U $5f$ levels (around $0.2 e^-$) suggesting that the deviation from Vegard's law is caused by valence instability [8].

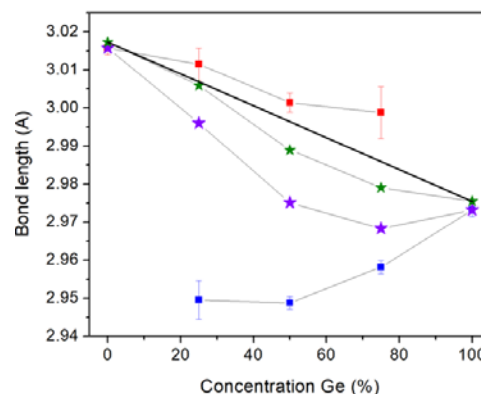


Figure 1 Evolution of the U-Al (blue squares), U-Ge (red squares) and average U-Al/Ge distances (purple stars) obtained from EXAFS as a function of the Ge concentration. Distances determined from XRD (green stars) and the linear relation expected from the Vegard's law (black line).

REFERENCES

1. W.C. Thurber, R. Beaver, Oak Ridge National Lab., Tenn., 1959 <https://doi.org/10.2172/4260852>, Tech. rep.
2. D. Rabin, R.Z. Shneck, G. Rafailov, I. Dahan, L. Meshi, E. Brosh, *J. Nucl. Mater.* **464** (2015) 170–184.
3. G. Rafailov, I. Dahana, L. Meshi, *Acta Crystallogr. B* **70** (2014) 580.
4. H.J. Ryu, Y.S. Kim, G.L. Hofman, J.M. Park, C.K. Kim, *J. Nucl. Mater.* **358** (2006) 52–56
5. A.V. Tyunis, V.A. Shaburov, Y.P. Smirnov, A.E. Sovestnov., *Phys. Solid State* **39** (9) (1997) 1337–1340.
6. C. Moussa, Z. El Sayah, G. Chajewski, A. Berche, M. Pasturel, L. Joanny, B. Stepnik, O. Tougait, *J. Solid State Chem.* **243** (2016) 168.
7. E. Burzo, P. Lucaci, *Solid State Commun.* **56** (1985) 537.
8. S. Le Tonquesse, M. Pasturel, V. Demange, A. Tayal, P. L. Solari, C. Prestipino, *J. Nucl. Mater.*, **526**, (2019), 151772

Structural Properties of TbMgNi_{4-x}Co_x Hydrides and Deuterides

V. Shtender^{1, 2}, V. Paul-Boncour¹, K. Provost¹, F. Couturas¹,
J-C. Crivello¹, R.V. Denys³, I.Yu. Zavaliy²

¹ICMPE (UMR 7182), CNRS, UPEC, 94320 Thiais, France

²Karpenko Physico-Mechanical Institute, NAS of Ukraine, 79060 Lviv, Ukraine

³HYSTORSYS AS, P.O. Box 45, Kjeller NO-2027, Norway

ABSTRACT

A large number of research has been performed on metal hydrides to improve their hydrogenation capacities, hydrogen absorption/desorption kinetics and thermodynamics for hydrogen storage applications [1]. Substantial work has been done to improve the thermodynamic properties of Mg-based compounds. It is already known that substitution of rare earth by Mg in the binary RT_2 , RT_3 , R_2T_7 and R_5T_{19} (R = rare earth and T = d -transition metals) intermetallic compounds increases their stability against hydrogen induced amorphization [2]. Different approaches have been applied to enhance the hydrogenation properties: partial substitution of R by another rare earth metal or by Mg; different combinations of d -transition metals and even replacing D by H to check if there is a significant isotope effect on the thermodynamic and structural properties [3].

Recently, R -Mg-Co(Ni) compounds attracted substantial interest due to their outstanding hydrogenation properties. For instance, it was shown that $RMgCo_4$ (R = Y, La, Pr, Nd) compounds absorb ~50% more hydrogen and at lower pressures than $RMgNi_4$ [4, 5].

In this work, TbMgNi_{4-x}Co_x (x = 0–4) intermetallics with SnMgCu₄ type cubic structure have been synthesized. Their hydrogenation properties have been studied in detail. The increase of Co content increases the stability of TbMgNi_{4-x}Co_x hydrides as demonstrated by the experimental results and confirmed by the first principles calculations. The structural investigation of the alloys and their hydrides (deuterides) was investigated by synchrotron radiation diffraction (ESRF and SOLEIL) and various crystal structures derived from the parent compound have been observed versus Co content and (H,D) isotope. These results will be presented and discussed in comparison with other $RMgCo(Ni)_4$ systems.

REFERENCES

1. M. P. Brown and K. Austin, *The New Physique*, Publisher City: Publisher Name, 2005, pp. 25-30.
2. M. P. Brown and K. Austin, *Appl. Phys. Letters* **85**, 2503-2504 (2004).
3. B. R. Jackson and T. Pitman, U.S. Patent No. 6,345,224 (8 July 2004)
4. V. V. Shtender, R. V. Denys, V. Paul-Boncour, A. B. Riabov, and I. Yu Zavaliy, *J. Alloy Compd.* **603**, 7 (2014).
5. V. V. Shtender, R. V. Denys, V. Paul-Boncour, Yu V. Verbovytsky, and I. Yu Zavaliy, *J. Alloy Compd.* **639**, 526 (2015).

Operando XAS Investigations on Mg-based Complex Hydrides as Anodes of Solid-state Li-ion Batteries

K. Provost¹, J. Zhang¹, V. Paul-Boncour¹, J. Monnier,
M. Latroche¹, S. Belin², F. Cuevas¹

¹ Univ. Paris Est Creteil, CNRS, ICMPE, UMR7182, 2 rue H. Dunant, F-94320, Thiais, France
² Synchrotron SOLEIL, Saint-Aubin, BP 48, 91192 Gif-sur Yvette Cedex, France

ABSTRACT

Metal hydrides (MH_x) are promising anode materials for Li-ion batteries thanks to their high specific capacity and low voltage. They operate through the conversion reaction $MH_x + xe^- + xLi^+ \rightleftharpoons M + xLiH$ [1]. In this context, Mg_2MH_x nanocrystalline complex hydrides ($M=Fe, Co, Ni$) synthesized by reactive ball milling [2] have been investigated as negative electrodes [3]. Using XAS, we showed in a previous study at RT using liquid electrolyte, that the lithiation reaction led to the formation of highly disordered metallic phases [4,5]. Different local orders around M atoms as well as decomposition of the intermetallic sublattice were observed: preservation of Mg_2Ni , partial demixion of Mg_2Co into Mg and $MgCo$, and full demixion of Mg_2Fe into $2Mg$ and nano- Fe , with a larger disorder for M atoms, compared to Mg . However, despite these differences, the reversibility of the conversion reaction (i.e. restoring of Mg_2MH_x hydrides upon delithiation) was very limited in all cases.

Recent findings have demonstrated that reversibility of hydrides as conversion materials can be improved in All-Solid-State Li-Ion Batteries (ASSLIB), using $LiBH_4$ as solid electrolyte at $120^\circ C$ [6-9]. In 2018, Huen and Ravensbaek reported that, contrary to RT studies, high reversibility is attained for Mg_2FeH_6 at $120^\circ C$ [10]. Ex-situ XRD and electrochemical potential profiles suggest the formation of MgH_2 hydride as intermediate, but scarce information was given on the transition metal. XRD data were not conclusive due to strong peak broadening and overlapping between diffraction peaks of the active material and $LiBH_4$ electrolyte.

In this work, we performed XAS *operando* studies at SOLEIL Rock-beamline on Mg_2NiH_4 and Mg_2CoH_5 in ASSLIB conditions ($120^\circ C$, $LiBH_4$ as solid electrolyte) at M -K edge. A partial reversibility could be obtained for both complex hydrides. Furthermore, first results show that the transition metal local environments obtained after complete lithiation in RT/liquid electrolyte vs. ASSLIB conditions are not the same. This difference might be at the origin of the various reversibility observed at RT and $120^\circ C$.

REFERENCES

1. Y. Oumellal, A. Rougier, G.A. Nazri, J. M. Tarascon and L. Aymard, *Nature Materials* **7**, 916-921 (2008)
2. J. Zhang, F. Cuevas, W. Zaïdi, J. P. Bonnet, L. Aymard, J.L. Bobet and M. Latroche, *J. Phys. Chem. C* **115**, 4971-4979 (2011)
3. W. Zaïdi, J. P. Bonnet, J. Zhang, F. Cuevas, M. Latroche, S. Couillaud, J.L. Bobet, M.T. Sougrati, J.C. Jumas and L. Aymard, *Int. J. Hydrogen Energy* **38**, 4798-4808 (2013)
4. J. Zhang, W. Zaïdi, V. Paul-Boncour, K. Provost, A. Michalowicz, F. Cuevas, M. Latroche, S. Belin, J. P. Bonnet and L. Aymard, *J. Mater. Chem. A* **1**, 4706-4717 (2013)
5. K. Provost, J. Zhang, W. Zaïdi, V. Paul-Boncour, J. P. Bonnet, F. Cuevas, S. Belin, L. Aymard and M. Latroche, *J. Phys. Chem. C* **118**, 29554-29567 (2014)
6. L. Zeng, T. K. Kawahito, S. Ikeda, T. Ichikawa, H. Miyaoka and Y. Kohima, *Chem. Commun.* **51**, 9773-9776 (2015)
7. L. Zeng, T. Ichikawa, K. Kawahito, H. Miyaoka and Y. Kohima, *ACS Appl. Mater. Interfaces* **9**, 2261-2266 (2017)
8. K. Kawahito, L. Zeng, T. Ichikawa, H. Miyaoka and Y. Kohima, *Mater. Trans.* **57**, 755-757 (2016)
9. P. Lopez-Aranguren, N. Berti, A.-H. Dao, J. Zhang, F. Cuevas, J.L. Bobet, M. Latroche and C. Cordy, *J. Power Sources* **357**, 56-60 (2017)
10. P. Huen and D.B. Ravensbaek, *Electrochem. Comm.* **87**, 81-85 (2018)

Formation of CoRu Nanoalloys: A Comprehensive Study by UV-visible and X-ray Absorption Spectrometries

L. Sicard,¹ B. Azeredo,¹ L. Barthe,² M. Giraud,¹ J. Peron,¹
J.-Y. Piquemal,¹ V. Briois²

¹ Université de Paris, ITODYS, CNRS, UMR 7086, 15 rue J-A de Baïf, F-75013 Paris, France

² Synchrotron SOLEIL, L'Orme des Merisiers, BP48, Saint-Aubin, 91192 Gif-sur Yvette, France

ABSTRACT

Bimetallic nanoparticles (NPs) have received growing interest for a wide range of applications such as catalysis, optics or magnetism.¹ By varying the composition and size of clusters of transition and noble metals nanoalloys, a fine control of the electronic state can be obtained and synergetic effects have been reported for different catalytic reactions.

We have prepared CoRu bimetallic nanoplatelets by reducing Ru(III) and Co(II) acetylacetonate (acac) salts in octan-1-ol which plays the role of both the solvent and the reducing agent and we tested them for the acceptorless dehydrogenation of alcohols. The key parameter to obtain homogeneously distributed Co and Ru atoms was to choose metal precursors and a solvent permitting a concomitant reduction of Ru(III) and Co(II). To determine precisely the reduction temperature and understand the mutual influence of a metal ion on the reduction of the other one, we have used two spectroscopy techniques: UV-visible and X-ray absorption (XAS). The first one allowed us to follow quantitatively the reduction of Ru(III) metal species: a quick reduction at *ca.* 170 °C was observed for pure Ru(acac)₃ as well as for a mixture with Co(acac)₂. Unfortunately, the reduction of Co(II) could not be followed by this technique. *In situ* XAS was thus carried out using a cell designed on purpose for this experiment on the Rock Soleil beamline. The spectra were processed using Principal Component Analysis (PCA) and Multivariate Curve Resolution with Alternating Least Squares (MCR-ALS).^{2,3} The results obtained at the Ru K-edge were in accordance with those obtained by UV-visible spectroscopy. However, the Co K-edge analysis showed a clear influence of the presence of Ru on the reduction of Co(II) species: the reduction of Co(II) species occurs at an early stage when adding Ru. Ru is known to be a promoter for the reduction of Co in Fischer Tropsch catalysis:⁴ the Ru(0) would form first and activate hydrogen, allowing the complete reduction of Ru(III) and Co(II) species by an autocatalytic process.⁵ Moreover the transformation of the precursor species towards metallic NPs occurs through the formation of an intermediate. All these results are highly valuable to rationalize the strategy to prepare homogeneous nanoalloys with a controlled composition.

REFERENCES

1. K.D. Gilroy, A. Ruditskiv, H.-C. Peng, D. Qin and Y. Xia, *Chem. Rev.* **116**, 10414–10472 (2016).
2. A. De Juan, J. Jaumot and R. Tauler, *Anal. Methods* **6**, 4964–4976 (2014),.
3. J. Jaumot, R. Gargallo, A. De Juan and R. Tauler *Chemom. Intell. Lab. Syst.* **76**, 101–110 (2005).
4. E. Iglesia, S. L. Soled, R. A. Fiato and G. H. Via, *J. Catal.* **143**, 345–368 (1993).
5. J. Hong, E. Marceau, A. Y. Khodakov, L. Gaberová, A. Griboval-Constant, J. S. Girardon, C. La Fontaine and V. Briois, *ACS Catal.* **5**, 1273–1282 (2015).

Sinogram Correction Method for Monochromatic Beam of a Synchrotron X-ray Source

D. N. Trinca and E. Libin

Institute of Measurement Science, Bratislava, Slovakia

ABSTRACT

Reconstruction algorithms for X-ray computed tomography (CT), and in particular iterative algorithms [1], have received increasing interest not only in conventional X-ray computed tomography, but also for synchrotron X-ray radiation, especially for the important goal of dose reduction. The recent researches based on total variation (TV) regularization propose some of the best iterative algorithms for X-ray CT [3,4]. The sinogram-based iterative reconstruction (SbIR) algorithm [2] has been recently proposed and evaluated with a number of X-ray CT examples; the comparisons show that in some cases the SbIR algorithm obtains better results than some variants of the TV regularization technique.

In this work, we propose a sinogram correction method that is suitable for X-ray sources such as monochromatic synchrotron X-ray radiation; from the simulations that we have run, the proposed correction method is worth including as a pre-processing step of iterative algorithms such as SbIR and SART, as in some cases it leads to a noticeable increase of the overall quality of the reconstruction.

The proposed correction method works as follows. If n_d is the number of detectors and n_v is the number of views in the experiment, let S_i be the sum of all sinogram values corresponding to view i , for $i=1,2,\dots,n_v$. If the X-ray source is monochromatic, then in principle all S_i values should be equal since the total attenuation for a view should be the same, regardless of the view (this assumption is reasonable since for a monochromatic X-ray source, noise present from undesired effects such as beam-hardening effects is almost inexistent). Thus let S be the sum of all sinogram values, thus S is the sum of all S_i values, and let $x = (S/n_v)$, so x is the mean of all S_i values. Thus if $S_{i,j}$ is the sinogram value corresponding to view i and detector j then we replace $S_{i,j}$ with $S_{i,j} * (x/S_i)$ before running an iterative algorithm.

REFERENCES

1. M. Beister, D. Kolditz and Kalender W.A., Iterative reconstruction methods in X-ray CT, *Physica Medica: European J. of Medical Physics* **28**, 94-108 (2012).
2. D. Trinca and E. Libin, Performance of the Sinogram-based Iterative Reconstruction in Sparse View X-ray Computed Tomography, *Journal of X-Ray Science and Technology* **27**, 37-49 (2019).
3. TVReg version 1.1 software package for 3D total variation regularization, Matlab code available at the Github software repository <https://github.com/jakobsj/TVReg>.
4. T.L. Jensen, J.H. Jorgensen, P.C. Hansen and S.H. Jensen, Implementation of an optimal first-order method for strongly convex total variation regularization, *BIT Numerical Mathematics* **52**, 329-356 (2012).

Significant Band Offset in 2D MoS₂/black Phosphorus Heterostructure

Z. Zhang^{a,b}

^a*Antares beamline, Synchrotron SOLEIL, Gif-sur-Yvette 91192, France*

^b*International Collaborative Laboratory of 2D Materials for Optoelectronics Science and Technology of Ministry of Education, Institute of Microscale Optoelectronics, Shenzhen University, Shenzhen 518060, China*

ABSTRACT

Vertical Van Der Waals semiconductor heterostructures with different materials have attracted tremendous interest not only for their outstanding properties such as strong interlayer interaction and ultrafast charge transfer process but also in optoelectronic applications such as photodiodes, light emitting diodes and solar cells with self-driven and rectifying features [1,2]. In general, the built-in potential and band offsets at the interface of the heterostructures play a key role in the performance of the devices. In this work, we report the determination of band offsets in the heterostructure of MoS₂/black phosphorus by using photoluminescence spectroscopy and micro X-ray photoemission spectroscopy [3]. We determine a type-II alignment between MoS₂ and black phosphorus with a significant valence band offset value of ~1.2 eV, which is in consistent with band alignment calculations. Our findings will offer new insights into the optoelectronic properties of MoS₂/black phosphorus heterostructure and will potentially boost the performance of new devices.

REFERENCES

1. Z. Chen, Z. Zhang, J. Biscaras and A. Shukla, *Journal of Materials Chemistry C*, 6, 12407-12412, (2018).
2. M. Huang, S. Li, Z. Zhang, X. Xiong, X. Li and Y. Wu, *Nature Nanotechnology*, 12, 1148-1154, (2017)
3. Z. Zhang, Z. Chen, M. Bouaziz, C. Giorgetti, H. Yi, J. Avila, B. Tian, A. Shukla, L. Perfetti, D. Fan, Y. Li and A. Bendounan, *ACS Nano*, 13, 11, 13486-13491, (2019)

Friday, January 17th

14:00 -17:00

Chemometry in Quick XAS tutorial (limited to the register participants)

Valérie Briois

Training room, T5 Building

Chemometry in QUICK XAS

ABSTRACT

Avec le développement des sources synchrotrons de 3^{ème} génération, donnant accès à des caractérisations temporelles inférieures à la seconde pour le suivi des cinétiques par spectroscopie d'absorption X (XAS), l'expérimentateur accède aujourd'hui à une description plus précise des espèces impliquées dans de tels procédés, pourvu bien sûr que le verrou de l'analyse des données ait pu être surmonté. En effet, les utilisateurs des lignes XAS résolues dans le temps doivent faire face à une quantité considérable de données en quelques minutes, rendant la stratégie standard d'évaluation et d'analyse des données XAS inefficace. De nouveaux outils doivent être proposés aux utilisateurs pour interactivement optimiser le déroulement d'une expérience et en extraire rapidement des résultats quantitatifs. Dans ce cadre, les outils chimiométriques combinant Analyse par Composantes Principales

(MCR-ALS) émergent comme une puissante méthode pour quantifier le nombre, l'évolution des espèces impliquées dans une réaction et leur nature grâce à la reconnaissance ou interprétation de leurs signatures caractéristiques en XAS [1-6]. Sur la ligne ROCK, une interface conviviale a récemment été développée pour manipuler les quantités de données obtenues pendant le suivi d'une réaction [7]. Des matrices normalisées de plusieurs centaines de spectres d'absorption sont rapidement générées après mesure, directement utilisables comme fichiers d'entrée pour l'analyse MCR-ALS sur la plate-forme Matlab utilisant les boîtes à outils mises à disposition par le groupe de Roma Tauler [8].

Dans cet atelier, après une courte introduction aux méthodes chimiométriques appliquées à la spectroscopie d'absorption X, une session pratique d'utilisation des outils disponibles sur la ligne ROCK pour la spéciation chimique déterminée par MCR-ALS d'un jeu de données Quick-XAS obtenus pendant le suivi d'une réaction sera réalisée.

L'utilisation d'ordinateurs ayant une licence Matlab étant requise, le nombre de participants est limité à 20.

REFERENCES

- [1] W. Cassinelli, L. Martins, A. R. Passos, S. H. Pulcinelli, C. V. Santilli, A. Rochet, V. Briois, *Cat. Today* 229, 114 (2014).
- [2] J. Hong, E. Marceau, A. Khodakov, L. Gaberova, A. Griboval-Constant, J. S. Girardon, C. La Fontaine, V. Briois, *ACS Catal.* 5, 1273 (2014).
- [3] A. Rochet, B. Baubet, V. Moizan, C. Pichon, V. Briois, *Comptes Rendus Chimie* 19, 1337 (2016)
- [4] H.W. P. Carvalho, F. Leroux, V. Briois, C. V. Santilli, S. H. Pulcinelli, *RSC Adv.* 8, 34670 (2018).
- [5] V. Girard, D. Chiche, A. Baudot, D. Bazer-Bachi, L. Lemaitre, V. Moizan-Baslé, A. Rochet, V. Briois, *C. Geantet, PCCP* 21, 8569, (2019).
- [6] A. Voronov, A. Urakawa, W. van Beek, N. E. Tsakoumis, H. Emercih, M. Ronning, *Analytica Chimica Acta*, 840, 20, (2014).
- [7] C. Lesage, E. Devers, C. Legens, G. Fernandes, O. Roudenko, V. Briois, *Catalysis Today* 336, 63, (2019)
- [8] J. Jaumot, A. de Juan, R ; Tauler, *Chemom. Intell. Lab. Syst.* 140, 1, (2015).

LIST OF COMMERCIAL EXHIBITORS

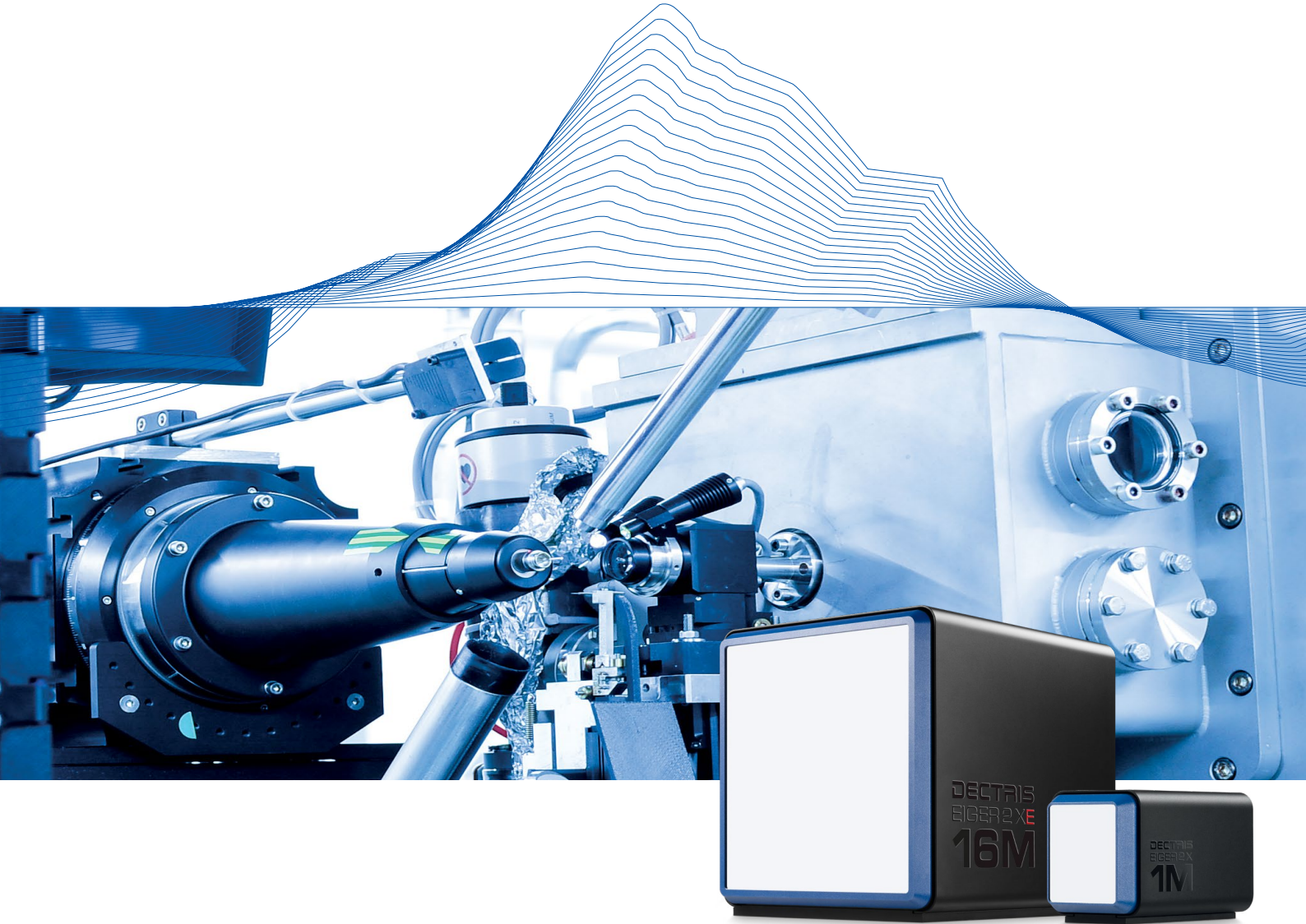
List of Commercial Exhibitors

Company		Website
	ALLECTRA	www.allectra.com
	ALTEC	www.altec-equipment.com
	CEGITEK	www.cegitek.com
	HITACHI	www.hitachi-hta.com
	MDC VACUUM	www.mdcvacuum.com
	MKS NEWPORT	www.newport.com
	PFEIFFER VACUUM	www.pfeiffer-vacuum.fr

List of Commercial Exhibitors

Company		Website
	<p>PI FRANCE SAS</p>	<p>www.pi.ws</p>
	<p>SAES GETTERS GROUP</p>	<p>www.saes-group.com</p>
	<p>SCHAEFER TECHNIQUES</p>	<p>www.schaefer-tech.com</p>
	<p>SCIENTA OMICRON</p>	<p>www.scientaomicron.com</p>
	<p>SCIENTEC</p>	<p>www.scientec.fr</p>
	<p>SPECS</p>	<p>www.specs.com</p>
	<p>SYDOR TECHNOLOGIES</p>	<p>www.sydortechnologies.com</p>

COMPANIES ADVERTISEMENTS



FLYING SPEED FOR ON-THE-FLY SCANNING

Go for Ultimate Performance
with EIGER2 XE

- Hybrid Photon Counting technology
- Frame rate up to 2 kHz
- Count rate capability of 10^7 counts/s/pixel
- Two energy-discriminating thresholds



Find your optimal detector

Beamline Instrumentation

SOPHISTICATED COMPONENTS AND SYSTEM SOLUTIONS



High Stiffness Positioning Stages for Medium Load

- Standard travel range to 300 mm
- 50 kg payload capacity
- Stepper and DC motors
- Optional linear encoder



Sample Positioning in High Vacuum

- Motorized and piezo positioners
- Up to 6 degrees of freedom
- High precision and stability
- Vacuum compatible to 10^{-10} mbar



Engineered System for Complex Applications

- Application support and consulting
- Commissioning of turnkey solutions
- Multi-axis designs and parallel kinematic
- Customized software integration such as Epics, LabVIEW, Tango